STUDY ON ULTRASONIC MACHINING OF Al/Si BASED COMPOSITE AND Al/Cu ALLOY

A THESIS

SUBMITTED IN PARTIAL FULFILLMENT OF THE REQUIREMENT

FOR THE AWARD OF THE DEGREE OF

MASTER OF ENGINEERING

IN

PRODUCTION AND INDUSTRIAL ENGINEERING

SUBMITTED BY

PUNEET BANSAL

Roll No. 801182017

UNDER THE GUIDANCE OF

Dr.V.K.SINGLA

(Associate Professor)

DEPARTMENT OF MECHANICAL ENGINEERING

THAPAR UNIVERSITY

PATIALA – 147004, INDIA

JULY, 2013

CERTIFICATE

This is to certify that the thesis report entitled "**Study On Ultrasonic Machining of Al/Si Based Composite And Al/Cu Alloy**" is an authentic record of my study carried out as requirements for the award of degree of **MASTER OF ENGINEERING (PRODUCTION AND INDUSTRIAL ENGINEERING)** to Thapar University, Patiala, under the guidance of Dr. VINOD KUMAR SINGLA, Associate Professor, Department of Mechanical Engineering, Thapar University Patiala.

This report or the matter involved in this thesis is of desired standard and has not been submitted in any other University or Institute for the award of this degree.

Dr.V.K.SINGLA
Associate Professor
Mechanical Engineering Department
Thapar University, Patiala

Countersigned by

Dr. AJAY BATISH
Professor and Head,
Department of Mechanical Engineering,
Thapar University, Patiala-147004

Dr. S.K.MOHAPATRA
Dean of Academic Affairs,
Thapar University, Patiala-147004

ACKNOWLEDGEMENT

I am highly grateful to the authorities of Thapar University, Patiala for providing this opportunity to carry out the Thesis work. I would like to express a deep sense of gratitude and thanks profusely to my thesis guide Dr. V.K. SINGLA, Associate Professor, Mechanical Engineering Department, Thapar University Patiala and for his sincere and invaluable guidance, suggestions and sympathetic attitude which inspired me to submit this thesis report in the present form. I am highly thankful to Dr. Ajay Batish, Professor and Head of Mechanical Engineering Department and Dr. S.K. Mohapatra, Dean of Academic Affairs Thapar University, Patiala for his great support and encouragement for my thesis work. I am thankful to all faculty members of Mechanical Engineering Department, Thapar University Patiala for their intellectual support.

I would like also thanks to School of Physics and Material Science for providing the required testing facilities for my thesis work.

My special thanks to my family members specially my parents who loved me a lot and friends who constantly encouraged me to complete this study.

PUNEET BANSAL

ABSTRACT

Ultrasonic machining is one of the most widely used non-traditional machining processes for the machining of non-conductive, brittle materials. Unlike other processes, ultrasonic machining does not damage the work surface thermally which contributes to the successful performance of these materials in service. Ultrasonic vibration cutting as a cutting process has been widely used in the precision machining of difficult to cut materials due to an enhanced cutting stability and increased productivity. Ultrasonic machining is a technology driven process used for machining or finishing brittle abrasives or materials. The USM is effective and practical for all brittle materials, including glass, ceramics, carbides, and graphite roughness, micro-structure, surface hardness, material removal rate as output parameters. In the present study, Al/Si composite and Al/Cu alloy was machined. The effect of different input parameters namely Power Rating, Tool type, Slurry type, Slurry Concentration, Work piece and Grit Size on the output parameters namely MRR, TWR, SR and Hardness was studied. A number of factors and their different levels are selected. Based on factors and their levels number of experiments are selected using orthogonal array. The effect of various input parameters on output parameters is analysed using statistical technique such as ANOVA, Optimization and verification of the process parameters and the modelling of the results is done by applying Regression Analysis. Main effect plot and Residual plot for significant factors and S/N ratio have been used to determine the optimal design for each output response. SEM was done to see the distribution and presence of various particles in Al/Si composite and Al/Cu alloy. XRD was completed to analyze the various elements present in different composites.

ABBREVATIONS

ANOVA	Analysis of Variance
USM	Ultrasonic Machining
DOF	Degree of Freedom
V	Variation
MRR	Material Removal Rate
TWR	Tool Wear Rate
SR	Surface Roughness
SEM	Scanning Electron Microscope
XRD	X-Ray Diffraction
S/N	Signal to Noise Ratio
SS	Stainless Steel
HSS	High Speed Steel

NOTATIONS

OA	Orthogonal Array
A	Abrasive Slurry
B	Tool
C	Workpiece
D	Abrasive Grit Size
E	Slurry Concentration
F	Power Rating
V	Variation
CI	Confidence Interval
SS	Sum of Squares

TABLE OF CONTENTS

LIST OF FIGURES

.

LIST OF TABLES

CHAPTER 1
INTRODUCTION

With the development of technology, the scientists and technologists in the field of manufacturing are facing more and more challenges. Technologically advanced industries such as aeronautics, nuclear reactors and automobiles have been demanding high strength temperature resistant (HSTR) materials having high strength to weight ratio. Researchers in the area of materials science are developing materials having higher strength, hardness, toughness and other diverse properties. This also needs the development of improved cutting tool materials so that productivity is not hampered.

1.1 Introduction to non-traditional machining

In unconventional machining methods, there is no direct contact between the tool and work piece; hence the tool need not be harder than work piece. Further, in spite of the recent technical advancement, the conventional machining processes are inadequate to produce complex geometries shapes in hard and temperature resistant alloy and die steels. Keeping these requirements in mind, a number of non conventional methods have been developed. Below given classification of machining process based on type of energy used, the mechanism of metal removal, the source of energy requirement.

Non Traditional Machining (NTM) processes are characterized as follows:

- Material removal may occur with chip formation or even no chip formation may take place. For example in AJM, chips are of microscopic size and in case of Electrochemical machining material removal occurs due to electrochemical dissolution at atomic level.
- In NTM, there may not be a physical tool present. For example, in laser jet machining, machining is carried out by a laser beam. However in electrochemical machining there is a physical tool that is very much required for machining.
- In NTM, the tool need not be harder than the work piece material. For example, in EDM, copper is used as the tool material to machine hardened steels.

- Mostly NTM processes do not necessarily use mechanical energy to provide material removal. They use different energy domains to provide machining. For example, in USM, AJM, WJM mechanical energy is used to machine material, whereas in ECM electrochemical dissolution constitutes material removal.

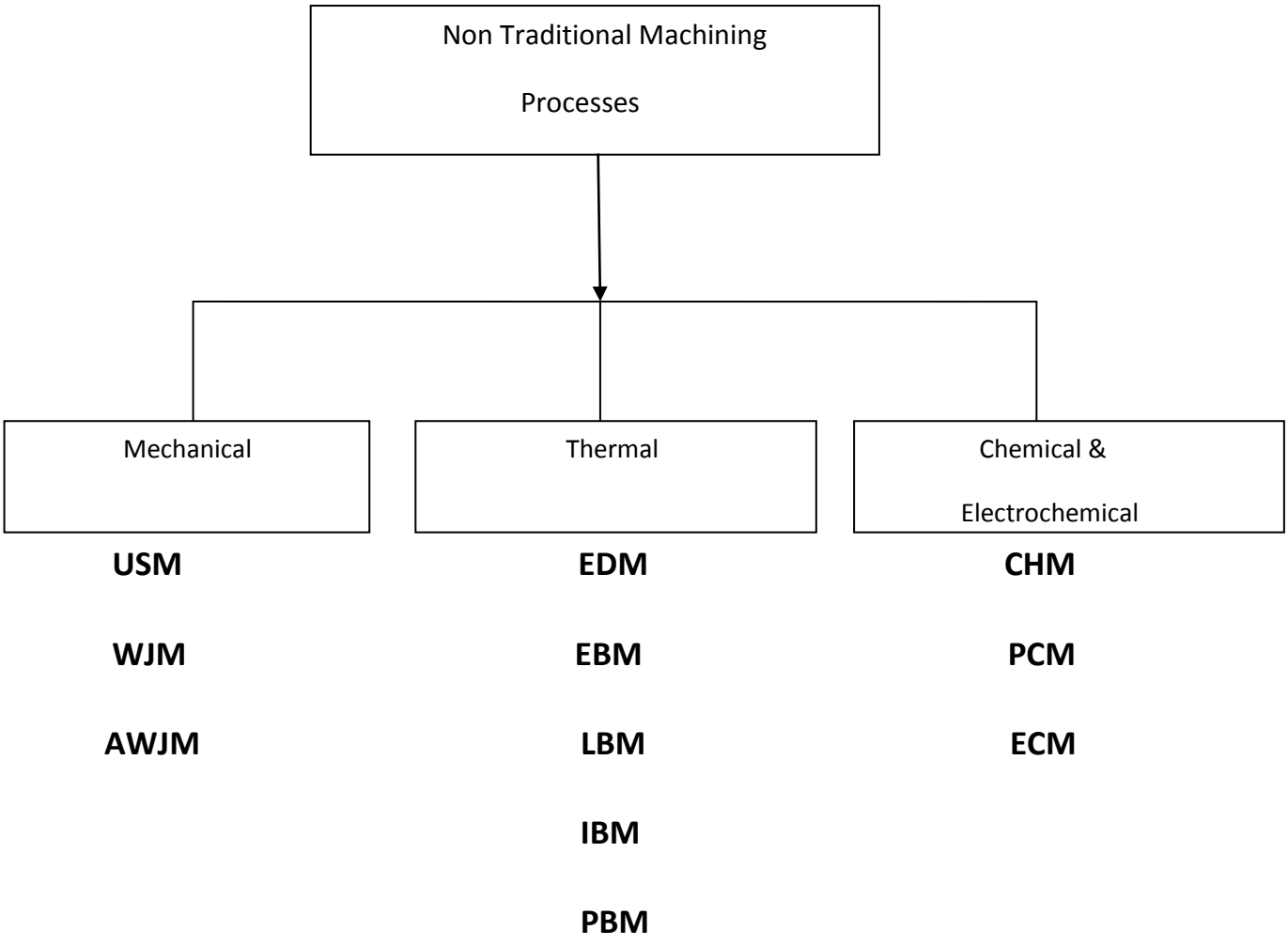

Figure 1.1 Classification of Non Traditional Machining Process [34]

- **Mechanical Energy (Mechanical Process) :** in mechanical processes, metal removal takes place either by a mechanism of simple shear or by erosion mechanism where high velocity particles are used as a transfer media and pneumatic/hydraulic pressure acts as source of energy. It includes ultrasonic machining, water jet machining and abrasive jet machining etc.
- **Thermal Energy (Thermal process):** thermal processes involve the application of very thin intense local heat. Here melting and vaporization from the small areas at the surface of the work piece removes material. The source of

energy used is amplified light, ionized material and high voltage. Examples are laser beam Machining, ion beam machining, plasma are machining, and electrical discharge machining.

- **Electrical Energy (Electro Chemical Processes):** Electrochemical processes involve removal of metal by mechanism of ion displacement. High current is required as the source of energy, and electrolyte acts as transfer media. It includes electro-chemical machining, electro chemical grinding etc.

- **Chemical Energy (Chemical Processes):** Chemical processes involve the application of resistant material (acidic or alkaline in nature) to certain portion of the work piece. The desired amount of material is removed from the remaining area of the work piece by subsequent application of an etching that converts the work piece material into a dissolve metallic salt. It includes chemical machining and photochemical machining.

1.2 Ultrasonic Machining

Ultrasonic Machining (USM) is a non-conventional mechanical material removal process used for machining both electrically conductive and non-metallic materials; preferably those with low ductility and a hardness above 40 HRC such as inorganic glasses, ceramics, quartz etc. The process came into existence in 1945 when L. Balamuth was granted the first patent for the process. USM has been variously termed ultrasonic drilling; ultrasonic cutting; ultrasonic abrasive machining and slurry drilling.

In USM, process operates at ultrasonic frequencies and typical frequencies used in the ultrasonic machining process range between 20 and 40 KHz. The equipment used is based upon a generator energizing a transducer which in turn causes an attached tool to vibrate. The power ratings range from 50 to 3000 W and a controlled static load is applied to the tool to provide feed in the longitudinal direction. Abrasive slurry, which is a mixture of abrasive material such as silicon carbide, boron carbide or alumina suspended in water or some suitable carrier medium is continuously pumped across the gap between the tool and work (25–60 μm). The vibration of the tool causes the abrasive particles held in the slurry to impact the work surface leading to material

removal by micro-chipping. The vibrating tool transfer energy to abrasive particles carried, within a slurry, underneath the tool tip. The interaction between these particles and the work piece result in the formation of mirror image of tool tip in the surface of the work piece.

USM is generally associated with low material removal rates, however its application is not limited by the electrical or thermal characteristics of the work material. Because the process is non-thermal and non-chemical, the materials processed are not altered either chemically or metallurgically. Holes as small as 76μm in diameter can be drilled, however the depth to diameter ratio is limited to 3:1. For efficient machining to take place, the tool and horn must be designed with consideration given to mass and shape so that resonance can be achieved within frequency range capability of the ultrasonic machine.

1.3 Need for ultrasonic machining

The process is regarded as competitive only when an operation cannot be practically and economically performed on conventional machining equipment. Ultimate value of USM lies in the ability to do work that cannot be practically accomplished in any other way because USM is non-chemical and non-thermal. Materials are not altered either chemically or metallurgically during ultrasonic machining. As Glass is a material difficult to machine by any means but good result have been obtained as a result of ultrasonic machining.

1.4 Historical background of Ultrasonic Machining (USM)

The history of ultrasonic machining (USM) began with a paper by R.W. Wood and A.L Loomis in 1927 and the first patent was granted to L. Balamuth in 1945. The use of ultrasonic in machining was first proposed by J.O. Farrer in 1945. Farrer was the patent agent on the first issued patent, British patent no.602801 (1945), issued to an American engineer, L. Balamuth, who discovered ultrasonic machining accidentally in 1942, while he was investigating the dispersion of solid in liquid by means of a magnetostrictively vibrating nickel tube. The United States patent, for the process, no.2580716 was issued in 1962.In 1960's Rozenberg's crediting to Farrer is an exquisite example of the unfortunate high frequency of "noise" when scientific information crosses language barriers.

The first report on the equipment and technology appeared during 1951-52 by 1954, the machine tools, using the ultrasonic principle, had been designed and constructed. Originally USM used to be a finishing operation for the component processed by the electro spark machines. However, this use becomes less important because of the development in electric discharge machining. But thenwith the boom in solid state electronics, the machining of electrically nonconducting, semi conductive, and brittle material become more and more important and, for this reason, ultrasonic machining again gained importance and prominence. In recent years, various types of ultrasonic machine tool have been developed. The USM technique is still far from perfect.

1.5 Principle of Ultrasonic Machining

It is the removal of material by the abrading action of grit-loaded liquid slurry circulating between the work piece and a tool vibrating perpendicular to the work face at high frequency and an amplitude in the order of 0.01mm to 0.06 mm. Ultrasonic machining, also known as Ultrasonic Impact Grinding, is a machining operation in which an abrasive slurry freely flows between the work piece and a vibrating tool. The tool is pressed against the work surface under a load of few kilograms and fed downwards continuously as the cavity is cut in the work. Fig 1.2 shows USM process principle. The tool never contacts the work piece and as a result the grinding pressure is rarely more, which makes this operation perfect for machining extremely hard and brittle materials, such as glass, ruby, diamond and ceramics.

The working process of an ultrasonic machine is performed when its tool interacts with the work piece or the medium to be treated. The tool is subjected to vibration in a specific direction, frequency and intensity. The vibration is produced by a transducer and is transmitted to the tool using a vibration system, often with a change in direction and amplitude. The work piece is placed under the face of the tool which is subjected to high frequency vibration perpendicular to the surface being machined. Abrasive slurry is conveyed to the working zone between the face of the tool and the surface being machined. The tool moves towards the workpiece and is subjected to a static driving force. Repetitive impact of the tool on the grains of the abrasive material, falling from the slurry onto the surface to be treated, lead to the fracture of the workpiece material and to the creation of a cavity with the shape mirror formed of the tool. The abrasive

particles are propelled or hammered against the workpiece by the transmitted vibrations of the tool. The particles then microscopically erode or "chip away'' at the workpiece.

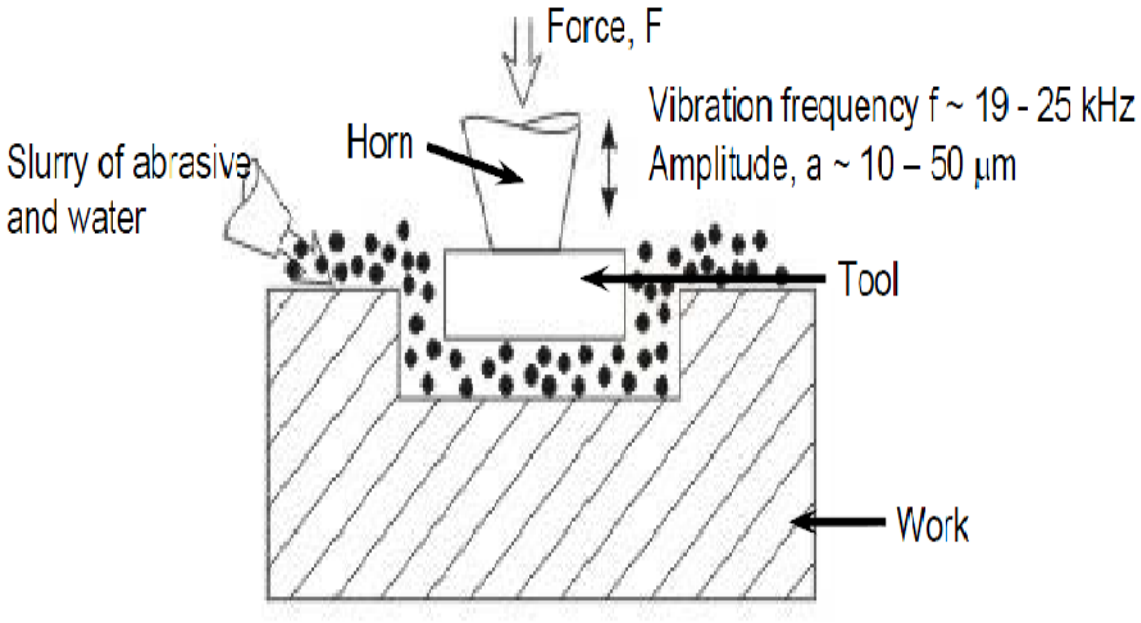

Figure. 1.2 USM process principle [33]

The USM equipment consist of an oscillator (high frequency current generator) that converts the 50Hz (c/s) power supply into high frequency (15 KHz to 30 KHz) power which in turn is converted into mechanical oscillations with the help of a magnetostrictive or piezo-electric transducer of the two type, the piezo-electric transducer are most efficient, i.e. they involve less loss of power and hence do not require cooling. The magnetiostrictive transducers generally found in old machines are less efficient due to high eddy current losses and hence may require cooling. The power rating of modern machines varies from 0.04 to 4 KW.

1.6 Elements of Ultrasonic Machining Process

The machining for USM ranges from small, table top sized units to large - capacity machine tools. In addition to part size capacity of USM machine, suitability for a particular application is also determined by the power rating. The power of USM machine is rated in watts and can range from 40 W to 2400 W. the material removal rate is directly related to the power capability of USM machine. The entire USM

machine share common subsystem regardless of the physical size or power. The ultrasonic machine process consists of the following basic element.

1.6.1 The ultrasonic power supply and transducer.

1.6.2 The tool holder

1.6.3 The tool

1.6.4 The abrasive slurry

1.6.5 The work-piece

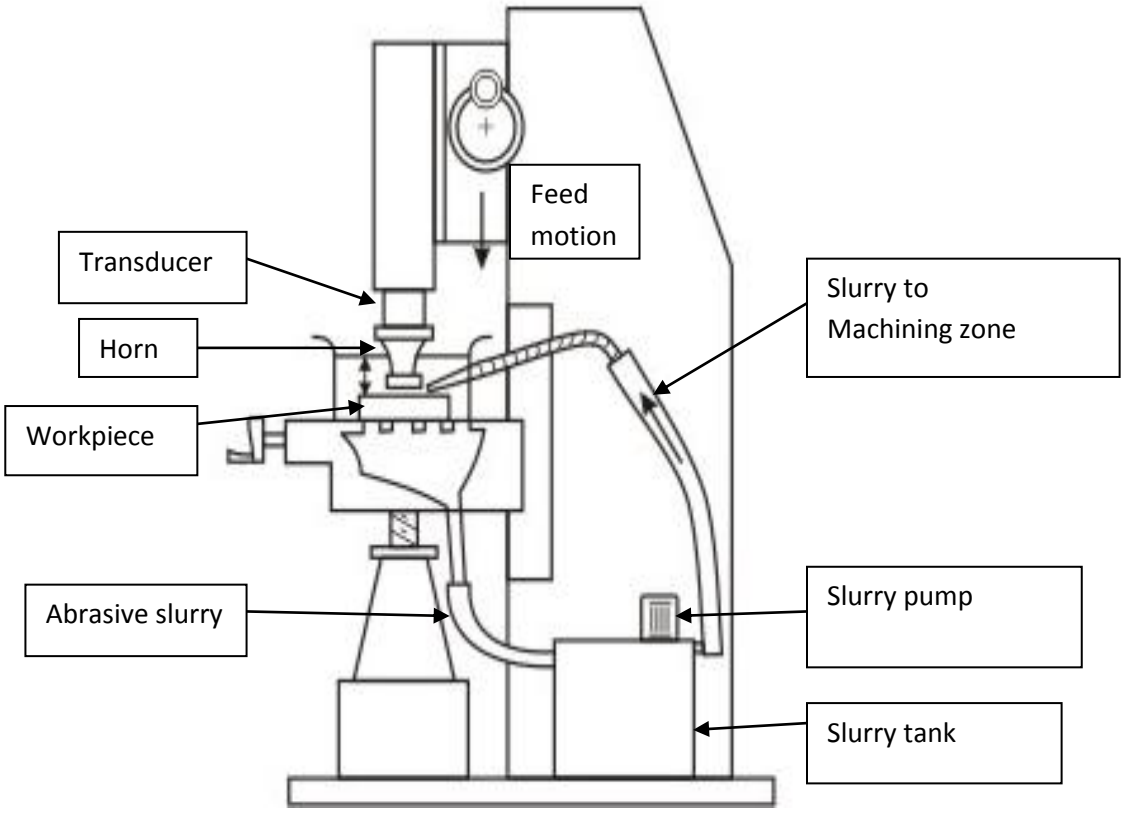

Figure. 1.3 Basic Elements of USM [33]

1.6.1 The ultrasonic power supply and transducer

The solid state variable output power supply with internal and external power control converts (50-60) Hz electrical power into 20,000 electrical power. This electrical signal is then supplied to the transducer for conversion into mechanical motion. The power

supply for an ultrasonic machine tool is more accurately characterized as a high power sine wave generator that offers the user control over both the frequency and power of generated signal.

The transducer is a device that converts energy from one form into another. In the case of transducer for USM, electrical energy is converted to mechanical motion. The two types of transducers used for ultrasonic machining are based on two different principles of operations:

1.6.1.1 Piezoelectric Transducer

These are used for USM to generate mechanical motion through the piezoelectric effect by which certain materials, such as quartz or lead will generate a small electric current when compressed. Conversely, when an electric current is applied to one of these material, the material increases minutely in size. When the current is removed, the material intently returns to its original shape. Piezoelectric transducer, by nature, exhibit an extremely high electro-mechanical conversion efficiency (up to 96%), which eliminates the need for water cooling of transducer. These transducers are available with power capabilities upto 900W.

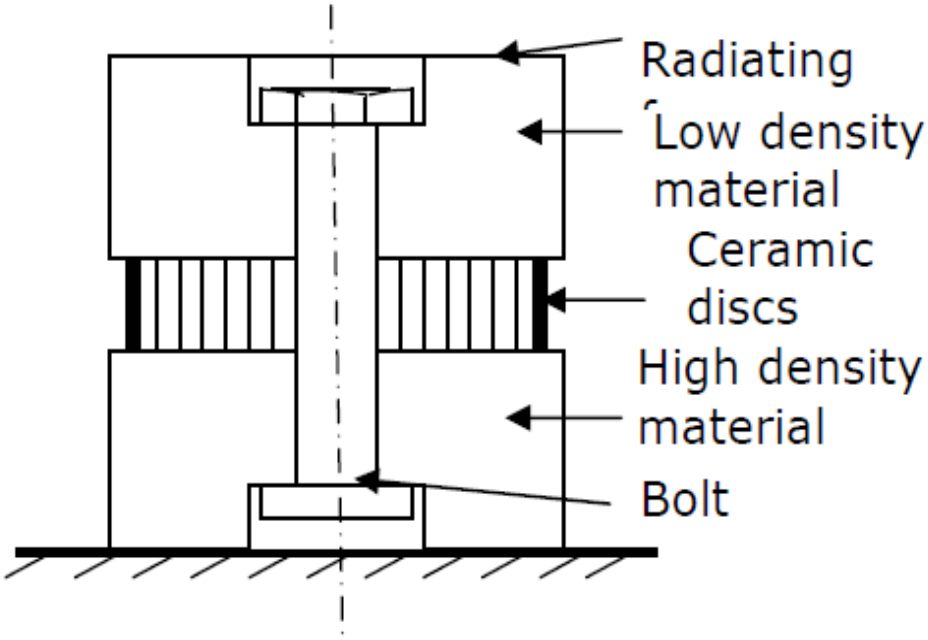

Figure 1.4 Piezoelectric ultrasonic transducer [50]

1.6.1.2 Magnetostrictive Transducer

These are usually constructed from a laminated stock of nickel or nickel alloy sheets which, when influenced by a strong magnetic field, will change length. Magnetostrictive transducers are rugged but have electro-mechanical conversion

efficiencies ranging from 20 to 30%. The lower efficiency results in the need to water cool magnetostrictive devices to remove the waste heat. Magnetostrictive transducers are available with power capabilities up to 2400W.The magnitude of the length change that can be achieved by both piezoelectric and magnetostrictive transducer is limited by the strength of transducer material. In both types of transducer the limit is approximately 0.025mm (0.01 in).

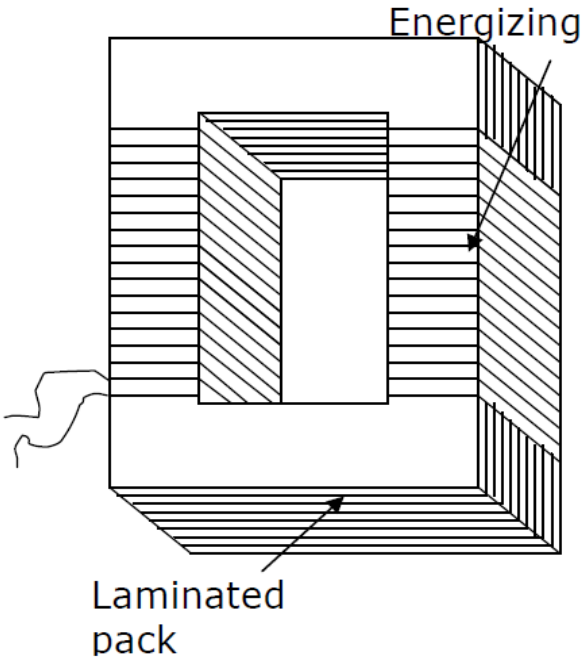

Figure 1.5 Magnetostrictive ultrasonic transducer [50]

1.6.2 The Tool Holder

The tool holder transfers the vibrations to the tool end and therefore, it must have adequate fatigue strength. Tool holder is removable part which is fastened to the concentrator and is made of mainly stainless steel. Generally, the shape of the tool holder is cylindrical or conical or a modified cone with the centre of mass of the tool on the centre line of the tool holder. It should be free from nicks, scratches and tool marks to reduce fatigue failures caused by the repeated reversal of stresses. In some ultrasonic machines, the trunk (horn) acts itself as a concentrator as well as the tool holder.

The horn or concentrator is a wave-guide, which amplifies and concentrates the vibration to the tool from the transducer. The three types of horns are shown in

fig.(1.7).The horn or concentrator can be of different shapes like Tapered or conical, Exponential and Stepped. Machining of tapered or stepped horn is much easier as compared to the exponential horn.

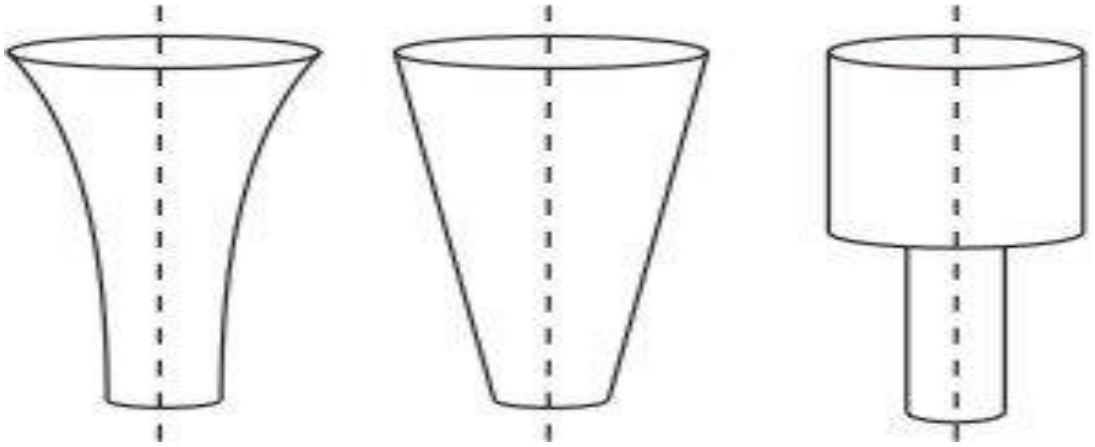

Figure.1.6 Different Horns used in USM [33]

1.6.3 The Tool

The tool should be so designed to provide the maximum amplitude of vibration at the free end at a given frequency. The material used should have high wear resistance, good fatigue strength and optimum values of hardness and toughness. For minimum tool wear, tools should be constructed from relatively ductile materials such as stainless steel, brass and mild steel. The harder the tool material the faster its wear rate will be. Depending on the abrasive used, work piece / tool wear ratios can range from 1:1 to 100:1

Tools can be joined to the horn either by soldering or brazing,screw fitting.Alternatively,the actual tool cofiguration can be machined to the end of the horn.Threaded joints have also been used conventionally to achieve the ease of tool changing,however problems such as self-loosening, loss of acoustic power and fatigue failure have been reported for such tools.

1.6.4 The Abrasive Slurry

Several abrasives are available in various sizes for ultrasonic machining (grit). The criteria for selection of an abrasive for a particular application include hardness, usable life, cost and particle size. In order of hardness, boron carbide, silicon carbide and

aluminium oxide are the most commonly used abrasives. The abrasive used for an application should be harder than the material being machined; otherwise the usable life time of the abrasive will be substantially shortened. Boron carbide is selected when machining the hardest work piece materials or when the highest material removal rates are desired. Although the cost is five to ten times greater than the next hardest abrasive, silicon carbide, the usable life of boron carbide is 200 machine operating hours before cutting effectiveness is lost and disposal is necessary. This compares with a usuable life time of approximately 60 hours for silicon carbide. The combination of high removal rates and extended life time justify the higher cost of boron carbide.

The size of the abrasive particles influences the removal rate and surface finish obtained. Abrasive for USM are generally avaliable in grit sizes ranging from 240 to 800 whilt the coarser grit exhibit the highest removal rates, they also result in the roughest surface finish and are therefore, used only for roughing operation, conversely , 800 grit abrasives will result in fine surface finishes but at a drastic reduction in material removal rate. The most popular general purpose abrasive used, based on the above considerations, is 320 boron carbide. The abrasive material is mixed with water to form the slurry. The most common abrasive concentration is 50% by weight. However this can vary from 30 to 60 percent. The thinner mixtures are used to promote efficient flow when drilling deep holes or when forming complex cavities. Table (1.1) shows the different types of abrasive used in USM with knoop hardness and relative cutting power.

Table 1.1.Abrasives used in USM

Abrasive	Knoop Hardness	Relative cutting power
Diamond	6500-7000	1
Cubic Boron Nitride	4700	.95
Boron Carbide (B4C)	2800	0.50-0.60
Silicon Carbide (SiC)	2480-2500	0.25-0.45
Alumina (Al2o3)	1850-1920	0.14-0.18

Once the abrasive has been selected and mixed with water, it is stored in a reservoir at the USM machine and pumped to the tool work piece interface by recirculating pumps

at rates up to 26.5 lit/min. Higher power ultrasonic machine require the addition of a light-duty cooling system to remove waste heat from the abrasive slurry.

1.6.5 Work-piece

There is no limitation to the range of material that can be machined by USM process, expect that they should not dissolve in the slurry media or react with it. While USM can be applied to ductile materials such as soft steel, copper, and brass but it is best suited to machining operation on hard, brittle materials that are not practical to process by other method. In general, USM is not recommended on the work materials which are softer than Rockwell Hardness Number HRC 45. Ultrasonic machining can be used for metals and non-metals, electrical conductors or non-conductor. The ultrasonic drilling technique is especially suited for hard materials like tungsten carbide, titanium carbide, ceramic and diamond. Materials which exhibit high hardness and which have impact brittleness can be successfully machined by this technique such materials are germanium, ferrites, glass and quartz.

1.7 Process Parameters of Ultrasonic Machining

The ultrasonic vibration machining method is an efficient cutting technique for difficult-to-machine materials. It is found that the USM mechanism is influenced by these important parameters.

Frequency of tool oscillation – greater than 20 kHz

Type of abrasive – Boron carbide, aluminium oxide and silicon carbide

Grain size or grit size of the abrasives -200-800

Depth to diameter ratio of holes – 31

Power – 50-3000 W

Workpiece material – electrically conductive and non-metallic workpiece

1.8 Organization of Thesis

Chapter 1 covers brief introduction to non-traditional machining, principle of Ultrasonic Machining, explanation of USM and its various process parameters.

Chapter 2 presents an avaliable literature on USM process. The avaliable literature has been categorized in different categories according to their applications. Summary of literature and gap in literature is also discussed.

Chapter 3 presents the methodology in brief which is being adopted. The detailed explanation of Taguchi and ANOVA is given. Objective and work plan is also discussed. The details of the machine used and workpiece used are also explained.

Chapter 4 presents the analysis and results of MRR. Results after the Analysis of Variance (ANOVA) and Taguchi Signal-to-Noise ratio are outlined in this chapter. Main effect plot and interaction plots for MRR are discussed in this chapter. Optimal design conditions have been discussed.

Chapter 5 presents the analysis and results of TWR. Results after the Analysis of Variance (ANOVA) and Taguchi Signal-to-Noise ratio are outlined in this chapter. .Main effect plot and interaction plots for TWR are discussed in this chapter. Optimal design conditions have been discussed.

Chapter 6 presents the analysis and results of SR. Results after the Analysis of Variance (ANOVA) and Taguchi Signal-to-Noise ratio are outlined in this chapter. .Main effect plot and interaction plots for SR are discussed in this chapter. Optimal design conditions have been discussed.

Chapter 7 presents the analysis and results of Rockwell Hardness. Results after the Analysis of Variance (ANOVA) and Taguchi Signal-to-Noise ratio are outlined in this chapter. .Main effect plot and interaction plots for Hardness are discussed in this chapter. Optimal design conditions have been discussed.

Chapter 8 presents the analysis of Ovality of the machined surface.

Chapter 9 presents the analysis of surface morphology which is used to understand the microstructure on the surface of workpiece material.

Chapter 10 presents the analysis of Al/Si composite and Al/Cu alloy of different composition by XRD.

Chapter 11 presents the results, conclusions and recommendation from the experimental work.

CHAPTER 2
LITERATURE REVIEW

This chapter gives an extensive review of literature upon various fields related to USM and its effects on material removal rate and tool wear rate along with hardness, surface roughness of the machined surface. The literature available on USM is given below.

2.1 Material removal mechanism

Kumar et al. [24] explored the use of Ultrasonic Machining, a non traditional machining process of pure titanium and evaluated material removal rate under controlled experimental conditions. A micro-model for prediction of material removal rate in ultrasonic machining of titanium using dimensional analysis was made. The surface finish obtained in USM of titanium was better than many other non-traditional machining processes. Optimum MRR in USM of titanium can be achieved by using a tool material of higher hardness along with a higher power rating, coarse grit size and a hard abrasive material. Also, power rating factor had emerged as most significant factor with followed by abrasive type and slurry grit size. Tool material factor can be termed as the least significant for MRR.

Singh and Khamba [39] applied Taguchi approach to model the material removal rate during ultrasonic machining of titanium and its alloys. Relationships between material removal rate and other controllable machining parameters such as power rating, tool type, slurry concentration, slurry type, slurry temperature and slurry size had been deduced by using Taguchi technique. The results suggested that Ultrasonic power rating significantly improved the material removal rate with contribution of 28%, followed by type of tool with contribution of 24.6%. The third significant factor was type of slurry with contribution of 13.3%.

Singh and Khamba [41] investigated Ultrasonic machining of titanium and its alloys. The material removal mechanisms involved and the effect of operating parameters on material removal rate, tool wear rate and work piece surface finish of titanium and its alloys were reviewed, for application in manufacturing industry.

Liu et al. [29] developed a physics-based cutting force model for Rotary Ultrasonic Machining (RUM) of brittle materials. The model used to predict the influences of input variables on cutting force. These predicted influences are compared with those determined experimentally. The trends of predicted influences of input variables on cutting force agree well with the trends determined experimentally. The result showed that cutting force increases as abrasive concentration, semi-angle of abrasive particle and feed rate increased. And also it was decreased as abrasive size, vibration amplitude, and spindle speed were increased.

Kumar and Khamba [22] established a relation between the mode of material removal rate and the energy input rate corresponding to the different process conditions. The results showed that the material removal in USM of titanium could be directly related to the energy input rate for the particular process settings used for machining. The higher level of input energy rate promoted the brittle fracture or cleavage of the work surface. For extremely small values of energy input purely ductile failure mode was observed. Also, minor fluctuations in the process variables such as slurry concentration caused significant alteration in the results. Hence, it was very important to maintain the fixed parameters as constant with the highest possible accuracy.

Chang and Bone [6] had given a novel analytical burr height model to predict the exit burr height in Vibration Assisted Drilling (VAD) of aluminium 6061-T6. He studied the effect of ultrasonic assistance on burr size, chip formation, thrust forces and tool wear and demonstrated that under suitable ultrasonic vibration conditions, the burr height and width reduced in comparison to conventional drilling. He concluded that the proposed model improved the accuracy of existing burr height model for conventional drilling by up to 36%, and also predicted the burr height for VAD within a 10% deviation from the men values of the experimental results.

Kumar and Khamba [23] used Stellite 6, a cobalt alloy and outlined the effectiveness of the ultrasonic machining in terms of tool wear rate of the tool used and the material removal rate of work piece produced. The optimum combination of various input factors as type of abrasive slurry, their size and concentration, nature of tool material

and power rating of the machine for the ductile chip formation had been determined by applying the Taguchi multi-objective optimization technique and F-test. He concluded that the optimum parameter values in the present operating conditions found are tool material followed by abrasive slurry and slurry concentration. The percentage contribution of factors in descending order for MRR was power rating, abrasive grit size tool material, abrasive slurry and slurry concentration.

Liao et al. [28] retrofitted tool holder of a machining center so as to provide axial resonant vibration. Experimental results showed that the chip size was reduced and proportion of segmented chips was increased. The thrust force in drilling was reduced. There was less variation of the torque and the usable life of the drill was prolonged. It was also found that the function of peck drilling can be replaced by the ultrasonic vibration assisted conventional drilling. The application of ultrasonic vibration in drilling prolonged tool life and hence fewer tools were needed.

Khoo et al. [20] concluded that the material removal rate increased due to applied static load, ultrasonic power, amplitude of tool vibration, rotational speed and grain size. The surface roughness or hole clearance tends to increase with the increase of vibration amplitude and abrasive grit size but decreased with high applied static load. He found that wear occured on both the end face and lateral face of the tool in RUM of advanced ceramics.

Ichida et al. [17] proposed a new Non-contact Ultrasonic Abrasive Machining (NUAM) method, that was performed using loose abrasives excited by ultrasonic energy in a liquid, and discussed its suitability for application to ultra-precision machining. He found that in order to apply the NUAM to the ultra-precision machining, it was necessary to conduct the removal processing in small-scale mode. It was conducted by the abrasive grains, excited by the ultrasonic energy only by inhibiting the generation of cavitation.

Wiercigroch et al. [46] postulate the main mechanism of the enhancement of material removal rate in ultrasonic machining with high amplitudes forces generated by impacts. This acted on the workpiece and helped to develop micro-cracking in the cutting zone. He modeled inherent non-linearity of the discontinous impact process model to

generate the pattern of the impact forces and explained the experimentally observed fall in MRR at higher static forces.

Babitsky [4] designed a prototype of an ultrasonic drilling system and improvements of machining characteristics of ultrasonic vibration were demonstrated. He studied vibration excitation and energy transfer during ultrasonically assisted drilling and found the profound effect on their cutting performance when there was superimposition of longitudinal vibration at ultrasonic frequencies onto the normal rotary motion of drilling bits.

Thomas and Babitsky [43] employed a three-dimensional finite element drill bit to understand the drill bit's vibrational characteristic. The drill bit considered displayed strong vibration mode conversion characteristics during both experimentation and numerical simulation. Its amplitude frequency response curve was also extremely peaky, indicating instability when controlled using traditional frequency control methods.

Brehl and Dow [5] combined Vibration-Assisted Machining (VAM) with small amplitude tool vibration to improve the fabrication process. VAM had been applied to difficult applications such as diamond turning of ferrous and brittle materials. It created microstructures with complex geometries for products like molds and optical elements, hard alloys such as Inconel or Titanium. He found VAM offered distinct advantages over conventional precision machining methods over a broad range operating conditions. These conditions were depth of cut, part size, tool and work materials with reduced tool forces and surface roughness.

Simon and Garry [7] introduced a high frequency and low amplitude vibration model in the direction of drill feed during drilling. It had a potential to reduce thrust forces and reduce exit burr height. A novel analytical burr height model predicted the exit burr height in the vibration assisted drilling of aluminium 6061-T6. The presented model incorporated the hypothesis that only positive portion of the thrust force contributed to burr formation. It included elastic spring back of the workpiece material to provide more accurate prediction.

Lia et al. [27] developed a three dimensional Finite Element Analysis (FEA) model to study the effect of three parameters (cutting depth, support length, and pre-tightening load) on the maximum normal stress. Von Mises Stress criterion were used to predict the relation between edge chipping thickness and support length. He proposed a possible solution to reduce the edge-chipping thickness by increasing the support length and the diameter of the blind hole in the fixture underneath the workpiece should be as small as possible.

Zhang et al. [49] proposed an effective micromachining technique for hard brittle materials. He introduced several innovative strategies such as rotated tool, machine tool preparation, and vibration-applied workpiece. Hole as small as 5 mm in diameter machined in quartz glass and silicon. Complex structures like spiral trenches had also been claimed true by the use of path-controlled scanning mode.

Wei et al. [45] proposed Ultrasonic Lapping and compared with conventional lapping in material removal process. He showed that material removal rate of ultrasonic lapping was nearly three times than that of the conventional lapping under the same condition. The ultrasonic lapping can produce a better tooth surface quality. The results of this set of experiments revealed that the optimum conditions for a high removal rate in the ultrasonic lapping experiment of spiral-bevel gears had a braking torque of 0.12 Nm, pinion rotational speed of 600 rpm and slurry concentration of 20%. The contributions by percentage of torque, speed and concentration to the removal rate was 8.13, 19.26 and 68.11, respectively.

2.2 Process Parameters

2.2.1 Abrasive Slurry Properties

Singh and Khamba [40] used stainless steel, titanium and high-speed steel as the tool and silicon carbide, boron carbide and alumina as abrasive slurry. The results suggested that with boron carbide slurry and stainless steel tool best material removal rate was obtained. Also relative hardness of tool-work piece affects the material removal rate in ultrasonic machining.

Ramulu et al. [36] reported that use of boron carbide abrasive resulted in material removal rate which was approximately 75% higher than the silicon carbide abrasive for the 400 grit size and 320% higher for 220 grit size while machining silicon carbide ceramics. The effect of slurry hardness on MRR had been found to be dependent on the other experimental conditions such as work material properties, tool properties, amplitude of vibration and static load; which could be regarded as the reason for a wide reason for a wide inconsistency of the results reported in the literature available on USM.

Choi et al. [8] explored the use of Chemical-Assisted Ultrasonic Machining for machining of glass. To obtain the chemical effects, a low concentration hydrofluoric acid solution was added to the slurry. The hybrid method was found to be superior in terms of material removal rate and integrity of the machined surface. The surface roughness was improved and the machining load was decreased significantly as compared to the conventional USM method.

Guzzo et al.[14] reported a substantial increase in MRR obtained by using abrasive of larger grain size on account of the increase in the stress caused by the impact of abrasive particle over the workpiece surface.

2.2.2 Work Piece Properties

Kumar [19] highlighted machining of brittle and fragile material under controlled experimental conditions and focused on parametric optimization of ultrasonic machining of pure titanium metal with TWR as response and validation of optimized value of TWR by conducting confirmatory experiments.

Hsu et al. [16] investigated the machining characteristics of Inconel 718, Nickel-base super alloy, by combining ultrasonic vibration with high-temperature-aided cutting. The influence of various machining parameters such as cutting speed, feed rate, working temperature and ultrasonic power on the machining characteristics are clarified. The percentage contributions in descending order was cutting tool, feed rate, working temperature and depth of cut for surface roughness and cutting force.

Pujana et al.[35] applied ultrasonic vibrations for drilling of Ti6Al4V workpiece samples. Several parameters of ultrasonic-assisted drilling such as feed force, chip formation by means of high-speed imaging and temperature measurement on the drill tip by means of infrared radiation thermometry were monitored. He found ultrasonic assistance offered lower feed force and higher process temperatures as compared to conventional drilling. Also concluded higher force reductions and higher temperature increments when vibration amplitude was increased.

Jadoun et al.[18] studied the effect of process parameters on production accuracy obtained through ultrasonic drilling of holes in alumina based ceramics using silicon carbide abrasive and production accuracy in ultrasonic drilling involving both dimensional accuracy (hole oversize) and form accuracy (out of roundness and conicity).The parameters considered were workpiece material, tool material, grit size of abrasive, power rating and slurry concentration. He found when hole-oversize was marginally increased, there was increase in alumina content in the work piece. Out- of-roundness decreased with increase in alumina content in the work piece. Conicity increased with the increase in alumina content in the work piece and increases almost linearly as the grain size increases.

Li et al. [30] introduced rotary ultrasonic machining (RUM) into drilling Ceramic Matrix Composites (CMC) materials and compared cutting forces and material removal rates (MRR) for machining of CMC with and without ultrasonic vibration. He found that high-quality holes on CMC panels can be achieved by RUM with proper machining parameters and feed rate had the most significant effects on cutting force. Spindle speed, feed rate and ultrasonic power had significant effects on MRR. Spindle speed and feed rate as well as their interaction had significant effects on hole quality.

Li et al. [31] studied the effects of three parameters (cutting depth, support length, and pre tightening load) on the maximum normal stress and Von Mises Stress in the region where the edge chipping initiates. Two failure criteria (the maximum normal stress criterion and Von Mises Stress Criterion) were used to predict the relation between the edge chipping thickness and the support length. Furthermore, a solution to reduce the edge chipping was proposed based upon the FEA simulations and verified by experiments.

Jianxin and Tiachiu [10] investigated the effect of properties and microstructure of work materials on the MRR in USM of alumina-based ceramic composites. MRR was reported to be low while machining composites of higher fracture toughness such as whisker-reinforced composites. The particle reinforced composites yielded higher values of MRR on account of their low fracture toughness. The composites of higher flexural strength demonstrated better surface integrity while machining with USM.

Majeed et al. [32] outlined the machining of Al2O3/LaPO4 composites using static increase in the hardness of the composite. Results showed that an LaPO4 improved the machining rate up to a critical limit after which it tends to stabilize. The use of hollow tools was also reported to improve the MRR obtained.

Gao et al. [13] designed ultrasonic grinding vibration device and created the theoretical models of surface roughness for ultrasonic vibration grinding. He studied on ultrasonic grinding of nano-zirconia ceramics and found critical ductile depth of cut was larger than that in common grinding and than that of traditional ZrO2 engineering ceramics.

Guzzo et al. [15] investigated potential of ultrasonic machining as a tool to produce seed crystals for hydrothermal growth of synthetic quartz with required surface finish and unconventional geometries observed that the density of dislocations, nucleated at the early stage of the growth period, increases with increasing roughness of the seed-crystal surface. Cutting rate and the surface roughness were dependent on the abrasive grit size. USM process can be adopted in the production of seed crystals with unconventional geometries to obtain synthetic quartz of good crystalline perfection.

Tawakoli and Azarhoushang [42] investigated on dry machining in order to decrease the negative environmental impact of the cutting fluids, diminishing problems concerning waste disposal demand. He found problems frequently occur in terms of high heat generation on grinding wheel surface, increasing the grinding energy ,wear of grinding wheel, low material removal rate and poor surface roughness, so to eliminate these problem application of ultrasonic vibration was done .The obtained result showed that the application of ultrasonic vibration eliminated the thermal damage on the work piece and a decrease of up to 60-70% of normal grinding forces and up to 30-50% of tangential grinding forces had achieved.

Wiercigroch et al. [47] showed that an introduction of high-frequency axial vibration which significantly enhances drilling rates compared to the traditional rotary type method. He found that a light static load causes the tool to be bounced off from the work piece, with only intermittent and small impact forces. When the static force was too large, the percussive effect disappears and the work piece was exposed to a static force decreasing drastically the drilling efficiency.

2.2.3 Tool characteristics

Azarhoushang et al. [3] presented the design of an ultrasonically vibrated tool holder and the experimental investigation of ultrasonically assisted drilling of Inconel 738-LC, The circularity, cylindricity, surface roughness and hole oversize of the ultrasonically and conventionally drilled work pieces were measured and compared. The obtained results showed that the application of ultrasonic vibration can improve the hole quality considerably, improvements of up to 60% had been achieved.

Adithan [1] had reported that stainless steel tools exhibit low tool wear as compared to tungsten carbide or mild steel tools. This was due to high resistance to cavitation erosion of stainless steel. In USM, hardness of the tool increases by work hardening, therefore the penetration of the abrasive grains into the tool decreases resulting in higher MRR.

Ramu et al. [2] reported an optimum slurry concentration range (1:5:7) from tool wear aspect in USM of transformation toughened ceramics.

Komaraiah and Reddy [21] investigated the influence of tool material properties i.e hardness on the material removal rate in USM of glass. Results showed that the MRR increased with an increase in the hardness of the tool material. The different tool materials were arranged in the increasing order of superiority as mild steel < titanium < stainless steel < silver steel < niamonic-80 A < thoriated tungsten. The tool materials used were found to undergo a significantly different amount of work-hardening, which contributed to the variation in their machining performance.

Kumar et al. [24] compared the machining performance of high carbon steel and titanium alloys in USM of titanium. High carbon steel tool was found to experience

more tool wear as compared to titanium alloy tool because of its higher hardness, poor toughness and impact strength as compared to titanium alloy tool.

2.2.4 Surface Properties

Dam et al. [9] investigated the material removal rate in ultrasonic drilling of several different ceramic materials. Results showed that for tougher work materials, the MRR observed was quite low as compared to the hard and brittle materials. However, the surface quality obtained (in terms of finish) was found to be superior for tough materials.

Lee and Chan [26] measured the effects on the material removal rate and the surface roughness on the amplitude of the tool tip, the static load applied and the size of the abrasive. He concluded that any increase in power rating, the static load applied and the grit size of the abrasive will result in an increase in the material removal rate and a roughening of the machined surface.

Dvivedi and Kumar [11] investigated ultrasonic drilling of commercially pure titanium and titanium alloy. Process parameters such as work piece, grit size, slurry concentration, power rating and tools were changed to explore their effect on the surface roughness. Average surface roughness was measured by using the Optical Profiling System. Two dimensional and three-dimensional contour plots were obtained from the profiling system to quantify and visualize the surface roughness. It was concluded that the effect of slurry concentration and grit size had a significant effect on surface roughness more than other parameters..

Shen et al. [37] investigated the effects of assisted ultrasonic vibration on the surface roughness of machined surfaces in micro-end-milling. He found ultrasonic vibration had a negative effect on the surface roughness of slot bottom surface in the ultrasonic vibration-assisted milling experiment and analyzed that ultrasonic vibration makes a brilliant contribution to the improvement of the surface roughness of vertical side wall surface of slot.

Wang et al. [44] investigated surface roughness using Rotary Ultrasonic Machining of Potassium Di hydrogen Phosphate (KDP) crystal. He investigated the influence of three process variables (spindle speed, ultrasonic power and federate) and tool design on

surface roughness in RUM of KDP. He found that the surface roughness obtained when using a tool with a chamfered corner was lower than that obtained using tools with right angle corners. Smaller diamond grains tended to produce smoother surface and within the tested range from (20% to 40%).

2.3 Summary of Literature Review

A lot of work has been done different work material, abrasive slurry, slurry concentration and grit size. Various investigators (8,36,40) have reported results indicating that the rate of material removal for a certain abrasive is a function of its concentration, grain size and hardness besides the feed system. On increasing the abrasive grit size or slurry concentration, an optimum value of MRR is reached. Investigations found that reported a substantial increase in MRR obtained while using abrasive larger grain size on account of the increase in the stress caused by the impact of abrasive particle over the workpiece surface[14]. Use of boron carbide abrasive resulted in material removal rates which were approximately 75% higher than the silicon carbide abrasive for the 400 grit size and 320% higher for 220 grit size while machining silicon carbide ceramics [36]. The effect of slurry hardness on MRR has been found to be dependent on the other experimental conditions such as work material properties, tool properties, amplitude of vibration and static load.

Investigators [1,2,3,24,48] investigated the influence of tool material properties i.e. hardness on the material removal rate in USM of glass. Results showed that the MRR increased in the increasing of superiority as mild steel < titanium < stainless steel < silver steel < niamonic-80 A < thoriated tungsten. The tool materials used were found to undergo a significantly different amount of work hardening which contributed to the variation in their machining performance [3].

Investigators [11,37,44] found materials which observed higher MRR were also reported to have higher surface roughness values. Work piece materials with higher ratio of hardness to elastic modulus involve inferior surface quality. Dam et al [9] concluded that the work materials can be graduated according to their respective machining rates, so that the most productive materials give the greatest surface

roughness and vice versa. Therefore, higher productivity is not obtained without cost as the surface roughness increases.

Results showed power [22,23,24,39,41] primarily determines the mass of the tool horn assembly that can be utilized for an application and the frontal cutting area of the tool can be supported. Linear increase in MRR while increasing the amplitude of vibration provided all other factors such as frequency of vibration and abrasive grit size are kept constant. The linear trend of MRR while increasing the amplitude has been found to be more prevalent when high impact strength materials are machined or fine abrasive powders are used for machining. MRR decreases owing to a reduction in the size of abrasive grains reaching the cutting interface [14,36].

Investigators [10,16,18,19,31] found work piece materials machined in this investigation were glass, ferrite, porcelain, alumina and tungsten carbide. MRR was reported to decrease with an increase in work material hardness and fracture toughness in almost linear fashion under controlled experimental conditions. The particle reinforced composites yielded higher values of MRR on account of their low fracture toughness. The composites of higher flexural strength demonstrated better surface integrity while machining with USM.

2.4 Gaps in Literature

It was concluded from the literature review that a limited study has been done on machining of metal matrix composite of Al/Si and Al/Cu alloy. As Ultrasonic Machining enhances the MRR and Surface roughness with Al/Si and Al/Cu as a workpiece, so there is need to work on metal matrix composite and alloy to find the advantage using USM through various input parameters.

2.5 Objective of the Present Work

The objective of the present work has been discussed below:

1) To study the effect of various input parameters like Power rating of the machine, type of abrasive slurry, Slurry Concentration, type of Tool, Workpiece and Grit size of abrasive.

2) The experimentation work will be planned by applying DOE (Design of Experiments) approach.
3) Analysis of results obtained from the experimentation work will be done using the Statistical Techniques such as ANOVA (Analysis of Variance).
4) The optimization and verification of results will be done. Also the modeling of results will be done by applying the Regression Analysis.
5) The machined samples will be studied to find surface morphology.

CHAPTER 3

EXPERIMENTATION AND DESIGN OF STUDY

3.1 Design Factors Selection

3.1.1 Process parameters selection

Various input process parameters can be varied in the USM process, each having its own impact on output parameters such as Material Removal Rate (MRR), Tool Wear Rate (TWR) and Surface Roughness (Ra). The input parameters that are varied:

1. Power Rating of the machine
2. Type of abrasive slurry
3. Concentration of abrasive slurry
4. Abrasive Grit Size
5. Tool Material
6. Work piece

3.1.2 Response variable selection

The response variables selected in this study were MRR, TWR, Surface Roughness and Rockwell Hardness. These Variables are defined as:

Material Removal Rate (MRR) is defined as the weight of material eroded from workpiece surface per unit time. It is measured as:

$$\text{MRR } (mm^3/\text{min}) = \frac{weig\,ht\ difference\ \ of\ w/p(gm)}{Mac\,hining\ \ time\ \ (min.)\times density\ \ of\ material\ \ (\frac{gm}{mm^3})} \qquad \text{(Equation 3.1)}$$

Tool Wear Rate (TWR) is defined as the weight of material eroded from tool surface per unit time. It is measured as:

$$\text{TWR } (mm^3/\text{min.}) = \frac{weig\,ht\ difference\ \ of\ tool\ (gm)}{Mac\,hining\ \ time\ \ (min.)\times density\ \ of\ material\ \ (\frac{gm}{mm^3})} \qquad \text{(Equation 3.2)}$$

Surface Roughness (Ra) of the machined surface of work piece is expressed in microns. The characteristic of the layer of the work material just below the machined surface is evaluated. It is the arithmetic average roughness of the deviation of the roughness profile from the central line along the measurement.

$$\text{Surface Roughness (Ra)} = \frac{1}{L}\int_0^L |h(x)dx| \qquad \text{(Equation 3.3)}$$

Where, h(x) is the value of roughness profile & L is evaluation length

Rockwell Hardness determines the hardness by measuring the depth of penetration of an indenter under a large load compared to the penetration made by a preload. Rockwell scale is a hardness scale based on the indentation hardness of a material. There are different scales, denoted by a single letter, that use different loads or indenters. The result is a dimensionless number noted as HRB where B is the scale letter.

3.1.3 Experimental Design

As the objective of study aimed to carry out result on ultrasonic machining on Al/Si Composite and Al/Cu Alloy (as Work Material) different factor levels have been decided depending upon commercial availability, experimental constraints and machine tool capacity. Table 3.1 shows different control variables and their levels.

Table 3.1 Control Variables and their Levels.

S.No.	Factors	Levels	Level 1	Level 2	Level 3
1	Abrasive Slurry	2	Al_2O_3	SiC	
2	Tool Material	2	HSS	SS	
3	Work piece	2	Al/Si Composite	Al/Cu Alloy	
4	Abrasive Grit Size	3	280	400	Mixture
5	Slurry Concentration (%)	3	30	25	35
6	Power Rating	3	100	150	200

For conducting the experiments, it was decided to follow the Taguchi method of experimental design so that the effect of all the parameters could be studied with minimum possible number of experiments and an appropriate orthogonal array had to be selected after taking into consideration the above design variables and experiments were performed as per the set of experiments designed in the orthogonal array. Signal to Noise ratios were also calculated to analyze the Ultrasonic Machining more accurately.

The Taguchi Method apparently has the following strengths:

1. Consistency in experimental design and analysis.
2. Reduction of time and cost of experiments.
3. Robustness of performance without removing the noise factors.

The whole procedure of Taguchi method is as under.

1. Establishment of objective functions.
2. Selection of factors and/or interactions to be evaluated.
3. Identifications of uncontrollable factors and test conditions.
4. Selection of number of levels for the controllable and uncontrollable factors
5. Calculate total degree of freedom needed.
6. Select the appropriate Orthogonal Array (OA).
7. Assignment of factors and/or interactions to columns.
8. Execution of experiments according to trail conditions in the array.
9. Analyze results.
10. Confirmation experiments.

3.1.4 Selection of Orthogonal Array

For the selection of a particular orthogonal array, the number of parameters, the number of levels and their possible interactions must be taken into consideration. The case under study contains four parameters, three of two levels and three of three levels. Now as per requirements of the study L36 orthogonal array comes out as one of the solution. The L36 orthogonal array is taken in table 3.2.

Table 3.2 L36 Orthogonal Array

Experiment No.	Abrasive Slurry	Tool	Work piece	Abrasive Grit Size	Slurry Concentration	Power Rating
	A	B	C	D	E	F
1	1	1	1	1	1	1
2	1	1	1	2	2	2
3	1	1	1	3	3	3
4	1	1	1	1	1	1
5	1	1	1	2	2	2
6	1	1	1	3	3	3
7	1	1	2	1	1	2
8	1	1	2	2	2	3
9	1	1	2	3	3	1
10	1	2	1	1	1	3
11	1	2	1	2	2	1
12	1	2	1	3	3	2
13	1	2	2	1	2	3
14	1	2	2	2	3	1
15	1	2	2	3	1	2
16	1	2	2	1	2	3
17	1	2	2	2	3	1
18	1	2	2	3	1	2
19	2	1	2	1	2	1
20	2	1	2	2	3	2
21	2	1	2	3	1	3
22	2	1	2	1	2	2
23	2	1	2	2	3	3
24	2	1	2	3	1	1
25	2	1	1	1	3	2
26	2	1	1	2	2	3
27	2	1	1	3	1	1
28	2	2	2	1	3	2
29	2	2	2	2	2	3
30	2	2	2	3	1	1
31	2	2	1	1	3	3
32	2	2	1	2	2	1
33	2	2	1	3	1	2
34	2	2	1	1	3	1
35	2	2	1	2	2	2
36	2	2	1	3	1	3

3.1.5 Signal-to-noise ratio for Response Characteristics

The parameters that influence the output can be categorized into two classes, namely controllable (or design) factors and uncontrollable (or noise) factors. Controllable factors are those factors whose values can be set and easily adjusted by the designer. Uncontrollable factors are the sources of variation often associated with operational environment. The best settings of control factors as they influence the output parameters are determined through experiments.

Controllable factors are divided into three main types:

- Those which affect the average levels of the response of interest, referred to as Target Control Factors (TCF), sometimes called Signal Factors.
- Those which affect the variability in the response, the Variability Control Factors (VCF).

At the heart of Taguchi philosophy is the quality loss function. The loss function promotes efforts to continually reduce the variation in product s functional characteristics. The change in quality characteristic of a product under investigation in response to a factor introduced in the experimental design is the 'signal' of the desired effect. The effect of the external factors (uncontrollable factors) as the outcome of quality characteristic is termed as 'noise'. The objective of any experiment is to achieve the best possible S/N Ratio.

Finding a correct objective function to maximize in an engineering design problem is very important. Depending upon the type of response, the following three types of S/N ratios are employed in practice:

Lower-the-Better type problem:
For lower-the-better type problem, the quality characteristic is always continuous and non-negative. Its most desirable value is zero. As there is no adjustment factor in such type of problems, the thrust is simply on minimizing the quality loss without adjustment-that is, we should minimize *Q = k (mean square of the quality characteristic)*

$Q = k\left\{\frac{1}{n}\sum_1^n y_i^2\right\}$

Minimizing 'Q' is equivalent to maximizing 'η' defined by the following equation:

N= LB: S/N ratio = -10 $log_{10}\left\{\frac{1}{n}\sum_1^n y_i^2\right\}$ (Equation 3.4)

In this case the signal remains unchanged, to make the quality characteristic equal to zero. Therefore, the S/N ratio measures only the effect of noise.

Higher-the-better type problem: In this type of problem, the quality characteristic is again continuous and non-negative and it is to be made as large as possible. There is no

adjustment factor to be used in this case as well and one is interested in maximizing the objective function expressed as:

$$\text{HB: S/N ratio} = -10\ log_{10}\left\{\frac{1}{n}\sum_{1}^{n}\frac{1}{y_i^2}\right\} \quad \text{(Equation 3.5)}$$

Nominal-the-best type problem: In the nominal-the-best type problem, the quality characteristic is continuous and non-negative, but its target value is non zero and assumes some finite value. For these types of problems, if the mean becA scaling factor can be used as an adjustment factor to shift the mean closer to the target for such type of problems.

the objective function that is to be maximized can be expressed as

$$\text{NB: S/N ratio} = 10\ log_{10}\ \{\frac{Y^{-2}}{S^2}\} \quad \text{(Equation 3.6)}$$

Where Yi is the sample mean & S is the sample standard deviation of n observations in each trial. For smaller-the-better type, target value is zero. For larger-the-better, inverse of each large value becomes a small value and again the target value is zero.

For this experimental work, the response characteristics have been studied and are shown in Table 3.3. The representation of factor level is shown in Table 3.4 as under:

Table 3.3 Response Variables

Response No.	**Response 1**	**Response 2**	**Response 3**	**Response 4**
Response Name	MRR	TWR	SR	Hardness
Response Units	mm^3/min	mm^3/min	Microns	HRB
Response Type	Higher-the-better	Lower-the-better	Lower-the-better	Higher-the-better

Table 3.4 Representation of Factor Level

Factors	Level 1		Level 2		Level 3	
Abrasive Slurry	A1	Al2O3	A2	SiC		
Tool Material	B1	SS	B2	HSS		
Work piece	C1	Al/Si	C2	Al/Cu		
Abrasive Grit Size	D1	280	D2	400	D3	Mix
Slurry Concentration (%)	E1	30	E2	25	E3	35
Power Rating	F1	100	F2	200	F3	150

3.2 Analysis of results using ANOVA

In statistics, analysis of variance (ANOVA) is a collection of statistical models, and their associated procedures, in which the observed variance is partitioned into components due to different explanatory variables. The initial techniques of the analysis of variance were developed by the statistician and geneticist R.A. Fisher in the 1920s and 1930s and are sometimes known as Fisher's ANOVA or Fisher's analysis of variance, due to the use of Fisher's F-distribution as part of the test of statistical significance.

The purpose of the statistical analysis of variance (ANOVA) is to investigate which design parameter significantly affects the material removal rate, tool wear rate & surface roughness. In my thesis, ANOVA table is made with help of **MINITAB 16** Software.

Various Formulas for ANOVA are:

Sum of Square, SS = $\sum_{i=1}^{N} Y_i^2 - \frac{T^2}{N}$ (Equation 3.7)

DOF = Levels of Parameters – 1

Variance = $\frac{SS}{DOF}$ (Equation 3.8)

F-test = $\frac{variation\ \ due\ to\ par\ ameter}{variation\ \ due\ to\ error}$ (Equation 3.9)

e-pooled = sum of SS due to error and SS of all insignificant factors

SS' = SS of significant factor – DOF of that factor × variation due to e -pooled

(Equation 3.10)

C% = $\frac{SS'}{Total\ SS} \times 100$ (Equation 3.11)

If **F-critical > F-test**

Only then the factor is significant for the given conditions.

Where DOF = Degree of Freedom

F test = Fisher's test

C% = Contribution Factor

3.3 Description of the machining set up

The ultrasonic drilling Machine used for the experimentation consisted of an ultrasonic spindle kit; a constant pressure feed system and slurry flow system. The maximum power input to the machine was 500 W. Figure 3.2 shows the static USM set up used for the experimentation.

The ultrasonic spindle kit comprises an ultrasonic spindle mounted with cylindrical horn, a power supply unit that converts 50 Hz electrical supply to high frequency 20 kHz output. This high frequency electric signal is applied to a piezoelectric transducer positioned in the spindle. The function of this transducer is to convert the applied electrical signal into mechanical vibrations.

Figure 3.1 Ultrasonic Machining Set up [Courtesy by: N.T.M Lab,T.U,Patiala]

The amplitude of vibration was in range of 25.3-25.8 μm with a frequency of 20 kHz +/- 200 Hz. The static load for feed rate was fixed at 1.636 Kg and slurry flow was maintained at 36.4 X 10^3 mm^3/min.

3.4 Measuring and test equipment used

As the tool materials used for the experimentation possess different values of densities, the tool wear rate in terms of 'change in volume' per unit time could be a better measure of the rate at which the different tool materials are eroded while machining takes place. Hence, the tool wear rate as well as material removal rate was calculated as reduction in volume per unit time (mm^3/min) so as to facilitate more accurate comparison of the TWR for different tool materials under varying process conditions. The details of important test equipment used in experimental study are given below:

3.4.1 Surface Roughness tester

The surface roughness had been analyzed by using Surface roughness tester "Perthometer M4Pi" in the Metrology lab at Mechanical Engineering department at Thapar University, Patiala. The basic specifications of Surface roughness tester "Perthometer M4Pi" are given as follows:

Figure 3.2 Perthometer M4Pi [Courtesy by: N.T.M Lab,T.U,Patiala]

(1) Principle of measurement – Stylus method
(2) Measurement ranges – 100 - 150 Jm
(3) Cut-off wavelengths – 0.08 – 0.25 – 0.8 – 2.5 mm
(4) Tracing lengths – 1.5 – 4.8 – 15 mm
(5) Number of sampling lengths – 1……5 selectable
(6) Parameters – Ra, Rq, Rz, Rmax, Rp, Rt, Mr (material ratio)
(7) Tolerance monitoring – Maximum/minimum for all parameters selected.

(8) Measuring unit - Jm, Jin selectable

3.4.2 Vickers's Hardness tester

The hardness of machined surface had been measured by using Vickers's hardness tester in SOM lab at Mechanical Engineering department at Thapar University, Patiala. The basic features of Vickers's hardness tester are given as follows:

Fig 3.3 Vicker Hardness tester [Courtesy by: S.O.M Lab,T.U,Patiala]

(1) Maximum capacity – 50 kgf

(2) Model No – VM-50

(3) Company – Fuel Instruments and Engineering Pvt. Ltd, Maharashtra (INDIA)

The hardness measurement is dependent on the diameter of indentation on the samples. The depth of penetration of an indenter under a large load is determined. The different scales, denoted by a single letter, that use different loads or indenters. The result is a dimensionless number noted as HRB, where B is scale letter.

3.4.3 Scanning Electron Microscope (SEM)

Microstructure was carried out of some selected samples on Scanning Electron Microscope (SEM), model JSM-6610 LV of Jeol, Japan available at IIT, Ropar.

Figure 3.4 Scanning Electron Microscope (SEM) [IIT Ropar]

Its resolution in high vacuum mode is 3nm. Its maximum magnification range is 3,00,000X. SEM of samples was carried out on three ranges, namely 200X, 800X and 1000X.

Microstructure was carried out of some selected samples on Scanning Electron Microscope (SEM), model JSM-6610 LV of Jeol, Japan available at IIT, Ropar. Its resolution in high vacuum mode is 3nm. Its maximum magnification range is 3,00,000x. SEM of samples was carried out on three ranges, namely 250x, 800x and 1000x.

3.4.4 Weighing Machine

Precision balance was used to measure the weight of the workpiece and tool. This machine capacity is 300gram and accuracy is 0.001 gram and Brand: SHINKO DENSSHI Co. Ltd., Japan. Model: DJ 300S.

3.5 Workpiece description

There is no limitation to the range of material that can be machined by USM process, except that they should not dissolve in the slurry media or react with it. While USM can be applied to ductile materials such as soft steel, copper, and brass but it is best suited to machining operation on hard, brittle materials that are not practical to process by other method. Ultrasonic machining can be used for metals and non-metals, electrical conductors or non conductor. The ultrasonic drilling technique is especially suited for hard materials like tungsten carbide, titanium carbide, ceramic and diamond. Material which exhibit high hardness and which have impact brittleness can be successfully machined by this technique. Such materials are germanium, ferrites, glass and quartz.

Table 3.5 Typical Composition of work piece material (%) Al/Si (Composite)

Si	Mg	Cu	Ni	Fe	Mn	Zn	Pb	Sn
12.5	0.30	1.05	0.60	0.55	0.17	0.09	Traces	Traces

Table 3.6 Typical Composition of work piece material (%) Al/Cu (Alloy)

Si	Mg	Cu	Ni	Fe	Mn	Zn	Pb	Sn
11.5	0.36	4.60	2.20	0.58	0.07	0.09	Traces	Traces

Figure 3.5 (Al/Si) Composite **Figure 3.6 (Al/Cu) Alloy**

The dimensions of work piece were 100×50×5.98 mm^3. Table 3.4 and 3.5 shows the chemical composition of work piece materials of Al/Si Composite and Al/Cu Alloy.
Density of Al/Si Composite = 2.507 gm/cc
Density of Al/Cu Alloy = 2.531 gm/cc

3.6 Cutting Tool used for the Ultrasonic Machining

For minimum tool wear, tools should be constructed from relatively ductile materials such as stainless steel, brass and mild steel. The harder the tool material the faster its wear rate will be. Depending on the abrasive used, work piece / tool wear ratios can

range from 1:1 to 100:1.The cutting tool have been used in this experiment are HSS and SS

Table 3.7 Typical Composition of cutting tool material

Material	Chemical Composition (%)	Density (g/cm3)
High Speed Steel	Fe (40.7) + C (.377) + Si (2.05) + Mn (18.0) + Cr (15.4) + Ni (6.57) + Cu (3.92) + Pb (0.35) + V (0.07) + W (0.80)	8.253
Stainless Steel	Fe (68.9) + C (.622) + Si (.836) + Mn (1.14) + Cr (5.48) + Ni (5.56) + Cu (0.19) + Pb (0.35) + V (4.42) + W (6.27)	7.947

3.6.1 Preparation of Cutting Tool

The cutting tool is made from the cylindrical piece of 16.48 mm diameter and 41.4 mm length by turning, facing processes done on the lathe machine. The shape and size of the cutting tool is shown in the figure (3.8)

Figure 3.7 Tool (SS and HSS)

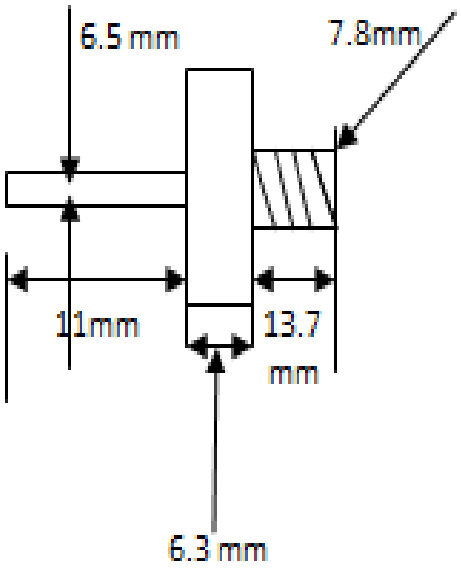

Figure 3.8 Dimensions of tool

The tool tip and tool holder comprises as a single piece. No brazing process done during the preparation of cutting tool. The threading process has been done to hold the tool in the horn.

3.7 Abrasive Slurry

The slurry used in ultrasonic machining process is a mixture of abrasive grains and a liquid carrier mainly water, kerosene, benzene, glycerol or thin oil. The ratio of abrasives to liquid can vary from 1:4 to 1:1 (by weight). Slurry can be fed externally or internally. In the case of external feeding, the slurry is pump fed by several jets covering the circumference of the tool or by a single jet. In the case of internal feeding hollow tools carry the abrasive slurry centrally to the work piece. The slurry is to be fed continuously to avoid any drying up at the tool face. Several abrasives are available in various particle (Grit) sizes for ultrasonic machining. The criteria for selection of an abrasive for a particular application include hardness, usable life, cost, shape and size of particles. The abrasive used for an application should be harder than the material being machined. Otherwise, the usable life time of the abrasive will be substantially shortened. The performance characteristics of an ultrasonic machining process have investigated by using the different abrasive slurry of different grit numbers. The slurry have been used during the experiments of Aluminium oxide and Silicon carbide.

CHAPTER 4

RESULTS AND ANALYSIS OF MRR

4.1 Introduction

The effects of parameters i.e. tool, workpiece, power rating, slurry concentration, type of slurry, grit size and interaction between tool and type of slurry, tool and workpiece, slurry type and workpiece were evaluated using ANOVA and factorial design analysis. A confidence interval of 95% had been used for the analysis. Total 36 experiments were performed and each experiment performs only at once.

4.2 Results for MRR

The results for MRR for each of the 36 treatment conditions are given in Table 4.1. The MRR is calculated from the loss of weight of tool during the performance trial:

$$\text{MRR} = \frac{W_i - W_f}{\rho t} \times 1000\ mm^3/\text{min} \qquad \text{(Equation 4.1)}$$

Where W_i = Initial weight of Workpiece (gm)

W_f = Final weight of Workpiece (gm)

t = time period of trial (minutes)

p = density of workpiece in gm/cc = 2.53 gm/cc

Table 4.1 RESULTS for MRR

Trail No.	Tool	Power Rating	Slurry Concentration (%)	Type of Slurry	Grit Size	Work piece	MRR mm^3/min	S/N Ratio	Mean
1	SS	100	30	SiC	280	Al/Si	1.861	3.1498	1.5370
2	SS	200	25	SiC	400	Al/Si	1.402	3.4780	1.5025
3	SS	150	35	SiC	Mix	Al/Si	2.587	8.5860	2.6935
4	SS	100	30	SiC	280	Al/Si	1.213	2.2123	1.2763
5	SS	200	25	SiC	400	Al/Si	1.603	4.4236	1.6040
6	SS	150	35	SiC	Mix	Al/Si	2.800	9.5862	2.8008
7	SS	200	30	SiC	280	Al/Cu	3.009	9.5684	3.0090
8	SS	150	25	SiC	400	Al/Cu	1.403	2.9412	1.4030
9	SS	100	35	SiC	Mix	Al/Cu	1.305	2.3122	1.3050
10	HSS	150	30	SiC	280	Al/Si	1.705	4.6345	1.7050
11	HSS	100	25	SiC	400	Al/Si	1.105	0.8672	1.1050
12	HSS	200	35	SiC	Mix	Al/Si	3.604	11.1357	3.6040
13	HSS	150	25	SiC	280	Al/Cu	2.498	8.7099	2.7640
14	HSS	100	35	SiC	400	Al/Cu	1.903	4.7642	1.7505
15	HSS	200	30	SiC	Mix	Al/Cu	2.013	7.0349	2.3015
16	HSS	150	25	SiC	280	Al/Cu	3.030	9.6584	3.0305
17	HSS	100	35	SiC	400	Al/Cu	1.598	3.9423	1.6001
18	HSS	200	30	SiC	Mix	Al/Cu	2.590	9.0043	5.5962
19	SS	100	25	Al_2O_3	280	Al/Cu	1.103	0.8515	1.1030
20	SS	200	35	Al_2O_3	400	Al/Cu	3.604	11.1357	3.6040
21	SS	150	30	Al_2O_3	Mix	Al/Cu	1.702	4.6192	1.7020
22	SS	200	25	Al_2O_3	280	Al/Cu	3.706	11.3781	3.7060
23	SS	150	35	Al_2O_3	400	Al/Cu	3.405	10.6423	3.4050
24	SS	100	30	Al_2O_3	Mix	Al/Cu	1.199	1.5764	1.1990
25	SS	200	35	Al_2O_3	280	Al/Si	3.204	10.1139	3.2040
26	SS	150	30	Al_2O_3	400	Al/Si	3.098	9.8216	3.0980
27	SS	100	25	Al_2O_3	Mix	Al/Si	1.105	0.8672	1.1050
28	HSS	200	35	Al_2O_3	280	Al/Cu	3.402	10.6347	3.4020
29	HSS	150	30	Al_2O_3	400	Al/Cu	2.395	7.5861	2.3950
30	HSS	100	25	Al_2O_3	Mix	Al/Cu	1.100	0.8279	1.1000
31	HSS	150	35	Al_2O_3	280	Al/Si	3.388	10.5989	3.3880
32	HSS	100	30	Al_2O_3	400	Al/Si	1.502	3.5334	1.5020
33	HSS	200	25	Al_2O_3	Mix	Al/Si	1.213	1.6772	1.2130
34	HSS	100	35	Al_2O_3	280	Al/Si	2.904	9.2599	2.9040
35	HSS	200	30	Al_2O_3	400	Al/Si	2.605	8.3162	2.6050
36	HSS	150	25	Al_2O_3	Mix	Al/Si	1.910	5.6207	1.9100

4.3. ANOVA of Means for MRR

The results for MRR were analyzed using ANOVA for identifying the significant factors affecting the performance measures. The Analysis of Variance (ANOVA) for the mean MRR at 95% confidence interval is given in Table 4.2 the variance data for each factor and their interactions were F-tested to find significance of each. ANOVA table shows that the Grit Size (F value 5.99), Concentration (F value 11.30) and Power Rating (F value 12.41) are the factors that are significant and affects MRR. The factors Slurry type, tool, workpiece and interactions are found insignificant. Table 4.3 shows ranks to various input parameters in terms of their relative significance.

Table 4.2 ANOVA of Means for MRR

Sources	SS	DF	(V)	F	F (CRITICAL)	SS'	% age Contribution	STATUS
Slurry Type(A)	0.6783	1	0.6783	2.209	4.45			Insignificant
Tool (B)	0.0002	1	0.0002	0.0006	4.45			Insignificant
Workpiece (C)	0.0411	1	0.0411	0.133	4.45			Insignificant
Grit Size (D)	3.6888	2	1.8444	5.99	3.59	3.1352	12.73	Significant
Slurry Concentration (E) (%)	6.9438	2	3.4716	11.30	3.59	6.3897	25.95	Significant
Power Rating (F)	7.6238	2	3.8119	12.41	3.59	7.0702	28.71	Significant
A×B	0.3937	1	0.3937	1.27	4.45			Insignificant
A×C	0.0042	1	0.0042	0.013	4.45			Insignificant
B×C	0.0157	1	0.0157	0.048	4.45			Insignificant
Residual Error	5.2339	17	0.3078					
Total	24.6234	29	0.8490					
e-pooled	6.3671	23	.2768				32.60	

Table 4.3 Response table of Means for MRR

Level	Type Of Slurry	Tool	Work piece	Grit Size	Slurry Concentration	Power Rating
1	2.364	2.243	2.277	2.672	1.691	1.461
2	2.057	2.238	2.205	2.237	2.105	2.446
3				1.813	2.926	2.815
Delta	0.307	0.005	0.072	0.859	1.235	1.354
Rank	4	6	5	3	2	1

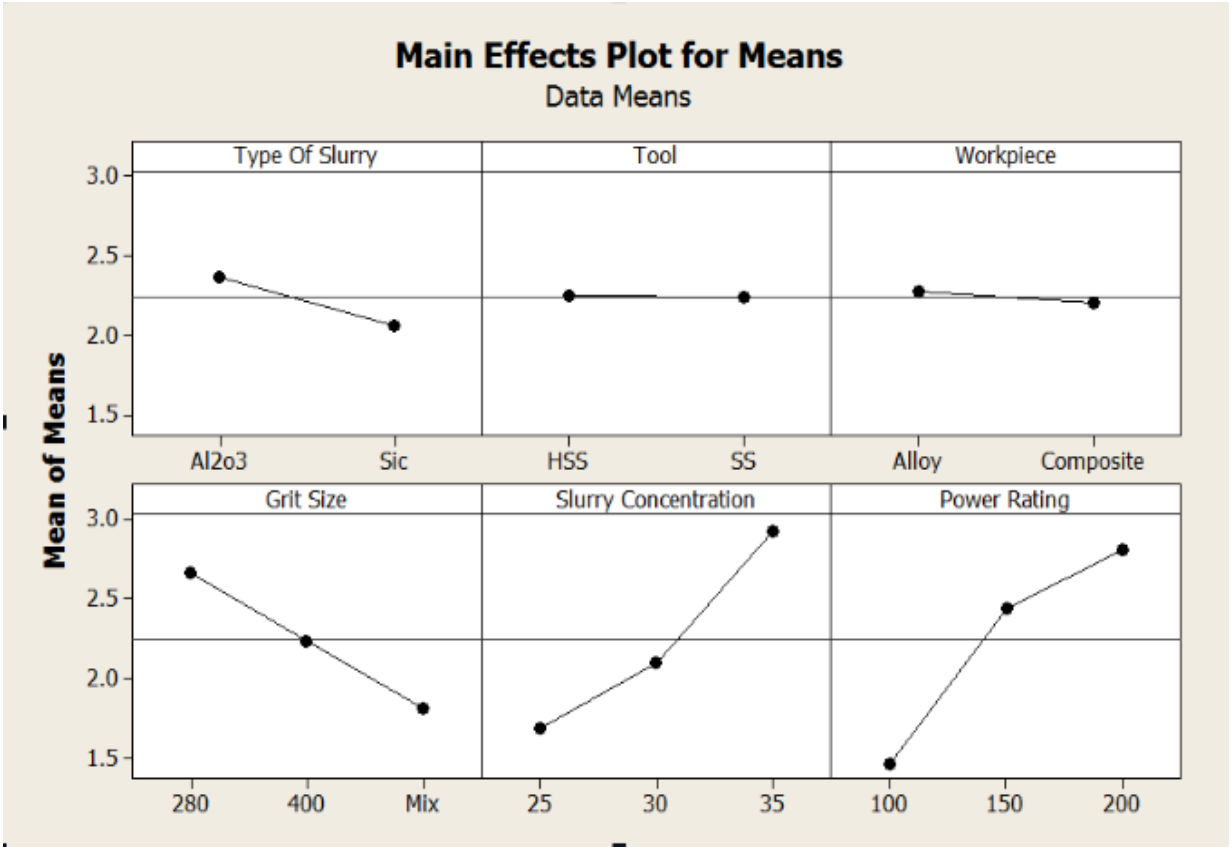

Figure 4.1: Main Effects Plot of Means for MRR

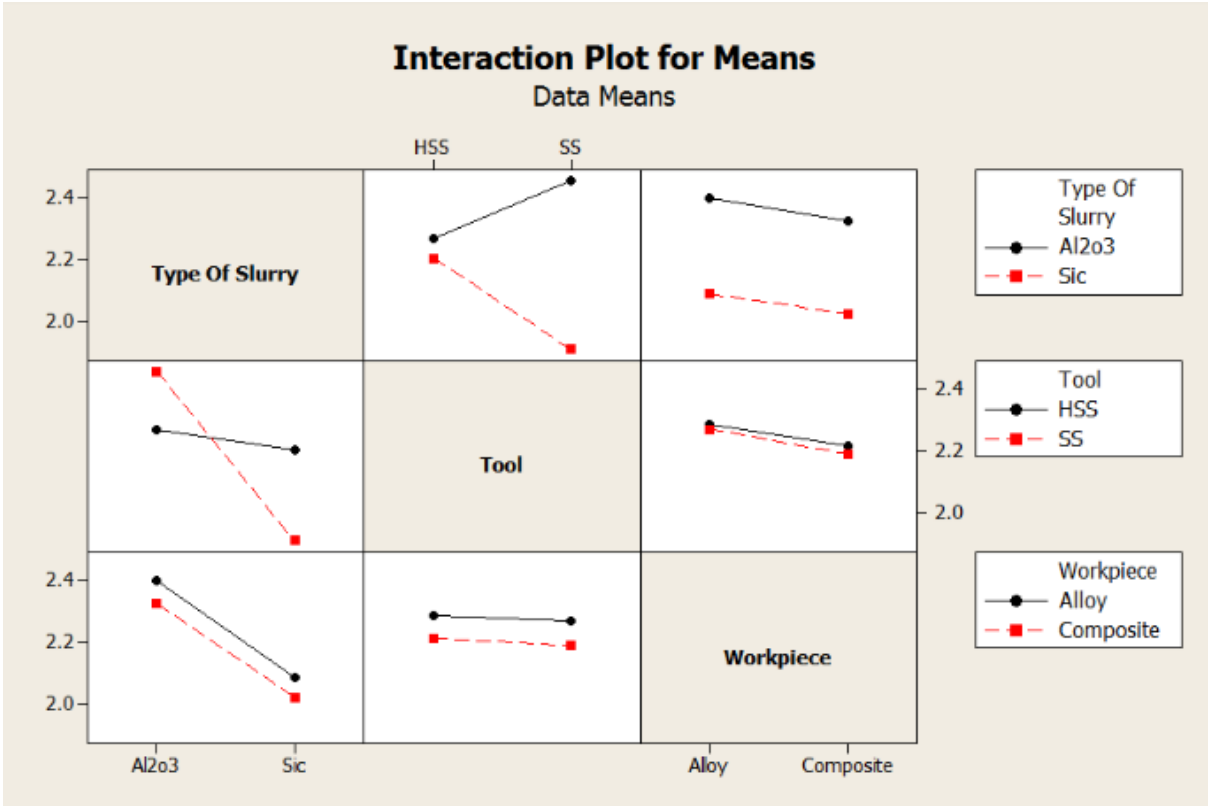

Figure 4.2: Interaction Plots of Means for MRR

4.4 ANOVA of S/N Ratio for MRR

The S/N ratio consolidates several repetitions into one value and is an indication of the amount of variation present. The S/N ratio has been calculated to identify the major contributing factors and interactions that cause variation in the MRR. MRR is "Higher is Better" type response which is given by:

HB: S/N ratio = -10 $log_{10}\left\{\frac{1}{n}\sum_1^n \frac{1}{y_i^2}\right\}$ (Equation 4.2)

Table 4.4 shows the ANOVA for S/N ratio for MRR at 95% confidence interval. The Slurry type is the most significant factor in affecting MRR followed by Power Rating and Tool type according to F-test. Main effect plot and residual plot for S/N ratios for MRR are shown in figure 4.3 and figure 4.4 respectively.

Table 4.4 ANOVA of S/N Ratio for MRR

Sources	SS	DF	(V)	F	F (CRITICAL)	SS'	% age Contribution	STATUS
Slurry (A)	7.432	1	7.432	1.573	4.45			Insignificant
Tool (B)	0.577	1	0.577	.0122	4.45			Insignificant
Workpiece (C)	0.489	1	0.489	.1035	4.45			Insignificant
Grit Size (D)	60.156	2	30.078	6.368	3.59	51.953	12.50	Significant
Slurry Concentration (E) (%)	119.633	2	59.816	12.664	3.59	112.03	26.95	Significant
Power Rating (F)	141.476	2	70.738	14.977	3.59	133.27	32.06	Significant
A×B	3.766	1	3.766	0.810	4.45			Insignificant
A×C	1.023	1	1.023	0.216	4.45			Insignificant
B×C	0.753	1	0.753	0.159	4.45			Insignificant
Residual Error	80.294	17	4.723					
Total	415.599	29	14.331					
e-pooled	94.334	23	4.1014				28.49	

Table 4.5 Response table of S/N ratio for MRR

Level	Type Of Slurry	Tool	Workpiece	Grit Size	Slurry Concentration	Power Rating
1	6.614	6.347	6.306	7.890	3.722	2.801
2	5.599	6.069	6.111	6.709	5.984	7.376
3				4.426	8.918	8.447
Delta	1.016	0.277	0.195	3.464	5.196	5.646
Rank	4	5	6	3	2	1

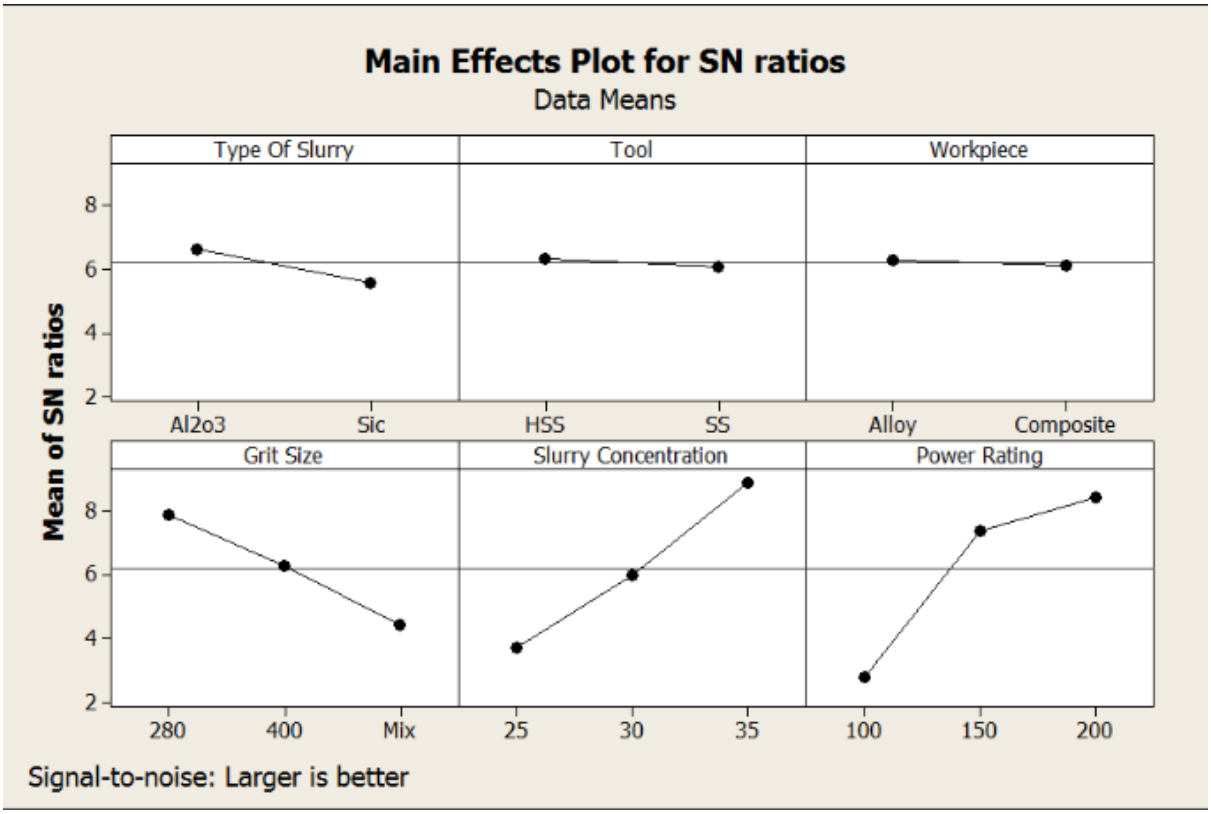

Figure 4.3 Main Effects Plot of S/N ratio for MRR

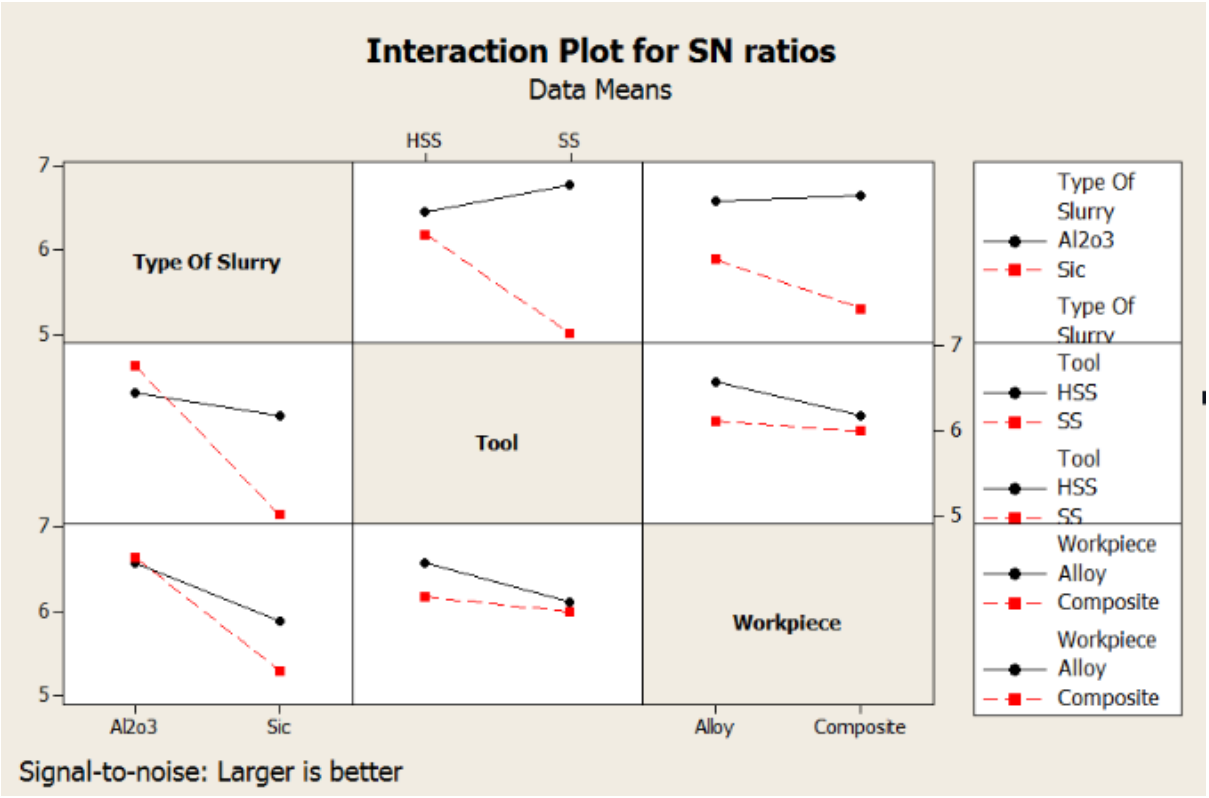

Figure 4.4 Interaction Plots of S/N ratio for MRR

4.5 Optimal design for MRR

In the experiment analysis, the main effect plot and interaction plot in figure 4.1 and figure 4.2 is used to estimate the mean MRR. From table 4.6 it is concluded that Mean and S/N ratio both are affected by Grit size, Slurry Concentration and Power rating. Also the interactions found insignificant in both the cases of Mean and S/N ratio.MRR to be achieved best when workpiece is machined by Grit size of 280 with slurry concentration 35% and Power rating 150.

Table 4.6: Significant Factors and Interactions

Factors	Affecting Mean		Affecting Variation	
	Contribution	**Best Level**	**Contribution**	**Best Level**
Slurry Type (A)				
Tool (B)				
Work piece (C)				
Grit Size (D)	Significant	Level 1 (280)	Significant	Level 1 (280)
Slurry Concentration (%) (E)	Significant	Level 3 (35)	Significant	Level 3 (35)
Power Rating (F)	Significant	Level 3 (150)	Significant	Level 3 (150)

Estimating the mean

In experimental analysis, MRR is a higher average response is better (HB) characteristic. Depending on the characteristic, different treatment combinations has been chosen to obtain satisfactory analysis. After conducting the experiments the optimum treatment condition within the experiments determined on the basis of prescribed combination of factor levels is determined to one of those in the experiment. The mean value of MRR ($\bar{T}$) is 1.733. The formulae for calculating the theoretical optimal value is as under:

$(MRR)_{opt}$ $=\bar{T} + (D_1\text{-}\bar{T}) + (E_3\text{-}\bar{T}) + (F_3\text{-}\bar{T})$ (Equation 4.3)

= 1.733 + (2.585 – 1.733) + (2.808 - 1.733) + (2.493 - 1.733)

= 4.42 mm^3/min

CI = $\sqrt{\frac{F_{\alpha,V1,V2}}{I]eff}}$ (Equation 4.4)

Where $F_{\alpha,V1,V2}$ = F ratio $\alpha = risk\ (0.05)$

Confidence = 1 - α

V_i = dof for mean which is always = 1

V_2= dof for error = V_e

ηeff = No. of tests under that condition using the particular factors

ηeff = N / (1+ dof_{D+E+F}) = 36 / (1+2+2+2) = 5.14

CI = $\sqrt{4.45 \times .276/5.14}$ = 0.488

So, the Confidence Interval around the MRR is given by 4.42 $\pm$ 0.48 mm^3/min.

CHAPTER 5

RESULTS AND ANALYSIS OF TWR

5.1 Introduction

The effects of parameters i.e. tool, workpiece, power rating, slurry concentration, type of slurry, grit size and interaction between tool and type of slurry, tool and workpiece, slurry type and workpiece were evaluated using ANOVA and factorial design analysis. A confidence interval of 95% had been used for the analysis. Total 36 experiments were performed and each experiment performs only at once.

5.2 Results for TWR

The results for TWR for each of the 36 treatment conditions are given in Table 4.1. The TWR is calculated from the loss of weight of tool during the performance trial:

$$\text{TWR} = \frac{T_i - T_f}{\rho t} \times 1000\ mm^3/\text{min} \qquad \text{(Equation 5.1)}$$

Where T_i = Initial weight of Tool (gms)

T_f = Final weight of Tool (gms)

t = time period of trial (minutes)

p = density of Tool in gms/cc

Table 5.1 Results for TWR

Trail No.	Tool	Power Rating	Slurry Concentration (%)	Type of Slurry	Grit Size	Work piece	TWR mm^3/ min	S/N Ratio	Mean
1	SS	100	30	SiC	280	Al/Si	0.3506	9.1174	0.35005
2	SS	200	25	SiC	400	Al/Si	0.2998	10.4764	0.29935
3	SS	150	35	SiC	Mix	Al/Si	0.2509	12.0186	0.25065
4	SS	100	30	SiC	280	Al/Si	0.3495	9.0174	0.34951
5	SS	200	25	SiC	400	Al/Si	0.2989	11.0123	0.29901
6	SS	150	35	SiC	Mix	Al/Si	0.2504	9.0623	0.25045
7	SS	200	30	SiC	280	Al/Cu	0.2994	10.4750	0.29940
8	SS	150	25	SiC	400	Al/Cu	0.2704	11.3599	0.27040
9	SS	100	35	SiC	Mix	Al/Cu	0.2510	12.0065	0.25100
10	HSS	150	30	SiC	280	Al/Si	0.3980	8.0023	0.39800
11	HSS	100	25	SiC	400	Al/Si	0.3214	9.8591	0.32140
12	HSS	200	35	SiC	Mix	Al/Si	0.3448	9.2487	0.34480
13	HSS	150	25	SiC	280	Al/Cu	0.4482	6.9958	0.44690
14	HSS	100	35	SiC	400	Al/Cu	0.3779	8.7269	0.36595
15	HSS	200	30	SiC	Mix	Al/Cu	0.4245	6.7879	0.45660
16	HSS	150	25	SiC	280	Al/Cu	0.4456	7.8562	0.44560
17	HSS	100	35	SiC	400	Al/Cu	0.3540	9.1175	0.35406
18	HSS	200	30	SiC	Mix	Al/Cu	0.4887	6.6485	0.48872
19	SS	100	25	Al_2O_3	280	Al/Cu	0.2706	11.3534	0.27060
20	SS	200	35	Al_2O_3	400	Al/Cu	0.3448	9.2487	0.34480
21	SS	150	30	Al_2O_3	Mix	Al/Cu	0.3105	10.1588	0.31050
22	SS	200	25	Al_2O_3	280	Al/Cu	0.4002	7.9545	0.40020
23	SS	150	35	Al_2O_3	400	Al/Cu	0.3669	8.7090	0.36690
24	SS	100	30	Al_2O_3	Mix	Al/Cu	0.3445	9.2562	0.34450
25	SS	200	35	Al_2O_3	280	Al/Si	0.3001	10.4547	0.30010
26	SS	150	30	Al_2O_3	400	Al/Si	0.2775	11.1347	0.27750
27	SS	100	25	Al_2O_3	Mix	Al/Si	0.2559	11.8386	0.25590
28	HSS	200	35	Al_2O_3	280	Al/Cu	0.5185	5.7050	0.51850
29	HSS	150	30	Al_2O_3	400	Al/Cu	0.4856	6.2744	0.48560
30	HSS	100	25	Al_2O_3	Mix	Al/Cu	0.4104	7.7359	0.41040
31	HSS	150	35	Al_2O_3	280	Al/Si	0.3500	9.1186	0.35000
32	HSS	100	30	Al_2O_3	400	Al/Si	0.3002	10.4518	0.30020
33	HSS	200	25	Al_2O_3	Mix	Al/Si	0.4789	6.3951	0.47890
34	HSS	100	35	Al_2O_3	280	Al/Si	0.2995	10.4721	0.29950
35	HSS	200	30	Al_2O_3	400	Al/Si	0.3885	8.2122	0.38850
36	HSS	150	25	Al_2O_3	Mix	Al/Si	0.3472	9.1884	0.34720

5.3 ANOVA of Means for TWR

The results for TWR were analyzed using ANOVA for identifying the significant factors affecting the performance measures. The Analysis of Variance (ANOVA) for the mean TWR at 95% confidence interval is given in Table 4.2. The variance data for each factor and their interactions were F-tested to find significance of each. ANOVA table shows that the Grit size (F value 5.02), Slurry concentration (F value of 8.74) and Power rating (F value of 9.60) are found to be significant and effects TWR. The Type of slurry, Tool, Workpiece and interactions B×E, B×F and E×F are found to be insignificant. Table 5.3 shows ranks to various input parameters in terms of their relative significance.

Table 5.2 ANOVA of Means for TWR

Sources	SS	DF	(V)	F	F (CRITICAL)	SS'	% age Contribution	STATUS
Slurry type (A)	0.6783	1	0.6783		4.73			Insignificant
Tool (B)	0.3002	1	0.3002		4.73			Insignificant
Workpiece (C)	0.0411	1	0.0411		4.73			Insignificant
Grit Size (D)	3.9868	2	1.984	5.02	3.89	3.40	13.83	Significant
Slurry Concentration (E) (%)	6.9430	2	3.471	8.74	3.89	6.36	25.83	Significant
Power Rating (F)	7.6230	2	3.811	9.60	3.89	7.04	28.59	Significant
B×E	0.2583	2	0.129		3.89			Insignificant
B×F	0.1705	2	0.085		3.89			Insignificant
E×F	0.4560	4	0.114		3.26			Insignificant
Residual Error	4.7628	12	0.396					
Total	24.623	29	0.849					
e-pooled	6.665	23	0.289				31.75	

Table 5.3 Response Table of Means for TWR

Level	Type Of Slurry	Tool	Work piece	Grit Size	Slurry Concentration	Power Rating
1	2.364	2.243	2.277	2.672	1.691	1.461
2	2.057	2.238	2.205	2.237	2.105	2.446
3				1.813	2.926	2.815
Delta	0.307	0.005	0.072	0.859	1.235	1.354
Rank	4	6	5	3	2	1

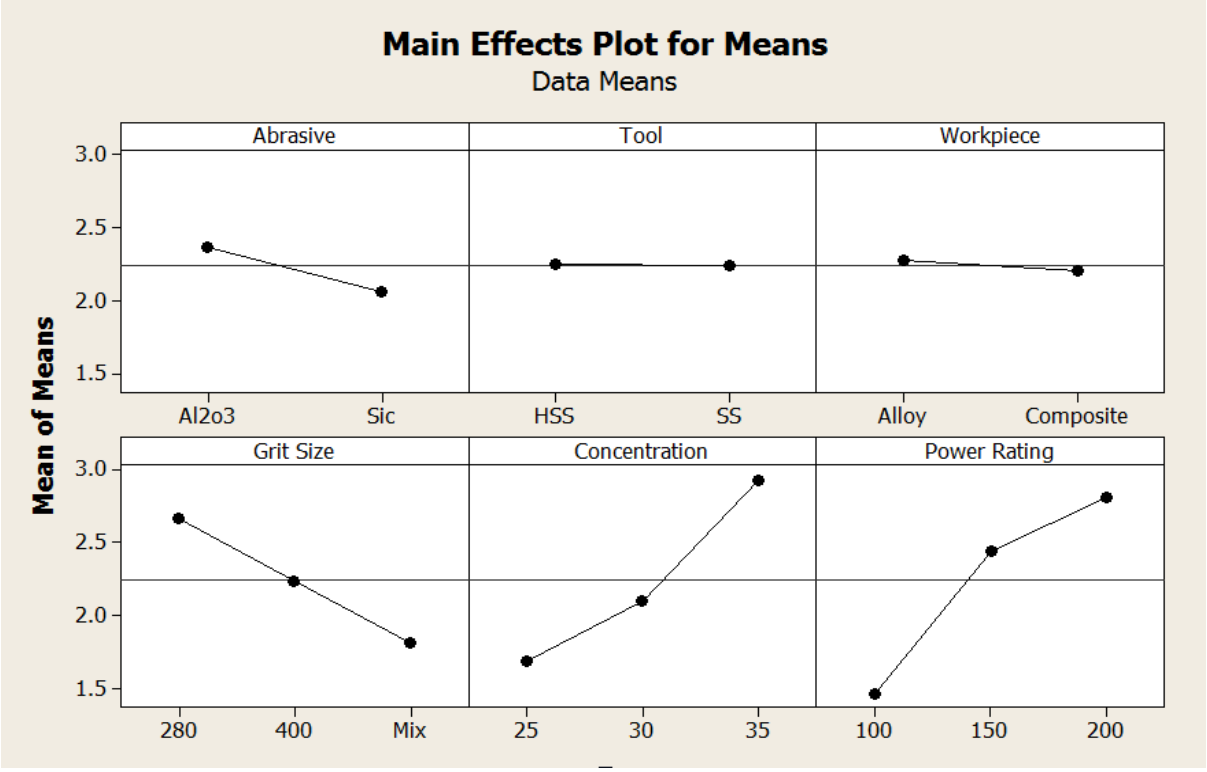

Figure 5.1 Main Effects Plot of Means for TWR

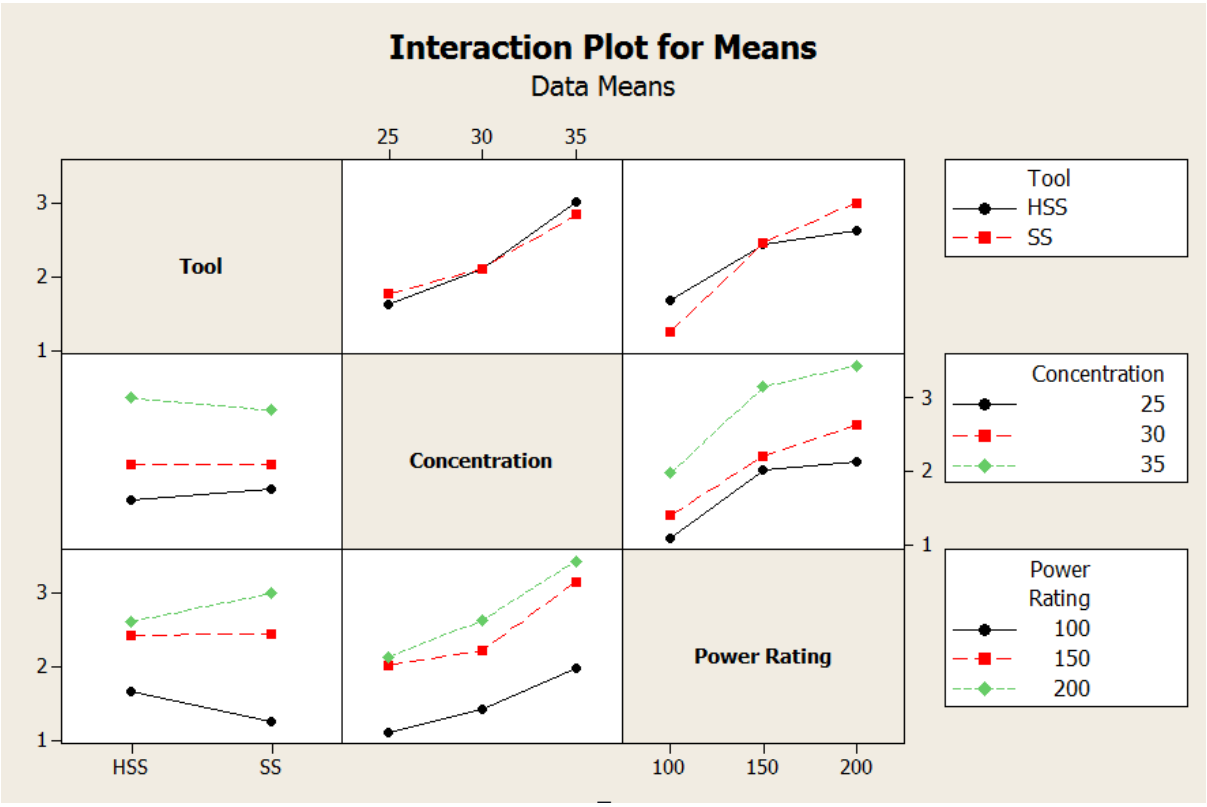

Figure 5.2 Interaction Plot of Means for TWR

4.4 ANOVA of S/N Ratio for TWR

The S/N ratio consolidates several repetitions into one value and is an indication of the amount of variation present. The S/N ratio has been calculated to identify the major contributing factors and interactions that cause variation in the TWR. TWR is "Lower is Better" type response which is given by:

LB: S/N ratio = -10 $log_{10}\left\{\frac{1}{n}\sum_1^n y_i^2\right\}$ (Equation 5.2)

Table 5.4 shows the ANOVA for S/N ratio for TWR at 95% confidence interval. The power rating is the most significant factor in affecting TWR followed by slurry concentration and grit size according to F-test. Main effect plot and residual plot for S/N ratios for TWR are shown in figure 5.3 and figure 5.4 respectively.

Table 5.4 ANOVA of S/N Ratio for TWR

Sources	SS	DF	(V)	F	F (CRITICAL)	SS'	% age Contribution	STATUS
Slurry Type (A)	5.77	1	5.77	0.968	4.73			Insignificant
Tool (B)	0.049	1	0.049	0.008	4.73			Insignificant
Workpiece (C)	0.397	1	0.397	0.066	4.73			Insignificant
Grit Size (D)	62.29	2	31.15	5.223	3.89	54.17	13.14	Significant
Slurry Concentration (%) (E)	118.56	2	59.28	9.910	3.89	110.44	26.80	Significant
Power Rating (F)	137.39	2	68.68	11.523	3.89	129.24	31.36	Significant
A×F	3.170	2	1.58	0.265	3.89			Insignificant
B×F	3.966	2	1.98	0.332	3.89			Insignificant
D×F	8.496	4	2.12	0.356	3.26			Insignificant
Residual Error	71.57	12	5.96					
Total	412.10	29	14.21					
e-pooled	93.42	23	4.061				28.69	

Table 5.5 Response table of S/N ratio for TWR

Level	Type Of Slurry	Tool	Workpiece	Grit Size	Slurry Concentration	Power Rating
1	6.614	6.384	6.343	7.983	3.746	2.891
2	5.713	6.128	6.169	6.330	6.089	7.395
3				4.456	8.934	8.482
Delta	0.896	0.257	0.174	3.528	5.189	5.591
Rank	4	5	6	3	2	1

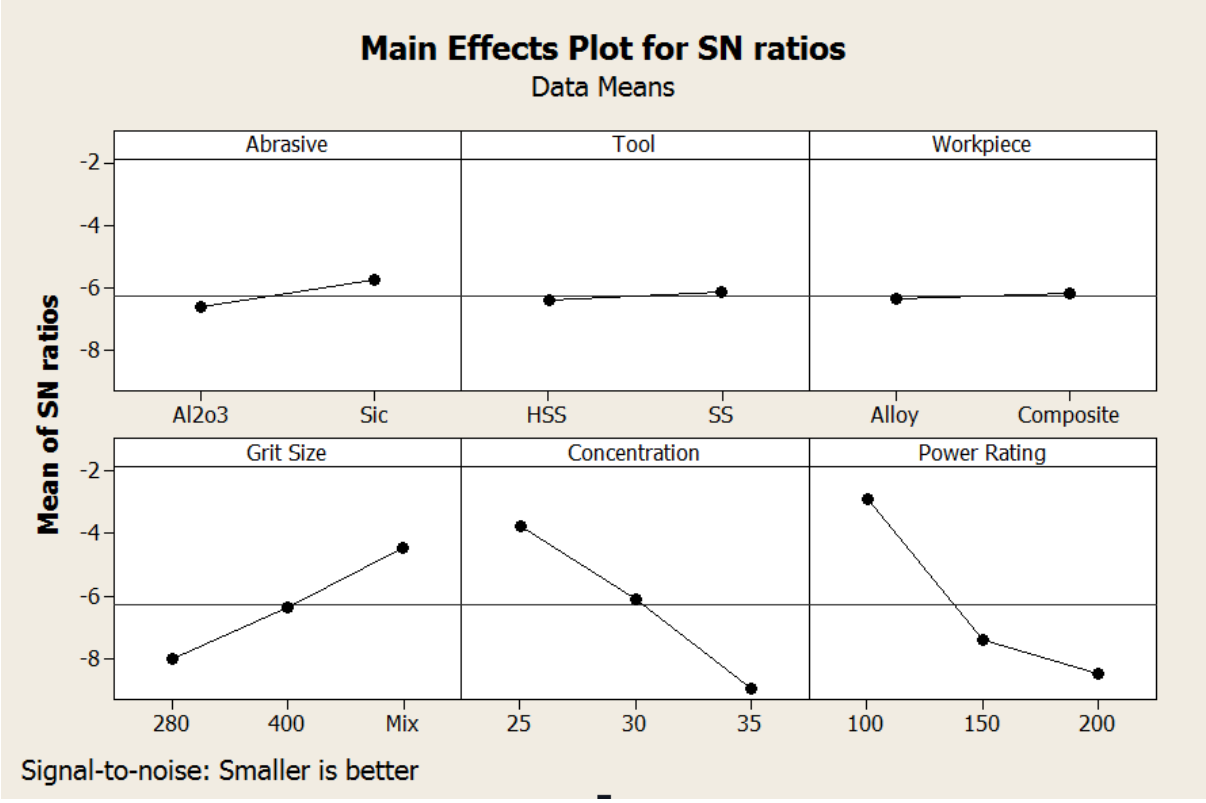

Figure 5.3 Main Effects Plot of S/N ratio for TWR

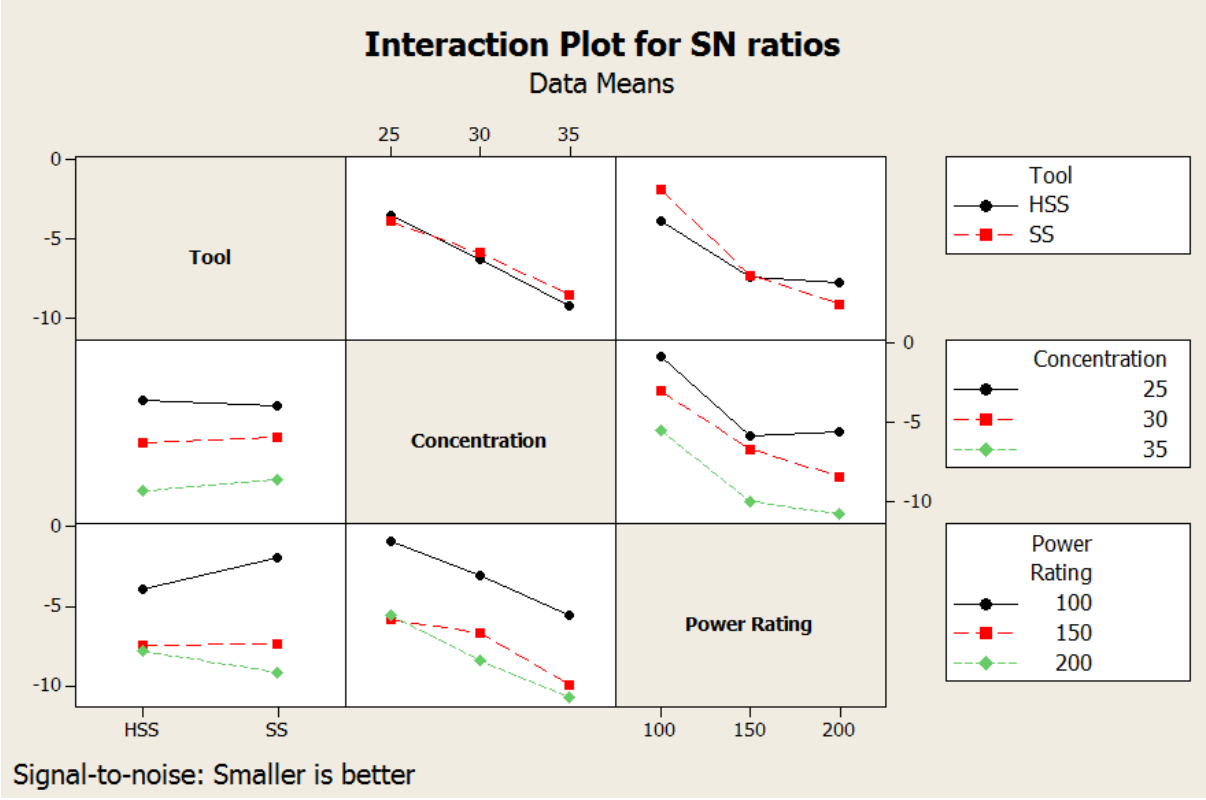

Figure 5.4 Interaction Plots of S/N ratio for TWR

5.5 Optimal design for TWR

In the experiment analysis, the main effect plot and interaction plot in figure 5.1 and figure 5.2 is used to estimate the mean MRR. From table 5.6 it is concluded that in case of Mean, lowest TWR is observed when workpiece is machined by Grit size (Mix), Slurry concentration (30%) at Power rating (100). It is observed that Type of slurry, Tool, Workpiece and interactions A×F, B×F, D×F were not affecting TWR. While in case of S/N ratio, best results are obtained when workpiece is machined by Grit size (280), Slurry concentration (35%) at Power rating (150). Remaining factors are found insignificant. So, TWR to be achieved best when workpiece is machined by Grit size (Mix), Slurry concentration 30% and Power rating 100.

Table 5.6: Significant Factors and Interactions

Factors	**Affecting Mean**		**Affecting Variation**	
	Contribution	**Best Level**	**Contribution**	**Best Level**
Type of slurry(A)				
Tool (B)				
Work piece (C)				
Grit Size (D)	Significant	Level 3 (Mix)	Significant	Level 1(280)
Slurry (Concentration (%) (E)	Significant	Level 1 (30)	Significant	Level 3 (35)
Power Rating(F)	Significant	Level 1 (100)	Significant	Level 3 (150)

Estimating the mean

In experimental analysis, TWR is a lower average response is better (LB) characteristic. Depending on the characteristic, different treatment combinations has been chosen to obtain satisfactory analysis. After conducting the experiments the optimum treatment condition within the experiments determined on the basis of prescribed combination of factor levels is determined to one of those in the experiment. The mean value of TWR ($\bar{T}$) is 0.3520. The formulae for calculating the theoretical optimal value is as under:

$$(TWR)_{opt} = \bar{T} + (D_3\text{-}\bar{T}) + (E_1\text{-}\bar{T}) + (F_1\text{-}\bar{T}) \qquad \text{(Equation 5.3)}$$

$$= .3520 + (.3464 - .3520) + (.3681\text{-}.3520) + (.3238\text{-}.3520)$$

= .3697 mm^3/min

CI = $\sqrt{\frac{F_{\alpha,V1,V2}}{\eta eff}}$ (Equation 5.4)

Where $F_{\alpha,V1,V2}$ = F ratio $\alpha = risk\ (0.05)$

Confidence = 1 - α

V_i = dof for mean which is always = 1

V_2= dof for error = V_e

ηeff = No.of tests under that condition using the particular factors

ηeff = N / (1+ dof_{D+E+F}) = 36 / (1+2+2+2) = 5.14

CI = $\sqrt{4.75 \times 0.289 / 5.14}$

= .0516

So, the Confidence Interval around the TWR is given by 0.3697 $\pm$ 0.051 mm^3/min.

CHAPTER 6

RESULTS AND ANALYSIS OF SURFACE ROUGHNESS

6.1 Introduction

The effect of parameters i.e. tool, power rating, workpiece, slurry concentration, type of slurry, grit size was evaluated using ANOVA and factorial design analysis. A confidence interval of 95% has been used for the analysis. Total 36 experiments were performed and each performs only at once.

6.2 Results for Surface Roughness

Surface Roughness is measured from the centre of every sample. It is a 'Lower is Better' phenomena. Total 36 experiments are performed to measure the surface roughness of every sample and the following results are obtained:

Table 6.1: Results for Surface Roughness

Trail No.	Tool	Power Rating	Slurry Concentration (%)	Type of Slurry	Grit Size	Work piece	Sourface Roughness μm	S/N Ratio	Mean
1	SS	100	30	SiC	280	Al/Si	1.80	-5.15	1.81
2	SS	200	25	SiC	400	Al/Si	1.95	-5.91	1.97
3	SS	150	35	SiC	Mix	Al/Si	1.85	-5.36	1.85
4	SS	100	30	SiC	280	Al/Si	1.82	-5.30	1.82
5	SS	200	25	SiC	400	Al/Si	2.00	-6.06	2.01
6	SS	150	35	SiC	Mix	Al/Si	1.86	-5.40	1.87
7	SS	200	30	SiC	280	Al/Cu	2.56	-8.16	2.56
8	SS	150	25	SiC	400	Al/Cu	1.75	-4.86	1.75
9	SS	100	35	SiC	Mix	Al/Cu	1.70	-4.60	1.70
10	HSS	150	30	SiC	280	Al/Si	1.83	-5.24	1.83
11	HSS	100	25	SiC	400	Al/Si	1.72	-4.71	1.72
12	HSS	200	35	SiC	Mix	Al/Si	1.81	-5.15	1.81
13	HSS	150	25	SiC	280	Al/Cu	1.96	-5.46	1.87

14	HSS	100	35	SiC	400	Al/Cu	1.69	-4.66	1.71
15	HSS	200	30	SiC	Mix	Al/Cu	1.86	-5.25	1.83
16	HSS	150	25	SiC	280	Al/Cu	1.79	-5.05	1.78
17	HSS	100	35	SiC	400	Al/Cu	1.73	-4.78	1.75
18	HSS	200	30	SiC	Mix	Al/Cu	1.80	-5.15	1.82
19	SS	100	25	Al_2O_3	280	Al/Cu	1.78	-5.00	1.78
20	SS	200	35	Al_2O_3	400	Al/Cu	1.86	-5.39	1.86
21	SS	150	30	Al_2O_3	Mix	Al/Cu	1.69	-4.55	1.69
22	SS	200	25	Al_2O_3	280	Al/Cu	2.10	-6.44	2.10
23	SS	150	35	Al_2O_3	400	Al/Cu	1.82	-5.20	1.82
24	SS	100	30	Al_2O_3	Mix	Al/Cu	1.69	-4.55	1.69
25	SS	200	35	Al_2O_3	280	Al/Si	2.06	-6.27	2.06
26	SS	150	30	Al_2O_3	400	Al/Si	1.86	-5.39	1.86
27	SS	100	25	Al_2O_3	Mix	Al/Si	1.79	-5.05	1.79
28	HSS	200	35	Al_2O_3	280	Al/Cu	2.06	-6.27	2.06
29	HSS	150	30	Al_2O_3	400	Al/Cu	1.90	-5.57	1.90
30	HSS	100	25	Al_2O_3	Mix	Al/Cu	1.87	-5.43	1.87
31	HSS	150	35	Al_2O_3	280	Al/Si	1.91	-5.62	1.91
32	HSS	100	30	Al_2O_3	400	Al/Si	1.76	-4.91	1.76
33	HSS	200	25	Al_2O_3	Mix	Al/Si	2.01	-6.06	2.01
34	HSS	100	35	Al_2O_3	280	Al/Si	1.86	-5.39	1.86
35	HSS	200	30	Al_2O_3	400	Al/Si	1.96	-5.84	1.96
36	HSS	150	25	Al_2O_3	Mix	Al/Si	1.89	-5.29	1.89

6.3 ANOVA of Means for Surface Roughness

The results for SR were analyzed using ANOVA for identifying the significant factors affecting the performance measures. The Analysis of Variance (ANOVA) for the mean SR at 95% confidence interval is given in Table 6.2. The variance data for each factor and their interactions were F-tested to find significance of each. ANOVA table shows that the Grit size (F value 7.530), Power rating (F value 13.24) and interaction between slurry type and tool (F value 6.97) are the significant factors that are affecting SR. The type of slurry, tool, workpiece, concentration and the interactions D×E and D×F are

found to be insignificant. Table 6.3 shows ranks to various input parameters in terms of their relative significance.

Table 6.2 ANOVA of Means for SR

Sources	SS	DF	(V)	F	F (CRITICAL)	SS'	% age Contribution	STATUS
Slurry Type (A)	0.0012	1	0.0012	0.102	4.84			Insignificant
Tool (B)	0.0031	1	0.0031	0.264	4.84			Insignificant
Workpiece (C)	.00004	1	.00004	0.003	4.84			Insignificant
Grit Size (D)	0.1765	2	0.0882	7.530	2.98	0.1541	18.39	Significant
Slurry Concentration (%) (E)	0.0085	2	0.0042	0.363	2.98			Significant
Power Rating (F)	0.3101	2	0.1550	13.24	2.98	0.2876	34.32	Significant
A×B	0.0816	1	0.0816	6.970	4.84	.0704	8.40	Significant
D×E	0.0799	4	0.0199	1.700	3.36			Insignificant
D×F	0.0477	4	0.0119	1.017	3.36			Insignificant
Residual Error	0.1288	11	0.0117					
Total	0.8378	29	0.0288					
e-pooled	0.2692	24	0.0112				38.89	

Table 6.3: Response Table of Means for SR

Level	Type Of Slurry	Tool	Work piece	Grit Size	Slurry Concentration	Power Rating
1	1.882	1.866	1.880	1.984	1.876	1.769
2	1.869	1.887	1.873	1.832	1.889	1.838
3				1.813	1.865	2.023
Delta	0.013	0.020	0.006	0.171	0.024	0.253
Rank	5	4	6	2	3	1

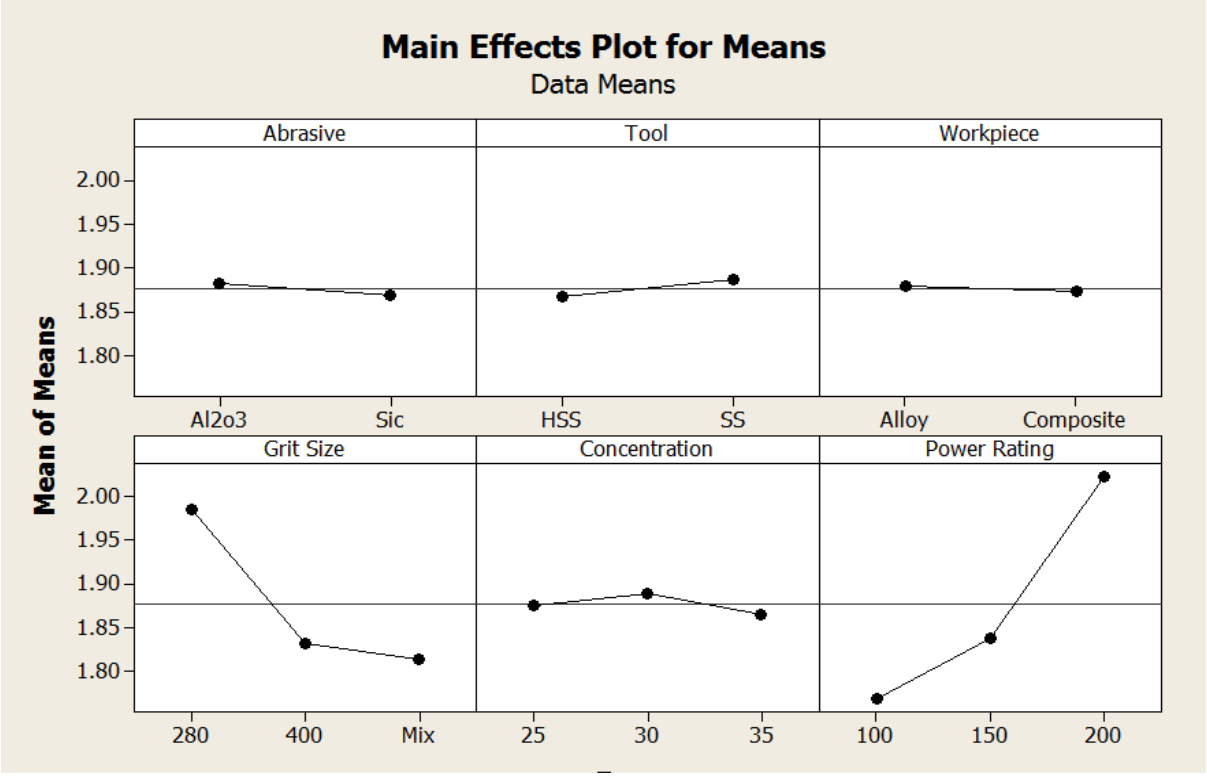

Figure 6.1 Main Effects Plot of Means for Surface Roughness

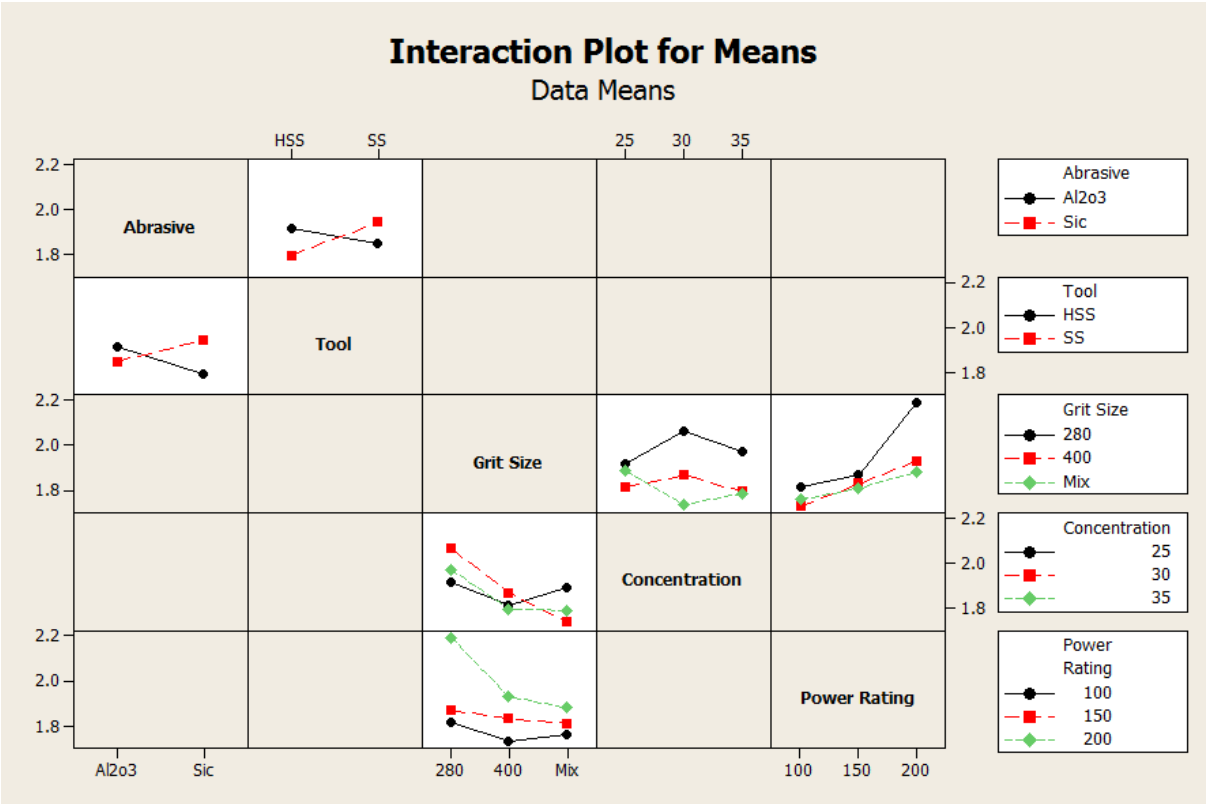

Figure 6.2 Interaction Plots of Means for Surface Roughness

6.4 ANOVA of S/N Ratio for Surface Roughness

The S/N ratio consolidates several repetitions into one value and is an indication of the amount of variation present. The S/N ratio has been calculated to identify the major contributing factors and interactions that cause variation in the SR. SR is "Lower is Better" type response which is given by:

LB: S/N ratio = -10 $log_{10}\left\{\frac{1}{n}\sum_1^n y_i^2\right\}$ (Equation 6.2)

Table 6.4 shows the ANOVA for S/N ratio for SR at 95% confidence interval. The power rating is the most significant factor in affecting SR followed by the Grit size and interaction A×B according to F-test. Main effect plot and residual plot for S/N ratios for SR are shown in figure 6.3 and figure 6.4 respectively

Table 6 .4: ANOVA of S/N Ratio for SR

Sources	SS	DF	(V)	F	F CRITICAL	SS'	% age Contribution	STATUS
Slurry Type (A)	0.0637	1	0.0637	0.305	4.54			Insignificant
Tool (B)	0.0219	1	0.0219	0.105	4.54			Insignificant
Workpiece (C)	0.0037	1	0.0037	0.017	4.54			Insignificant
Grit Size (D)	3.3382	2	1.6691	8.012	3.68	2.9216	19.07	Significant
Concentration (E)	0.1193	2	0.0596	0.286	3.68			Insignificant
Power Rating (F)	6.0797	2	3.039	14.589	3.68	5.6631	36.96	Significant
A×B	1.4839	1	1.4839	7.119	4.54	1.0673	6.92	Significant
A×D	0.5286	2	0.2643	1.2749	3.68			Insignificant
A×F	0.5486	2	0.2743	1.3136	3.68			Insignificant
Residual Error	3.1259	15	0.2083					
Total	15.3135	29	0.5280					
e-pooled	4.411	24	0.1839				37.05	

Table 6.5: Response table of S/N ratio for SR

Level	Type Of Slurry	Tool	Workpiece	Grit Size	Slurry Concentration	Power Rating
1	5.474	5.409	5.431	5.905	5.449	4.949
2	5.380	5.463	5.442	5.246	5.465	5.282
3				5.158	5.395	6.078
Delta	0.094	0.054	0.011	0.747	0.071	1.128
Rank	3	5	6	2	4	1

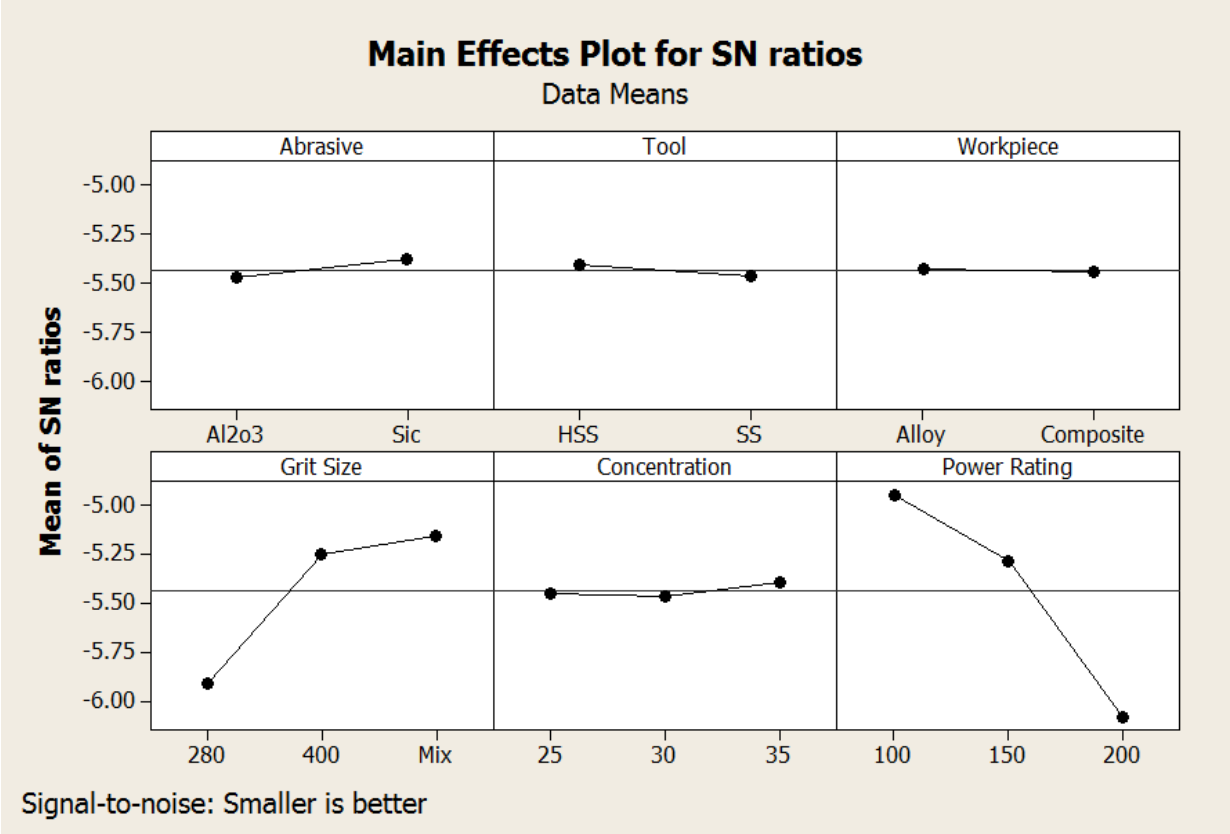

Figure 6.3 Main Effects Plot of S/N ratio for Surface Roughness

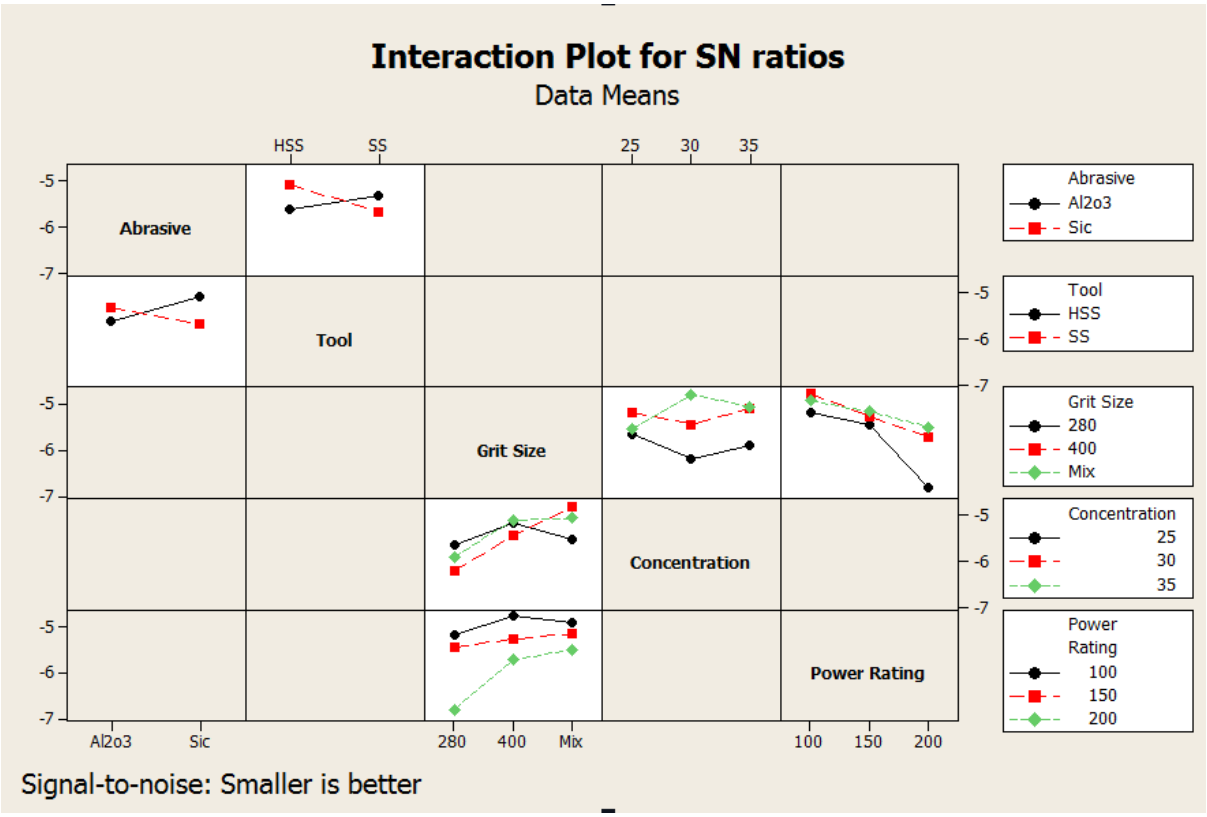

Figure 6.4 Interaction Plot of S/N ratio for Surface Roughness

6.5 Optimal design for SR

In this experimentation analysis, the main effect plot and interaction plot in Figure 6.1 and Figure 6.2 were used to estimate the mean SR. From table 6.6 it is concluded that lowest SR is observed when workpiece was machined at Power rating (150) and Grit size (Mix). It is also observed that the interaction A×B is significant and affecting the SR.

Table 6.6 Significant Factors and Interactions

Factors	Affecting Mean		Affecting Variation	
	Contribution	Best Level	Contribution	Best Level
Slurry				
Tool				
Work piece				
Grit Size	Significant	Level 3 (Mix)	Significant	Level 3 (Mix)
Concentration				
Power Rating	Significant	Level 1 (150)	Significant	Level 1 (150)
A×B	Significant		Significant	
D×E				
D×F				

Estimating the mean

In experimental analysis, SR is a lower average response is better (LB) characteristic. Depending on the characteristic, different treatment combinations has been chosen to obtain satisfactory analysis. After conducting the experiments the optimum treatment condition within the experiments determined on the basis of prescribed combination of factor levels is determined to one of those in the experiment. The mean value of SR ($\bar{T}$) is 1.87. The formulae for calculating the theoretical optimal value is as under:

$(SR)_{opt}$ = $\bar{T}$ + (D_3-$\bar{T}$) + (F_1-$\bar{T}$) (Equation 6.3)

= 1.87 + (1.87-1.82) + (1.87-1.84)

= 1.95 μm

CI = $\sqrt{\frac{F_{\alpha,V1,V2}}{\eta eff}}$ (Equation 6.4)

Where $F_{\alpha,V1,V2}$ = F ratio $\alpha = risk$ (0.05)

Confidence = 1 - α

V_1 = dof for mean which is always = 1

V_2 = dof for error = V_e

ηeff = No.of tests under that condition using the particular factors

ηeff = N / (1+ dof_{D+F+AB}) = 36 / (1+1+2+2) = 6

CI = $\sqrt{4.26 \times .0112 / 6}$ = 0.589

= 0.089

So the confidence interval around the Surface Roughness is given by 1.87 $\pm$ 0.09 μm .

CHAPTER 7

RESULTS AND ANALYSIS OF HARDNESS

7.1 Introduction

The Rockwell scale is a hardness scale based on the indentation hardness of a material. The Rockwell test determines the hardness by measuring the depth of penetration of an indenter under a large load compare to the penetration made by a preload.

7.2 Results for Hardness

The results for Hardness for each of the 36 treatment conditions are shown in table 7.1.

Table 7.1: Results for Hardness

Trail No.	Tool	Power Rating	Slurry Concentration (%)	Type of Slurry	Grit Size	Work piece	Hardness(HRB)	S/N Ratio	Mean
1	SS	100	30	SiC	280	Al/Si	40.25	31.12	40.37
2	SS	200	25	SiC	400	Al/Si	41.00	32.30	41.25
3	SS	150	35	SiC	Mix	Al/Si	40.00	32.14	40.50
4	SS	100	30	SiC	280	Al/Si	40.50	32.14	40.50
5	SS	200	25	SiC	400	Al/Si	41.50	32.36	41.50
6	SS	150	35	SiC	Mix	Al/Si	41.00	32.30	41.00
7	SS	200	30	SiC	280	Al/Cu	44.00	32.86	44.00
8	SS	150	25	SiC	400	Al/Cu	43.50	32.76	43.50
9	SS	100	35	SiC	Mix	Al/Cu	43.00	32.66	43.00
10	HSS	150	30	SiC	280	Al/Si	40.50	32.14	40.50
11	HSS	100	25	SiC	400	Al/Si	40.00	32.04	40.00
12	HSS	200	35	SiC	Mix	Al/Si	40.50	32.14	40.50
13	HSS	150	25	SiC	280	Al/Cu	44.00	32.91	44.25
14	HSS	100	35	SiC	400	Al/Cu	43.00	32.71	43.25
15	HSS	200	30	SiC	Mix	Al/Cu	43.50	32.76	43.50
16	HSS	150	25	SiC	280	Al/Cu	44.50	32.14	44.50
17	HSS	100	35	SiC	400	Al/Cu	43.50	32.76	43.50
18	HSS	200	30	SiC	Mix	Al/Cu	43.50	32.76	43.50
19	SS	100	25	Al_2O_3	280	Al/Cu	43.00	32.66	43.00
20	SS	200	35	Al_2O_3	400	Al/Cu	43.50	32.76	43.50
21	SS	150	30	Al_2O_3	Mix	Al/Cu	43.25	32.71	43.25
22	SS	200	25	Al_2O_3	280	Al/Cu	44.50	32.96	44.50

23	SS	150	35	Al_2O_3	400	Al/Cu	43.50	32.76	43.50
24	SS	100	30	Al_2O_3	Mix	Al/Cu	43.00	32.66	43.00
25	SS	200	35	Al_2O_3	280	Al/Si	42.00	32.46	42.00
26	SS	150	30	Al_2O_3	400	Al/Si	41.50	32.36	41.50
27	SS	100	25	Al_2O_3	Mix	Al/Si	41.25	32.30	41.25
28	HSS	200	35	Al_2O_3	280	Al/Cu	44.50	32.96	44.50
29	HSS	150	30	Al_2O_3	400	Al/Cu	43.50	32.76	43.50
30	HSS	100	25	Al_2O_3	Mix	Al/Cu	44.00	32.86	44.00
31	HSS	150	35	Al_2O_3	280	Al/Si	40.50	32.14	40.50
32	HSS	100	30	Al_2O_3	400	Al/Si	40.00	32.04	40.00
33	HSS	200	25	Al_2O_3	Mix	Al/Si	40.25	32.09	40.25
34	HSS	100	35	Al_2O_3	280	Al/Si	40.50	32.14	40.50
35	HSS	200	30	Al_2O_3	400	Al/Si	41.50	32.36	41.50
36	HSS	150	25	Al_2O_3	Mix	Al/Si	40.50	32.14	40.50

7.3. ANOVA of Means for Hardness

The results for Hardness were analyzed using ANOVA for identifying the significant factors affecting the performance measures. The Analysis of Variance (ANOVA) for the mean Hardness at 95% confidence interval is given in Table 7.2. The variance data for each factor and their interactions were F-tested to find significance of each. ANOVA table shows that the tool (F value 21.61), workpiece (F value 319.18) and power rating (F value 6.12) are the significant factors and affecting hardness. All other factors and interactions are found insignificant. Table 7.3 shows ranks to various input parameters in terms of their relative significance.

Table 7.2 ANOVA of Means for Hardness

Sources	**SS**	**DF**	**(V)**	**F**	**F (CRITICAL)**	**SS'**	**% age Contribution**	**STATUS**
Slurry (A)	0.323	1	0.323	1.77	4.75			Insignificant
Tool (B)	3.942	1	3.942	21.61	4.75	3.69	5.21	Significant
Workpiece (C)	58.22	1	58.22	319.18	4.75	57.96	81.86	Significant
Grit Size (D)	0.969	2	0.484	2.65	3.79			Insignificant
Slurry Concentration (E)	0.132	2	0.066	0.36	3.79			Insignificant
Power Rating (F)	2.235	2	1.117	6.12	3.79	1.733	2.44	Significant
B×D	0.143	2	0.071	0.39	3.79			Insignificant
B×F	0.125	2	0.062	0.342	3.79			Insignificant
D×F	2.393	4	0.598	3.28	3.36			Insignificant

Residual Error	2.188	12	0.182					
Total	70.802	29	2.440					
e-pooled	6.27	25	0.251					

Table 7.3: Response Table of Means for Hardness

Level	Type Of Slurry	Tool	Workpiece	Grit Size	Slurry Concentration	Power Rating
1	42.26	41.82	43.62	42.41	42.25	41.84
2	42.05	42.54	40.74	42.15	42.11	42.15
3				41.98	42.17	42.56
Delta	0.21	0.72	2.88	0.44	0.14	0.71
Rank	5	2	1	4	6	3

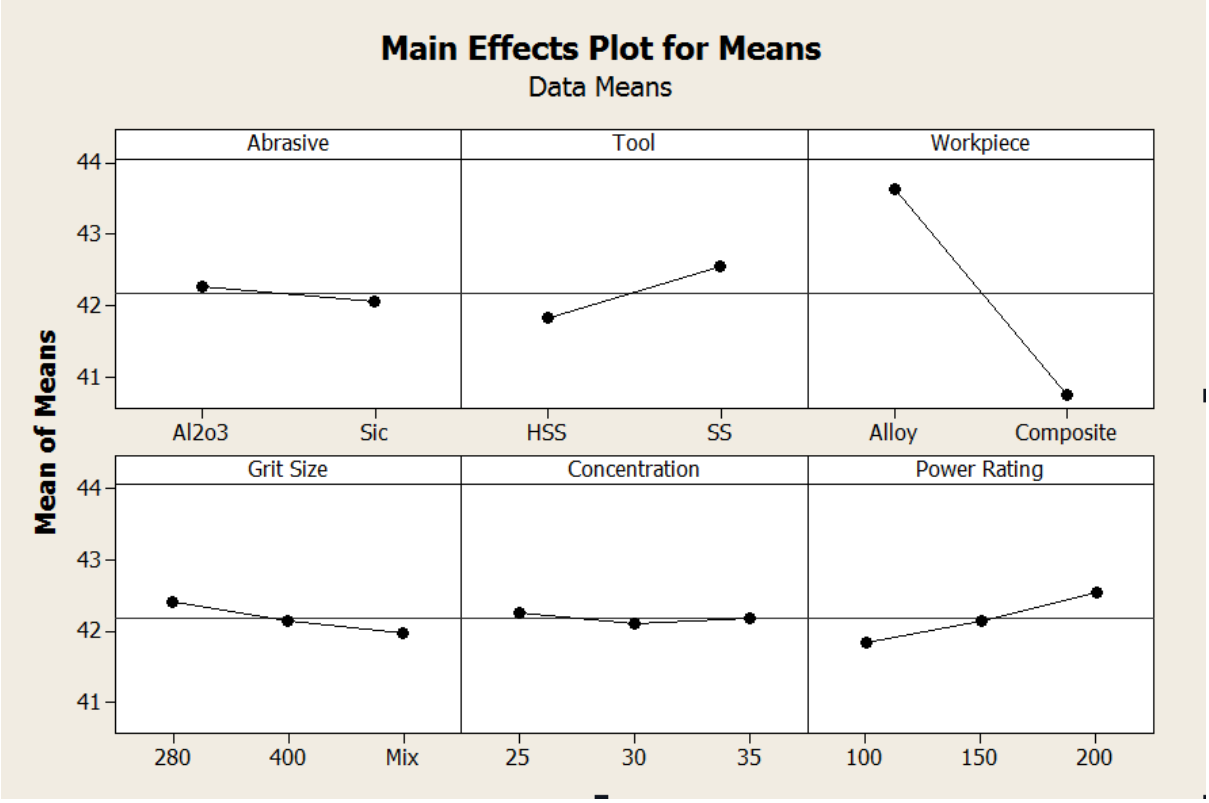

Figure 7.1 Main Effects Plot of Means for Hardness

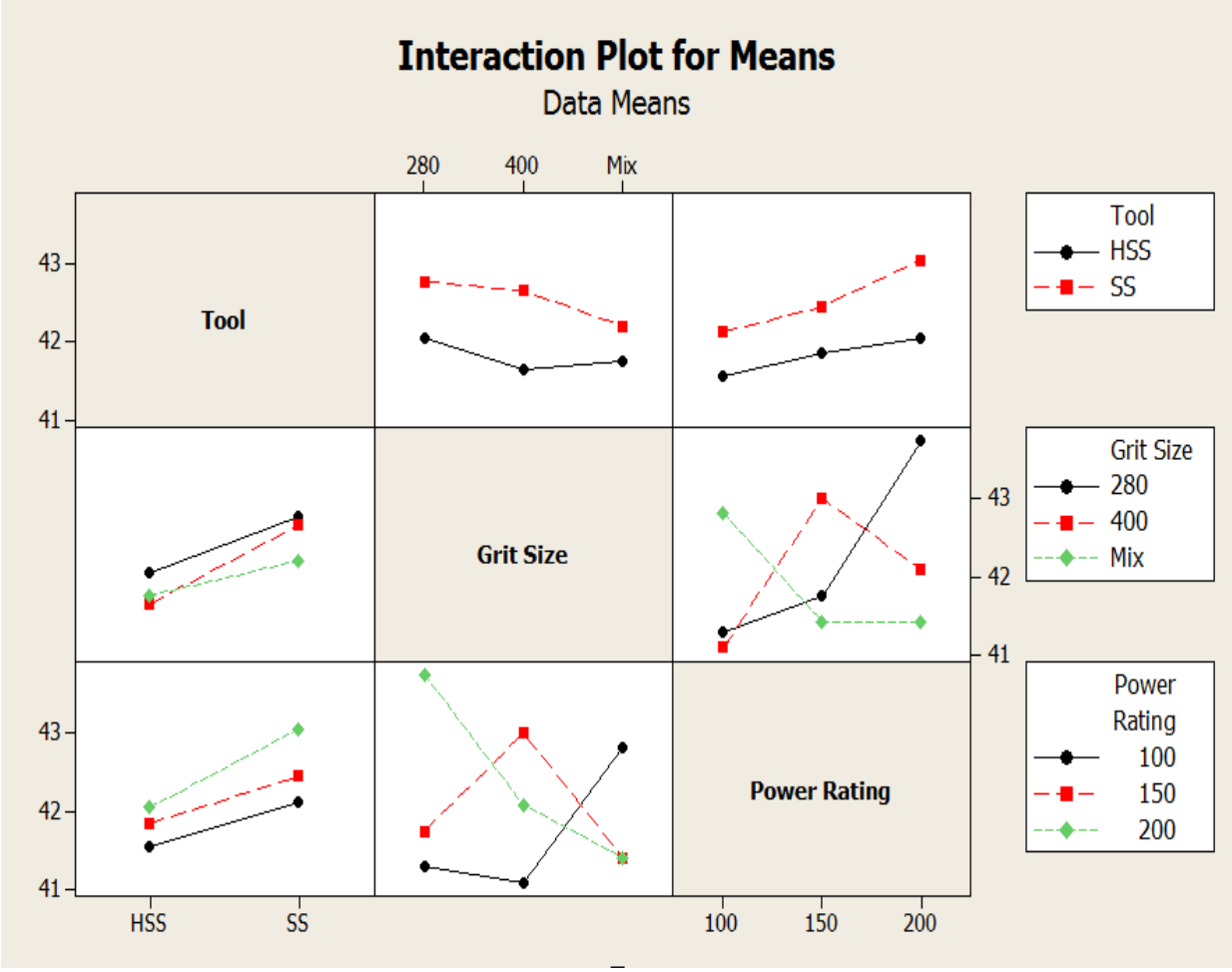

Figure 7.2 Interaction Plots of Means for Hardness

7.4 ANOVA of S/N Ratio for Hardness

The S/N ratio consolidates several repetitions into one value and is an indication of the amount of variation present. The S/N ratio has been calculated to identify the major contributing factors and interactions that cause variation in the hardness. Hardness is "Higher is better" type response which is given by:

$$\text{HB: S/N ratio} = -10\ log_{10}\left\{\frac{1}{n}\sum_1^n \frac{1}{y_i^2}\right\} \qquad \text{(Equation 7.1)}$$

Table 7.4 shows the ANOVA for S/N ratio for Hardness at 95% confidence interval. The workpiece is the most significant factor in affecting Hardness followed by tool and power rating according to F-test. Main effect plot for S/N ratios for Hardness are shown in figure 7.4 and figure 7.5 respectively.

Table 7.4: ANOVA of S/N ratio for Hardness

Sources	SS	DF	(V)	F	F (CRITICAL)	SS'	% age Contribution	STATUS
Slurry (A)	0.014	1	0.014	1.78	4.75			Insignificant
Tool (B)	0.174	1	0.174	21.8	4.75	0.16	5.39	Significant
Workpiece (C)	2.469	1	2.469	307.5	4.75	2.45	81.40	Significant
Grit Size (D)	0.038	2	0.019	2.375	3.79			Insignificant
Concentration (E)	0.004	2	0.002	0.30	3.79			Insignificant
Power Rating (F)	0.099	2	0.049	6.21	3.79	0.07	2.49	Significant
B×D	0.005	2	0.002	0.36	3.79			Insignificant
B×F	0.044	2	0.022	2.70	3.79			Insignificant
D×F	0.102	4	0.025	3.12	3.36			Insignificant
Residual Error	0.096	12	0.008					
Total	3.010	29	0.103					
e-pooled	0.306	25	0.012				10.72	

7.5: Response table of S/N ratio for Hardness

Level	Type Of Slurry	Tool	Workpiece	Grit Size	Slurry Concentration (%)	Power Rating
1	32.51	32.42	32.79	32.54	32.51	32.43
2	32.47	32.57	32.20	32.49	32.48	32.49
3				32.45	32.50	32.57
Delta	0.04	0.15	0.59	0.09	0.03	0.15
Rank	5	2	1	4	6	3

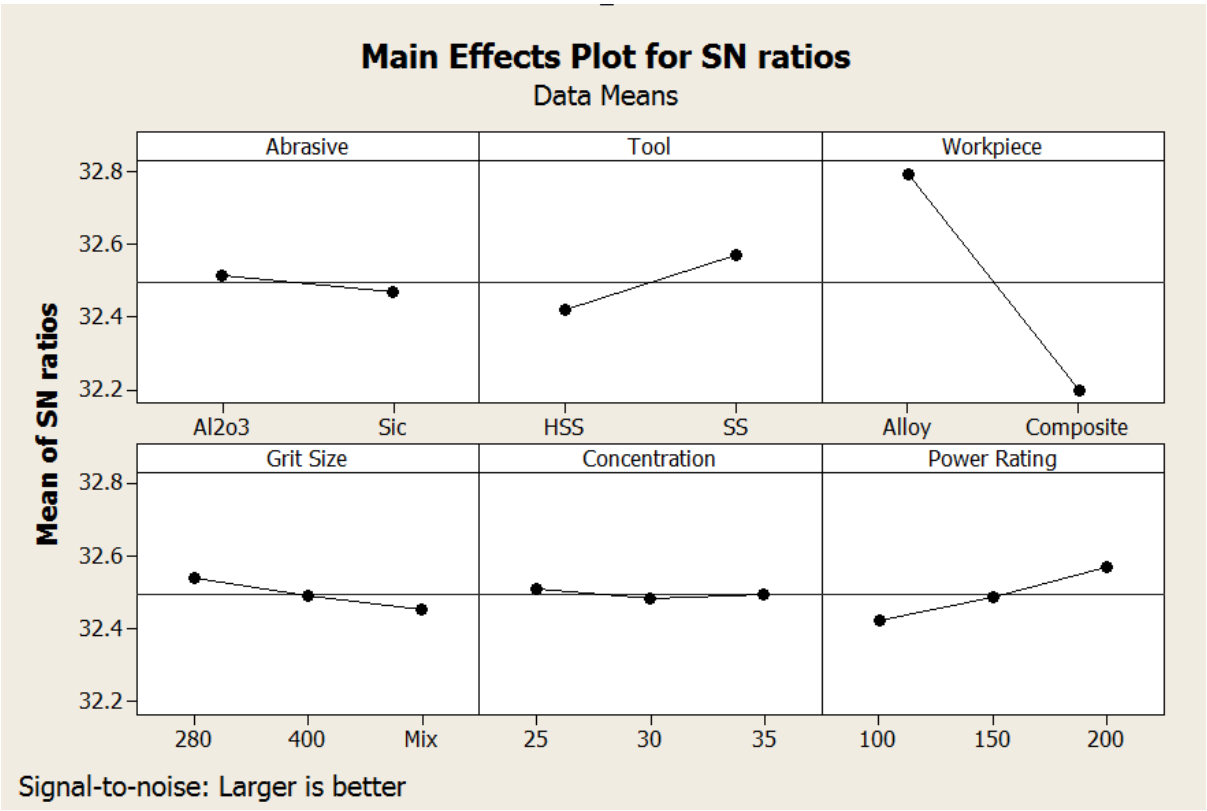

Figure 7.3 Main Effects Plot of S/N ratio for Hardness

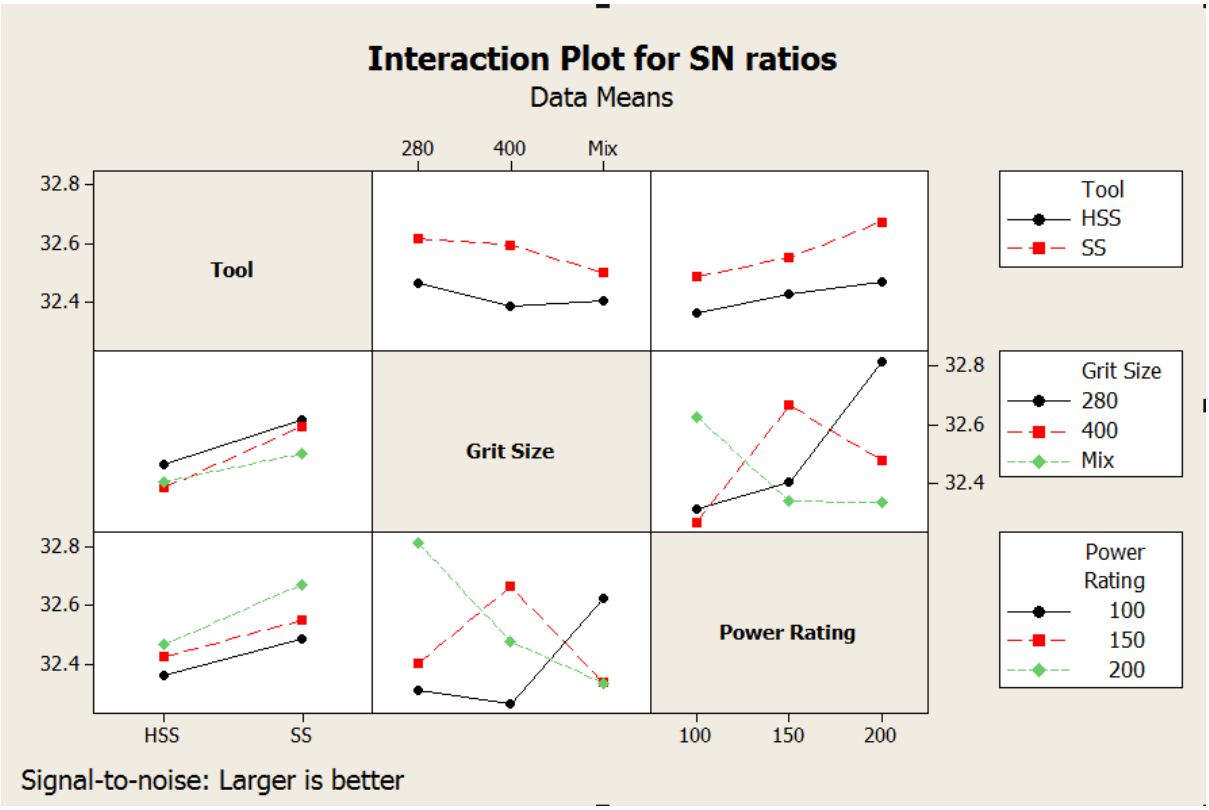

Figure 7.4 Interaction Plots of S/N ratio for Hardness

7.5 Optimal design for Hardness

In this experimentation analysis, the main effect plot and interaction plot in Figure 7.1 and Figure 7.2 were used to estimate the mean Hardness. From table 7.5 it is concluded that Mean and S/N ratio both are affected by Tool, Workpiece and Power Rating. All other factors and their interactions are found insignificant. Hardness assumed to be achieved best when workpiece Al/Si is machined by High Speed Steel Tool with Power Rating of 150.

Table 7.6: Significant Factors and Interactions

Factors	Affecting Mean		Affecting Variation	
	Contribution	**Best Level**	**Contribution**	**Best Level**
Slurry				
Tool	Significant	Level 2 (HSS)	Significant	Level 2 (HSS)
Work piece	Significant	Level 1 (Al/Si)	Significant	Level 1 (Al/Si)
Grit Size				
Concentration				
Power Rating	Significant	Level 3 (150)	Significant	Level 3 (150)

Estimating the mean

In experimental analysis, Hardness is a higher average response is better (HB) characteristic. Depending on the characteristic, different treatment combinations has been chosen to obtain satisfactory analysis. After conducting the experiments the optimum treatment condition within the experiments determined on the basis of prescribed combination of factor levels is determined to one of those in the experiment. The mean value of Hardness ($\bar{T}$) is 44.618. The formulae for calculating the theoretical optimal value is as under:

$(Hardness)_{opt}$ $=\bar{T} + (B_2\text{-}\bar{T}) + (C_1\text{-}\bar{T}) + (F_3\text{-}\bar{T})$ (Equation 7.2)

= 44.618 + (39.902 – 44.618) + (40.736 – 44.618) + (42.187-44.618)

= 33.589 HRB

CI = $\sqrt{\frac{F_{\alpha,V1,V2}}{\eta eff}}$ (Equation 7.3)

Where $F_{\alpha,V1,V2}$ = F ratio

$\alpha = risk\ (0.05)$

Confidence = 1 - α

V_1 = dof for mean which is always = 1

V_2= dof for error = V_e

ηeff = No.of tests under that condition using the particular factors

ηeff = N / (1+ dof_{B+C+F}) = 36 / (1+1+1+2) = 7.2

CI = $\sqrt{4.75 \times\ 0.251\ /7.2}$ = 0.4069

So, the Confidence Interval around the Hardness is given by 36.59 $\pm$ 0.407 HRB.

CHAPTER 8

OVALITY

8.1 Introduction

Ovality or Non circularity is the degree of deviation from perfect circularity of the cross section. Total 36 experiments were performed and each performs only at once.

8.2 Results for Ovality

Ovality is measured from the centre of every sample. It is a 'Lower is Better' phenomena. Total 36 experiments are performed to measure the Ovality of every sample by the profile projector and the following results are obtained:

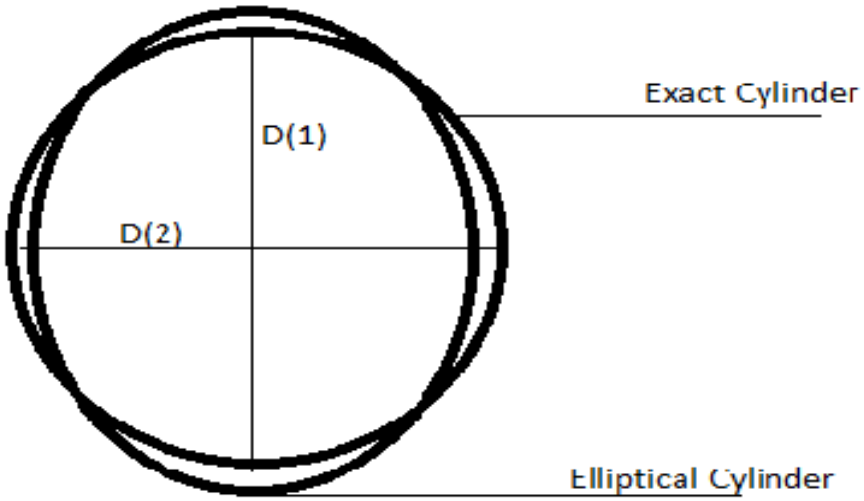

Figure 8.1: Measurement of circularity [49]

It is observed that when workpiece of Al/Si Composite was machined by SS tool, with SiC as abrasive slurry of 400 grit size at power rating of 200 and having slurry concentration 25%.

Table 8.1 Results for Ovality

Trail No.	Tool	Power Rating	Slurry Concentration (%)	Type of Slurry	Grit Size	Work piece	Dia.1	Dia. 2	Ovality
1	SS	100	30	SiC	280	Al/Si	6.592	6.547	
2	SS	200	25	SiC	400	Al/Si	6.660	6.616	
3	SS	150	35	SiC	Mix	Al/Si	6.645	6.675	
4	SS	100	30	SiC	280	Al/Si	6.624	6.671	
5	SS	200	25	SiC	400	Al/Si	6.644	6.732	Oval
6	SS	150	35	SiC	Mix	Al/Si	6.673	6.624	
7	SS	200	30	SiC	280	Al/Cu	6.648	6.661	
8	SS	150	25	SiC	400	Al/Cu	6.620	6.637	
9	SS	100	35	SiC	Mix	Al/Cu	6.598	6.602	
10	HSS	150	30	SiC	280	Al/Si	6.699	6.693	
11	HSS	100	25	SiC	400	Al/Si	6.613	6.698	
12	HSS	200	35	SiC	Mix	Al/Si	6.746	6.741	
13	HSS	150	25	SiC	280	Al/Cu	6.665	6.685	
14	HSS	100	35	SiC	400	Al/Cu	6.676	6.678	
15	HSS	200	30	SiC	Mix	Al/Cu	6.762	6.720	
16	HSS	150	25	SiC	280	Al/Cu	6.673	6.703	
17	HSS	100	35	SiC	400	Al/Cu	6.663	6.670	
18	HSS	200	30	SiC	Mix	Al/Cu	6.704	6.735	
19	SS	100	25	Al_2O_3	280	Al/Cu	6.610	6.567	
20	SS	200	35	Al_2O_3	400	Al/Cu	6.635	6.682	
21	SS	150	30	Al_2O_3	Mix	Al/Cu	6.599	6.593	
22	SS	200	25	Al_2O_3	280	Al/Cu	6.634	6.609	
23	SS	150	35	Al_2O_3	400	Al/Cu	6.669	6.636	
24	SS	100	30	Al_2O_3	Mix	Al/Cu	6.508	6.541	
25	SS	200	35	Al_2O_3	280	Al/Si	6.617	6.623	
26	SS	150	30	Al_2O_3	400	Al/Si	6.677	6.686	
27	SS	100	25	Al_2O_3	Mix	Al/Si	6.289	6.250	
28	HSS	200	35	Al_2O_3	280	Al/Cu	6.652	6.609	
29	HSS	150	30	Al_2O_3	400	Al/Cu	6.703	6.752	
30	HSS	100	25	Al_2O_3	Mix	Al/Cu	6.527	6.527	
31	HSS	150	35	Al_2O_3	280	Al/Si	6.674	6.639	
32	HSS	100	30	Al_2O_3	400	Al/Si	6.703	6.752	
33	HSS	200	25	Al_2O_3	Mix	Al/Si	6.678	6.642	
34	HSS	100	35	Al_2O_3	280	Al/Si	6.652	6.648	
35	HSS	200	30	Al_2O_3	400	Al/Si	6.770	6.776	
36	HSS	150	25	Al_2O_3	Mix	Al/Si	6.685	6.654	

CHAPTER 9

MICROSTRUCTURE OF MACHINED SURFACE (SEM ANALYSIS)

9.1 Introduction

Further analysis of the machined surfaces after confirmation experiments was performed to find out surface morphology and microstructure. Micro structural analysis of machined surface was studied by using Scanning Electron Microscope (SEM). In this work, the effect of various input parameters i.e. tool, power rating, work piece, slurry concentration, type of slurry, and grit size on the surface microstructure of the work piece material has been explored.

9.2 Microstructure Analysis

Microstructure analysis was carried out on selected samples using Scanning Electron Microscope to study the change in the microstructure after machining. The samples were prepared as per standard before SEM analysis on three different magnifications namely 250 X, 800 X and 1000 X.

9.3 Preparing Samples for SEM

The steps for the preparation of sample for SEM are given below:

All the samples are cut into size of 10 mm.

Clean the surface of sample with wire brush.

Clean the samples with acetone using cotton so as to remove debris from the machined surface.

9.4 SEM Analysis

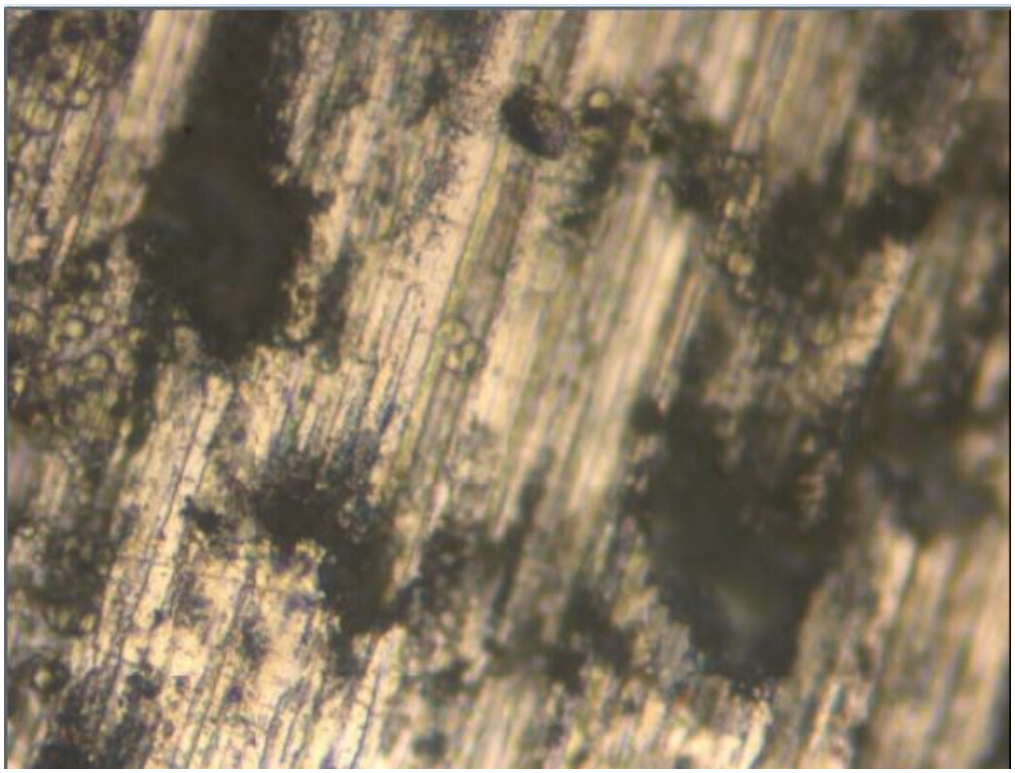

Figure 9.1: Micrograph at 50X of Al/Cu Alloy before machining.

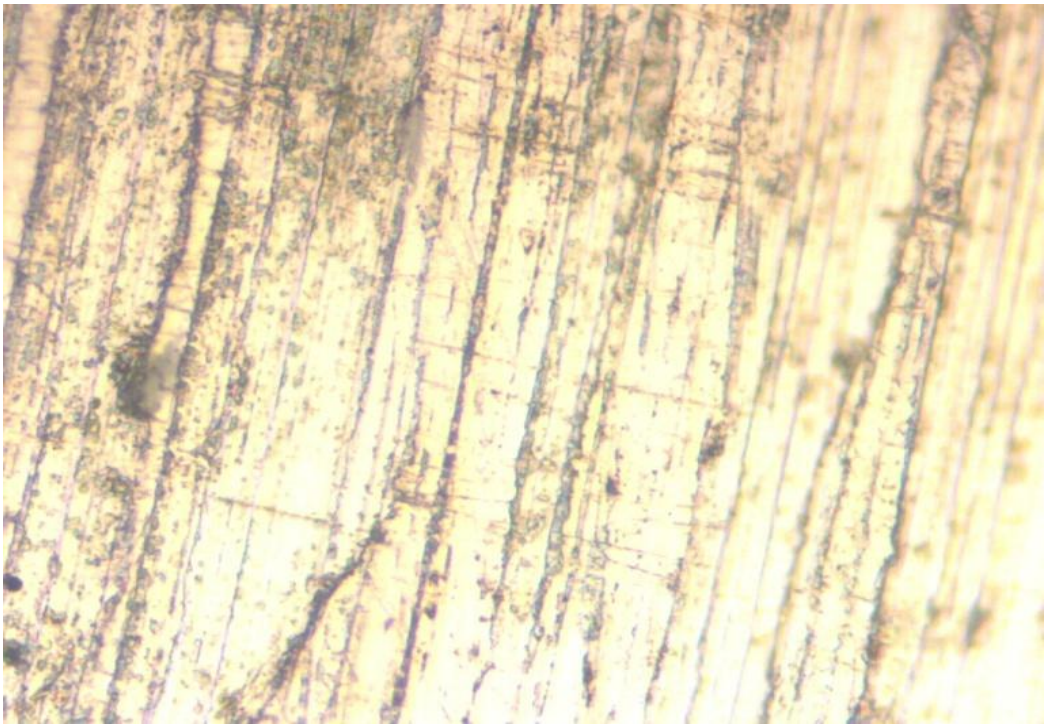

Figure 9.2: Micrograph at 50X of Al/Si Composite before machining.

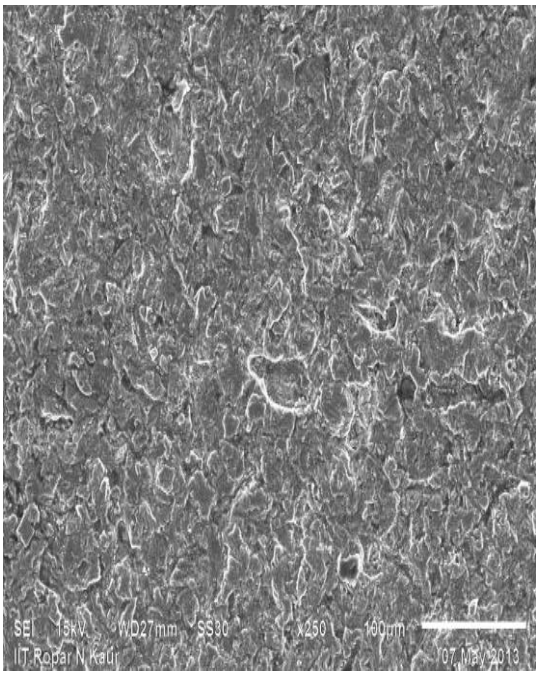

(a) 250

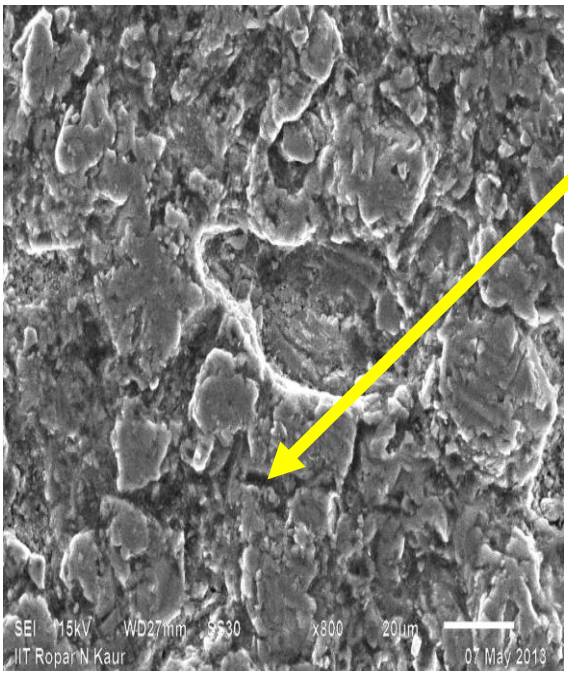

(b) 800

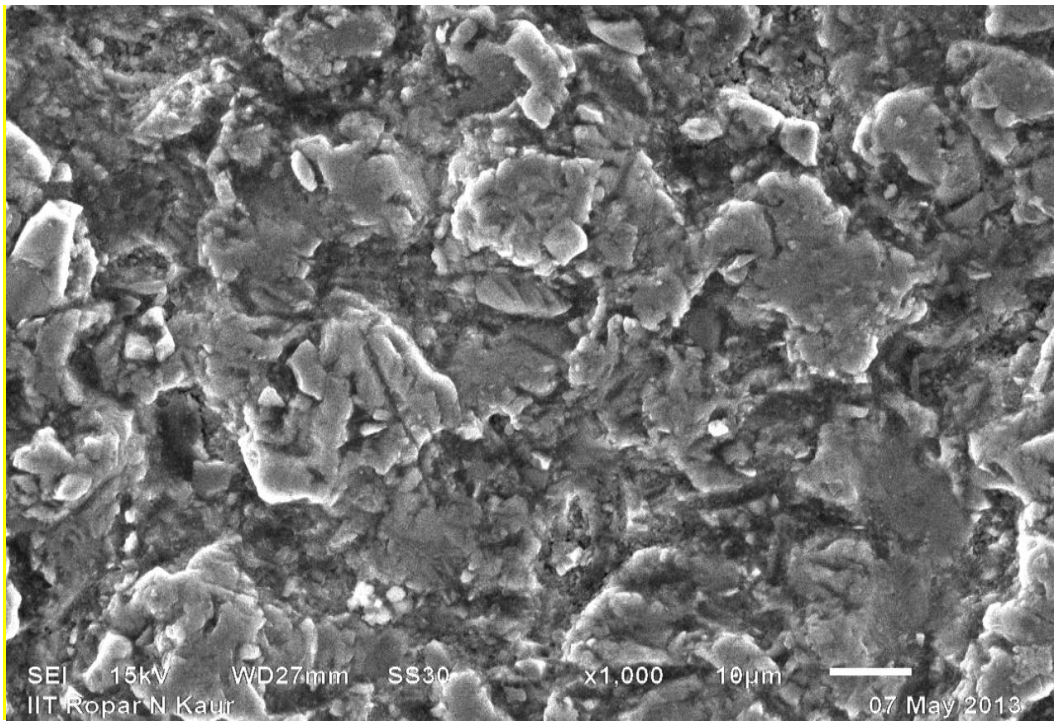

(c)1000

Figure 9.3: Micrograph of Al/Si Composite machined using SS tool with SiC as abrasive slurry SiC(Grit size 280, Slurry concentration 30% and Power rating 100W

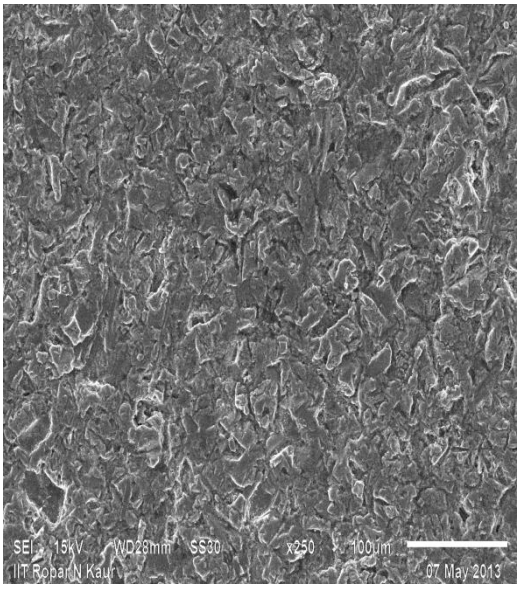

(a) 250

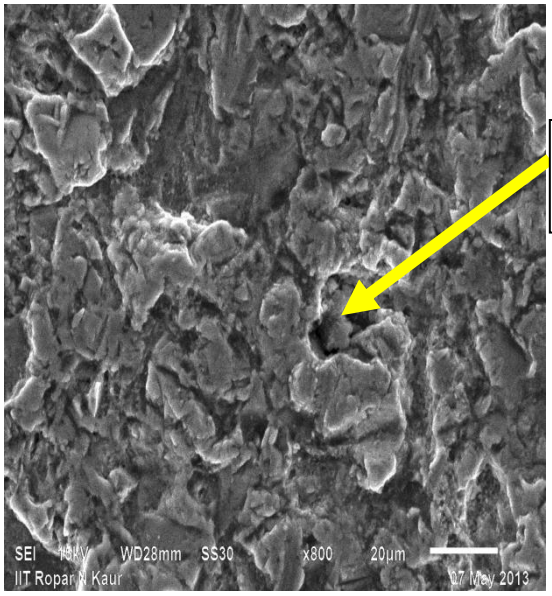

(b) 800

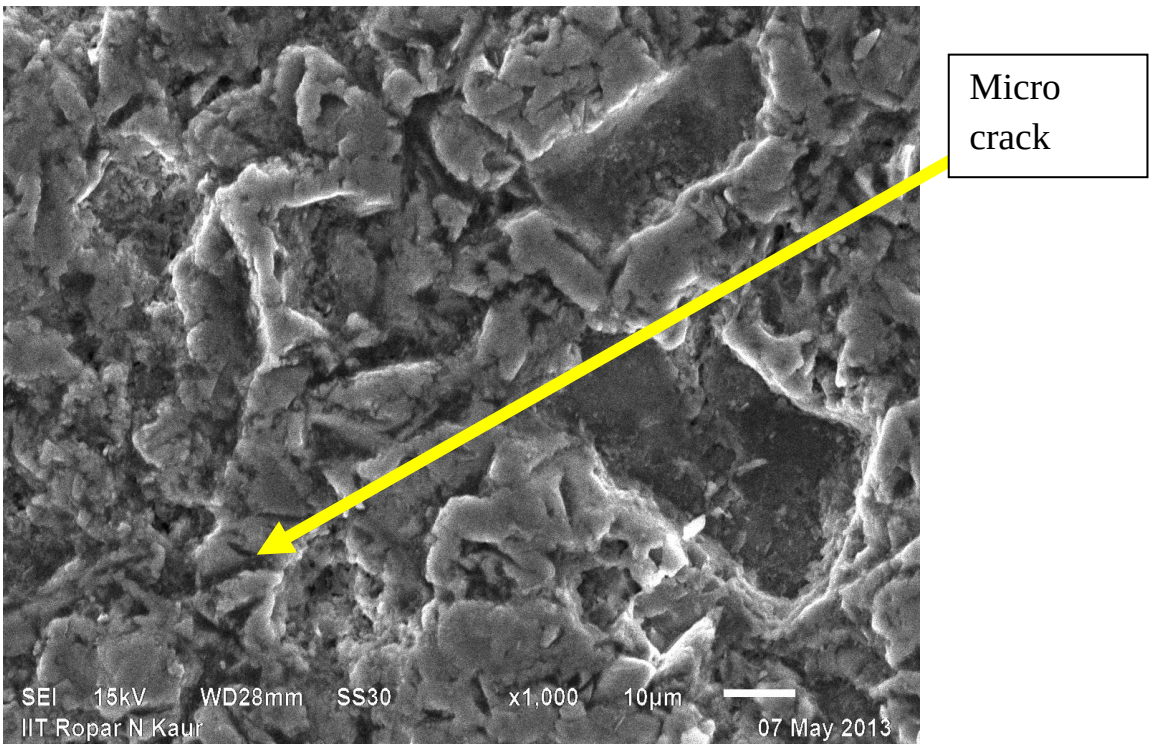

(c) 1000

Figure 9.4: Micrograph of Al/Si Composite machined using SS tool with SiC as abrasive slurry (Grit size Mix, Slurry concentration 35% and Power rating 150W)

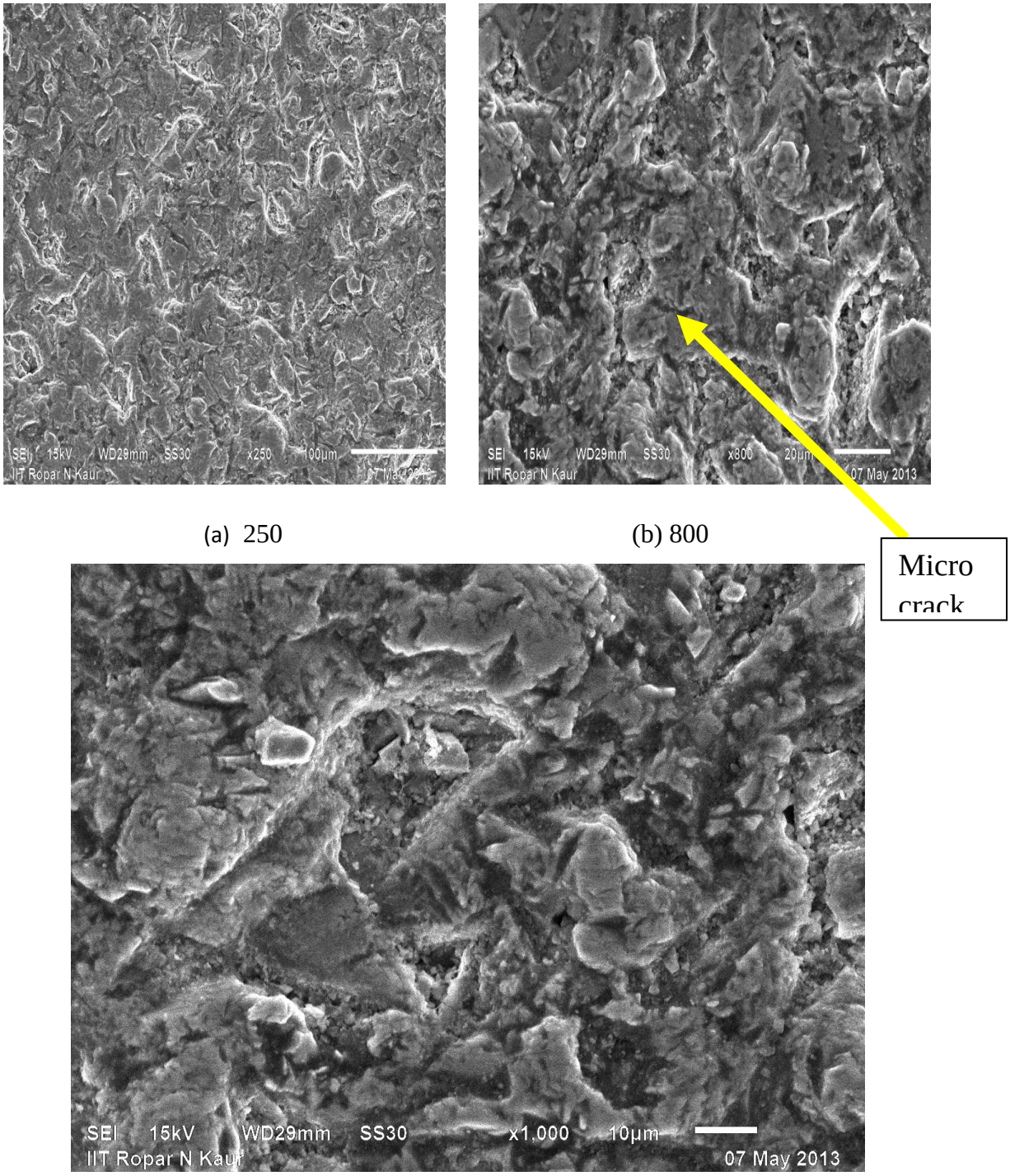

(a) 250

(b) 800

(c) 1000

Figure 9.5: Micrograph of Al/Cu Alloy machined using SS tool with SiC as abrasive slurry (Grit size 280, Slurry concentration 30% and Power rating 200W).

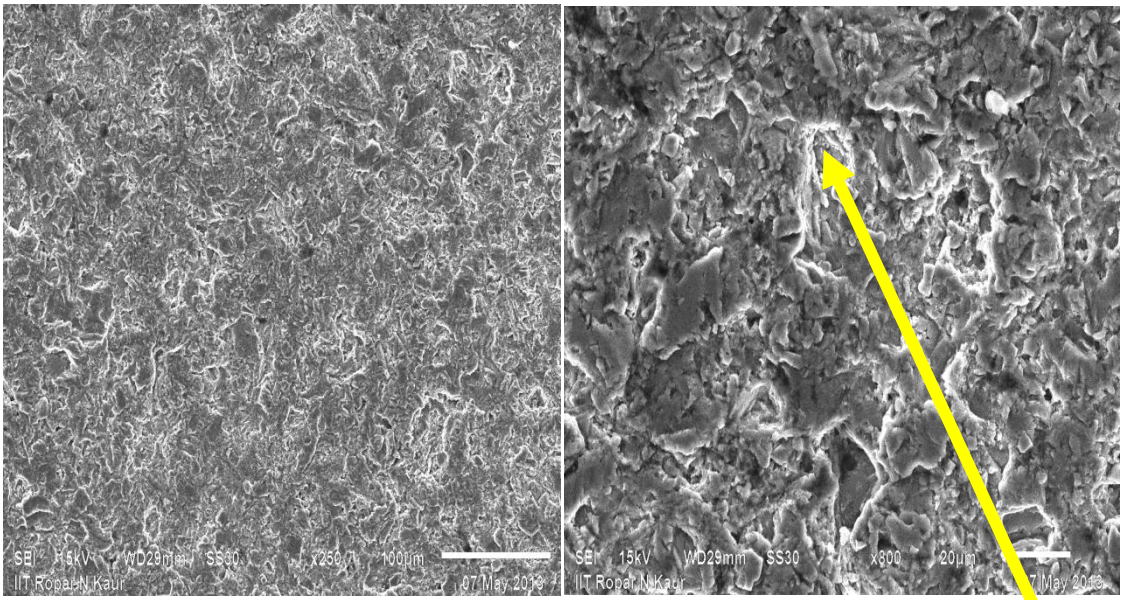

(a) 250 (b) 800

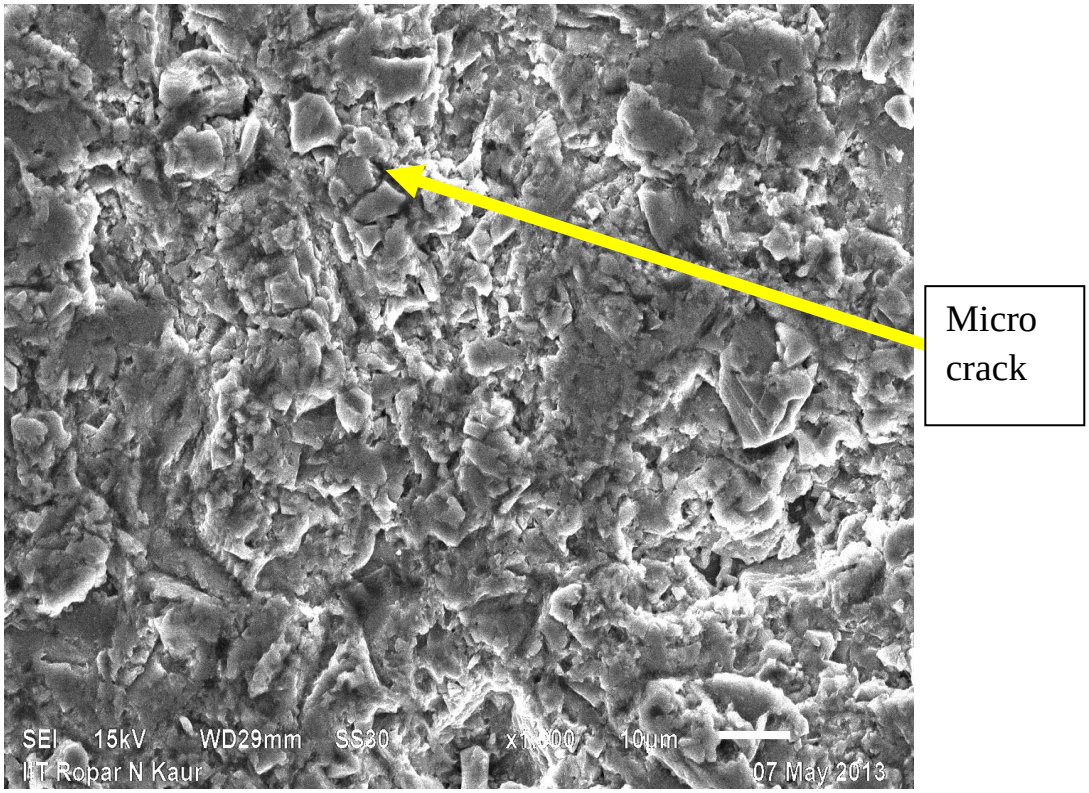

(c) 1000

Figure 9.6: Micrograph of Al/Cu Alloy machined using SS tool with SiC as abrasive slurry (Grit size Mix, Slurry concentration 35% and Power rating 100W).

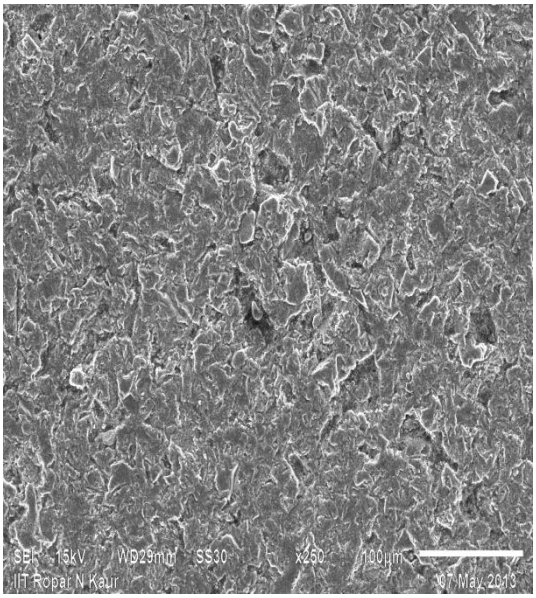

(a) 250

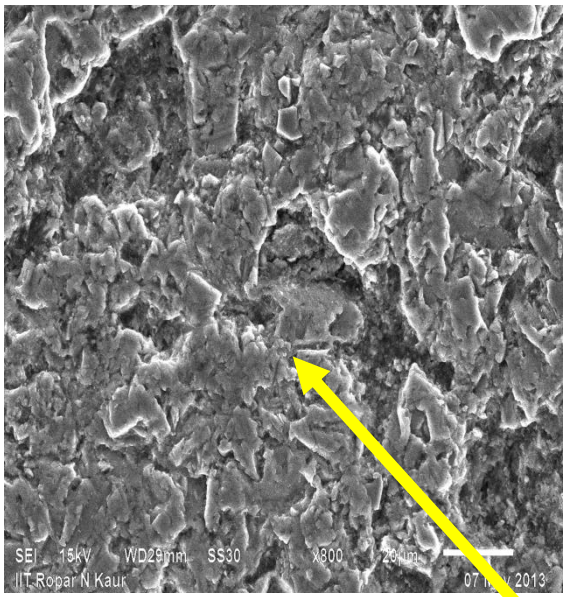

(b) 800

Micro crack

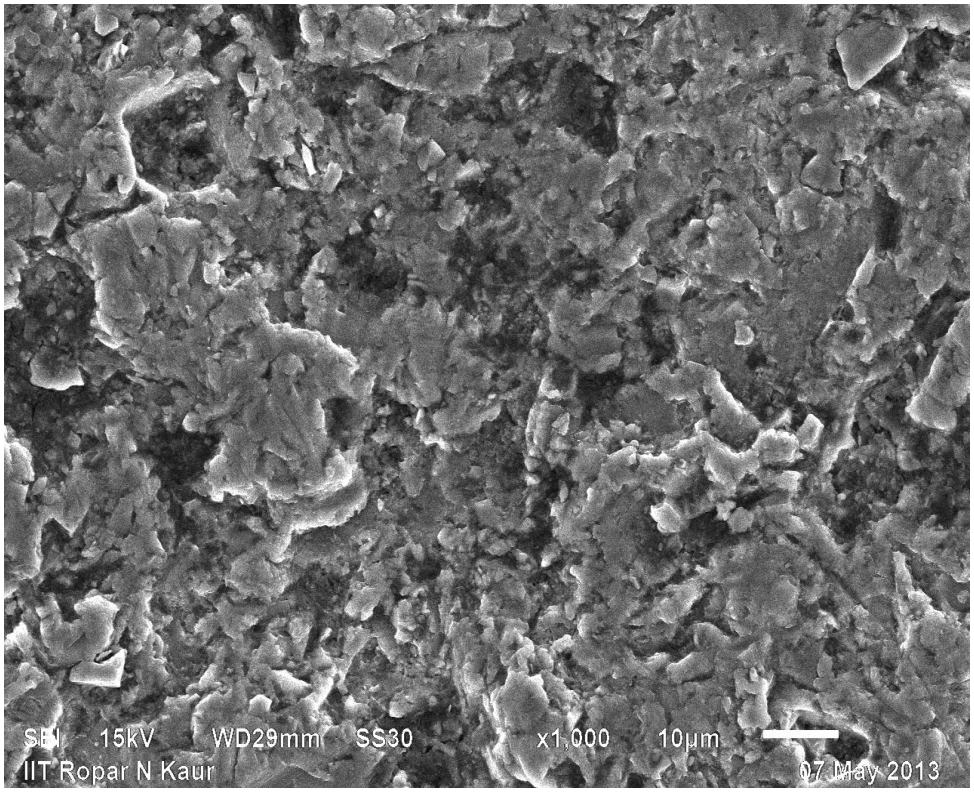

(c) 1000

Figure 9.7: Micrograph of Al/Si Composite machined using HSS tool with SiC as abrasive slurry (Grit size 280, Slurry concentration 30% and Power rating 150W).

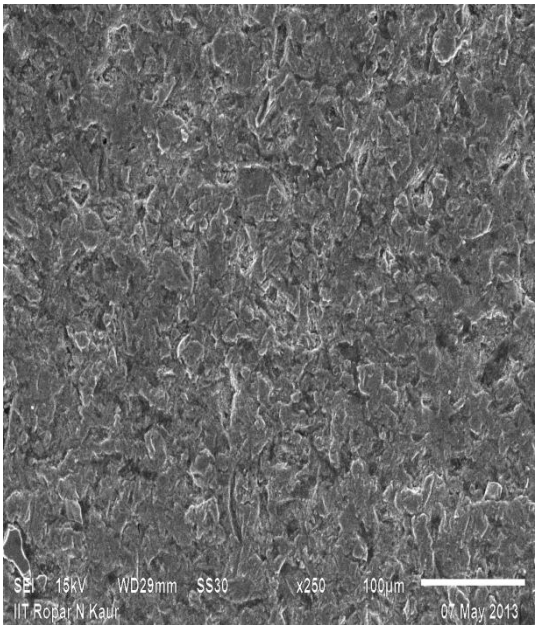

(a) 250

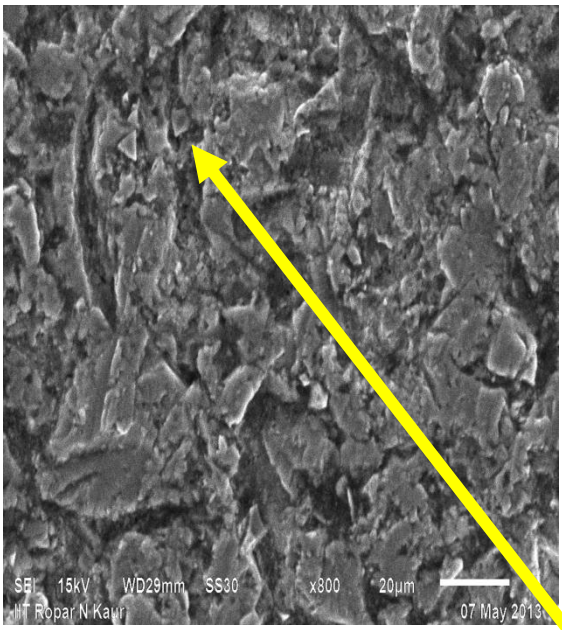

(b) 800

Micro crack

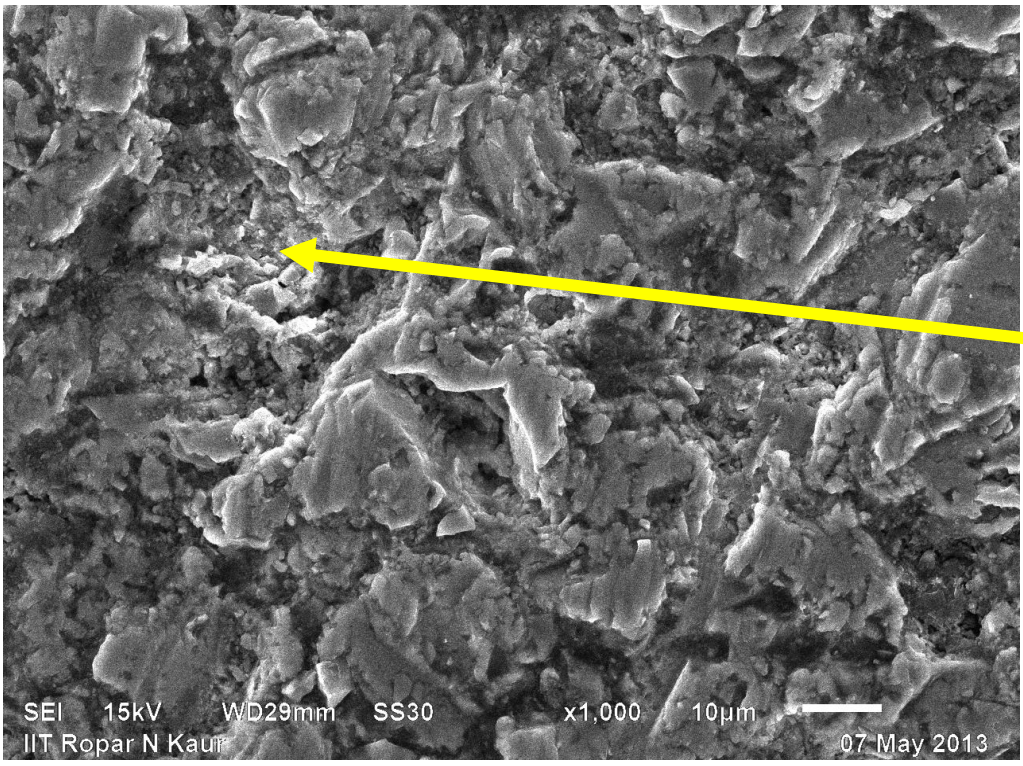

Blow hole

(c) 1000

Figure 9.8: Micrograph of Al/Cu Alloy machined using HSS tool with SiC as abrasive slurry (Grit size 280, Slurry concentration 25% and Power rating 150W).

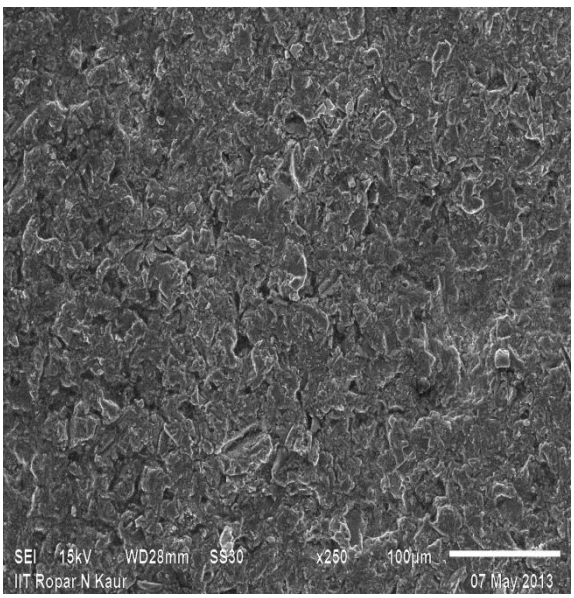

(a) 250

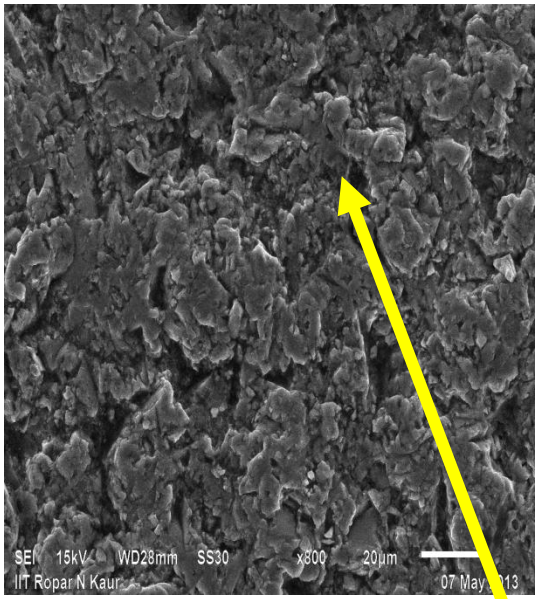

(b) 800

Micro cracks

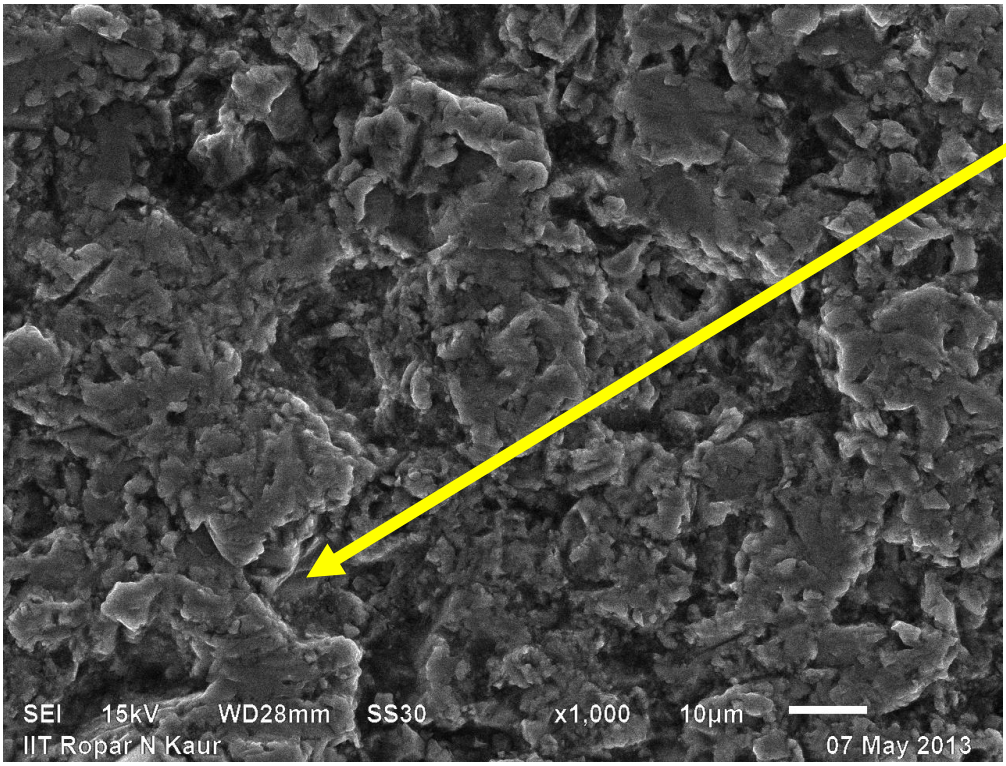

Blow hole

(c) 1000

Figure 9.9: Micrograph of Al/Cu Alloy machined by SS tool with Al_2O_3 as abrasive slurry (Grit size 280, Slurry concentration 25% and Power rating 100W).

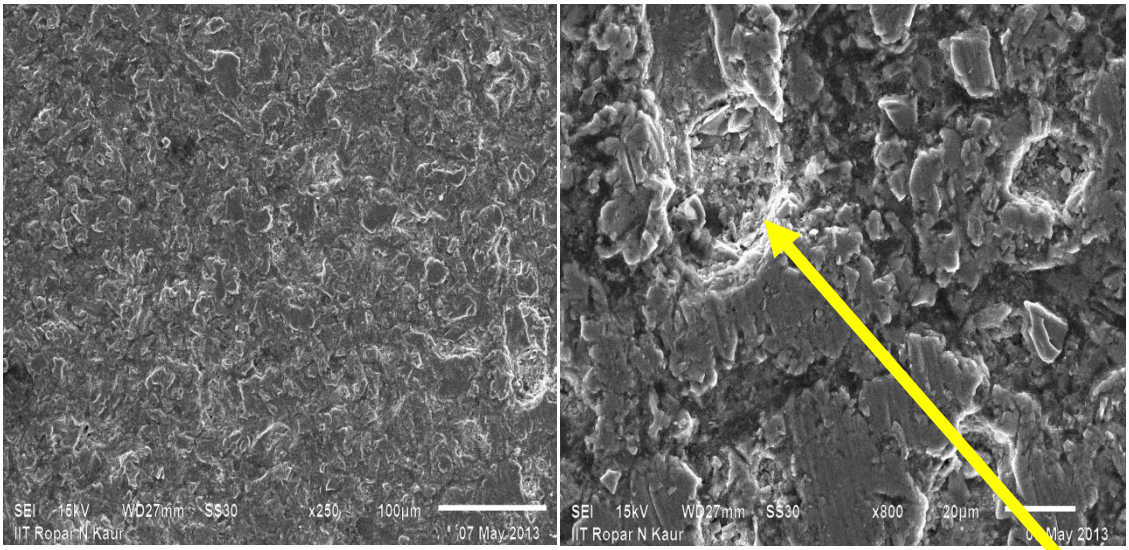

(a) 250 (b) 800

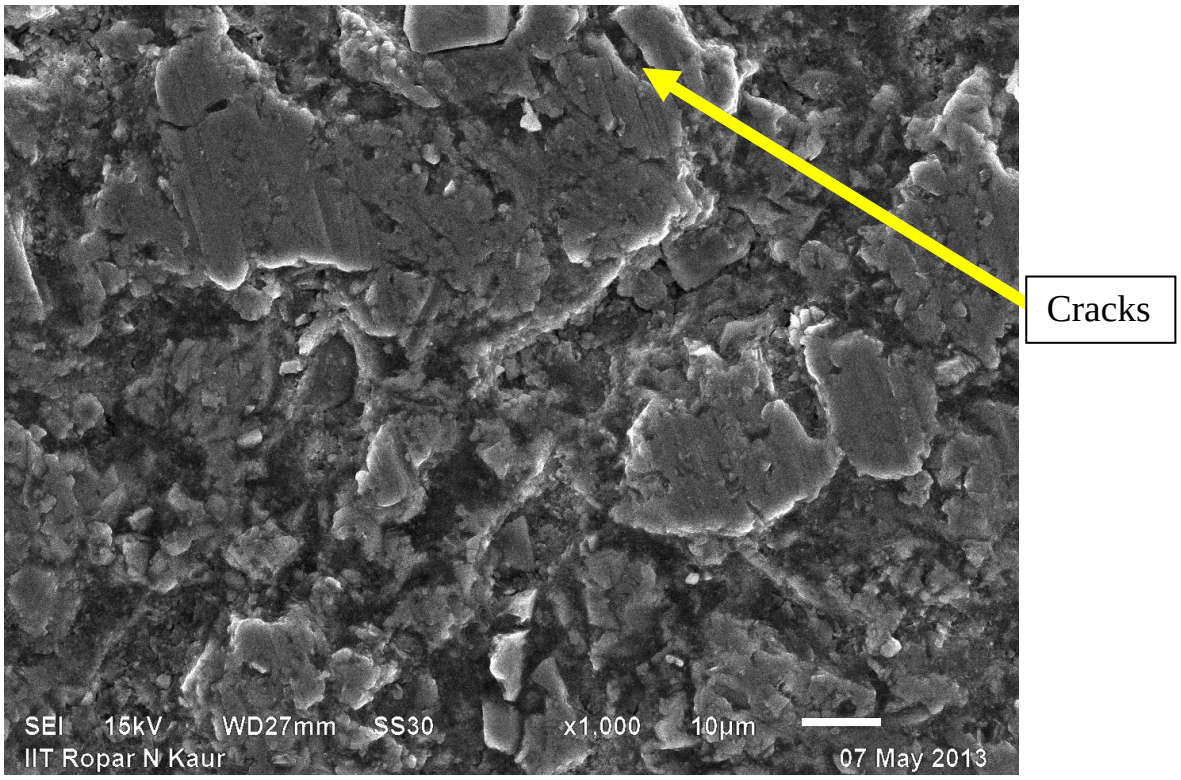

(c) 1000

Figure 9.10: Micrograph of Al/Si Composite machined using SS tool with Al_2O_3 as abrasive slurry (Grit size 400, Slurry concentration 30% and Power rating 150W).

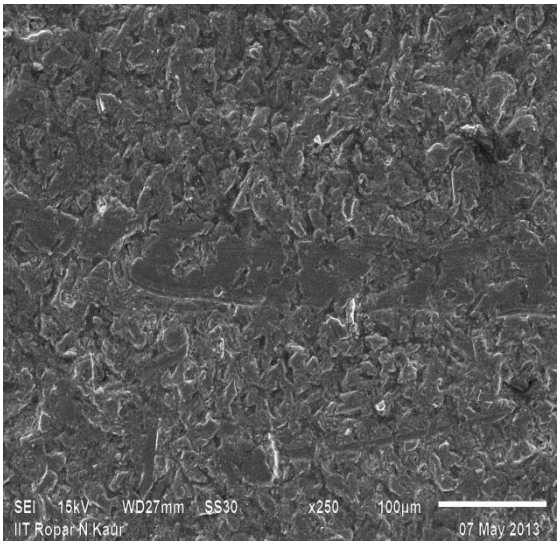

(a) 250

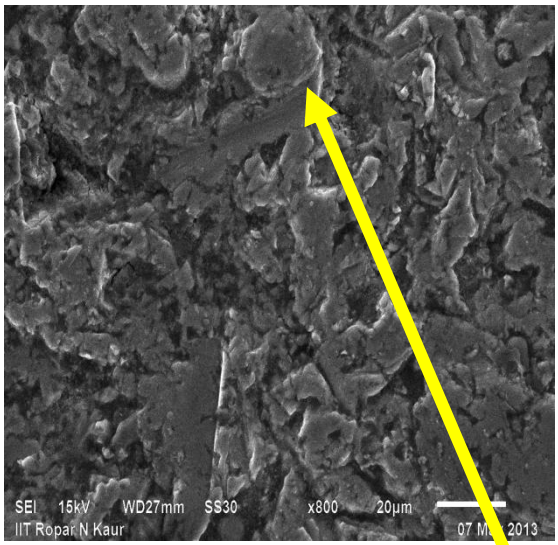

(b) 800

White layer

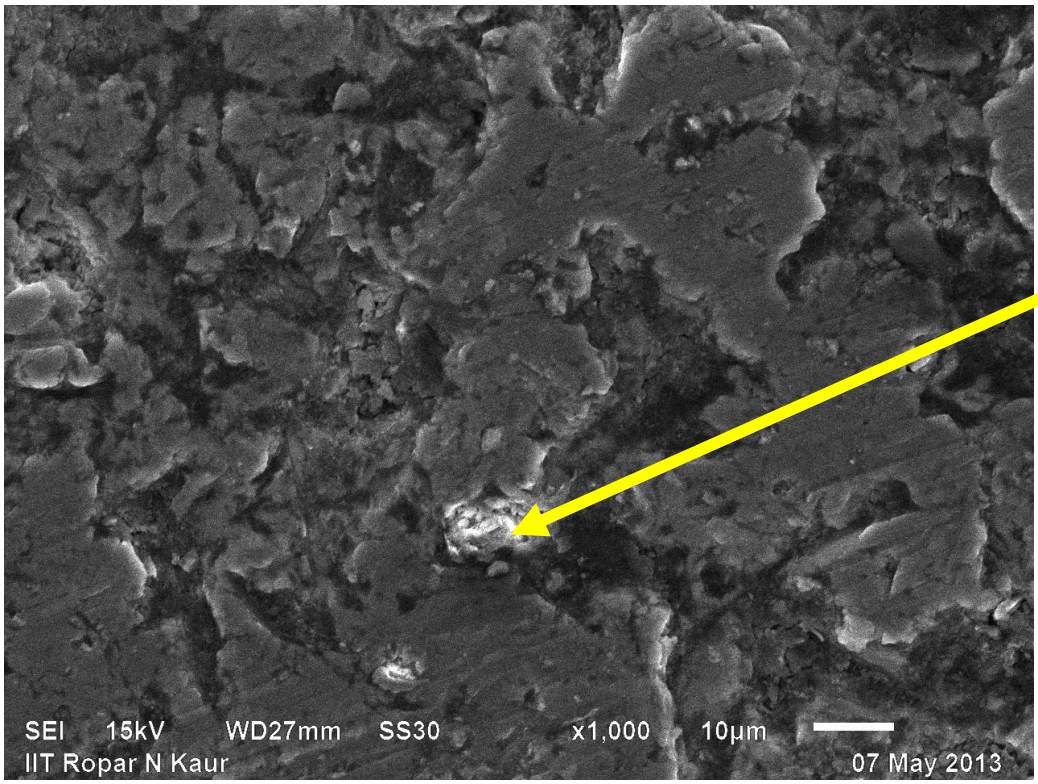

Blow hole

(c) 1000

Figure 9.11: Micrograph of Al/Si Composite machined using HSS tool with Al_2O_3 as abrasive slurry (Grit size 280, Slurry concentration 35% and Power rating 150W).

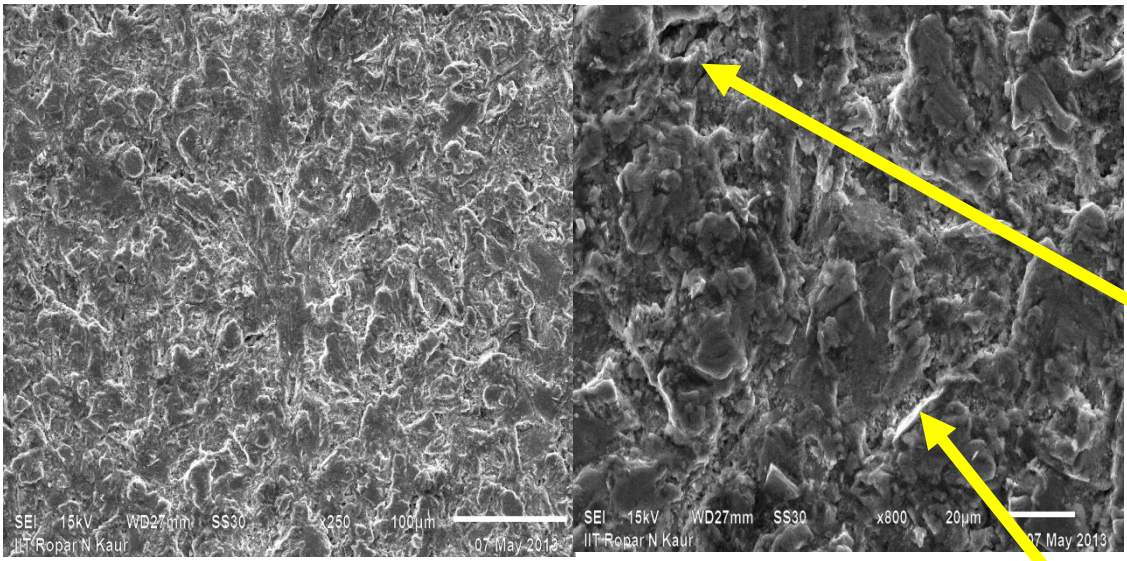

(a) 250 (b) 800

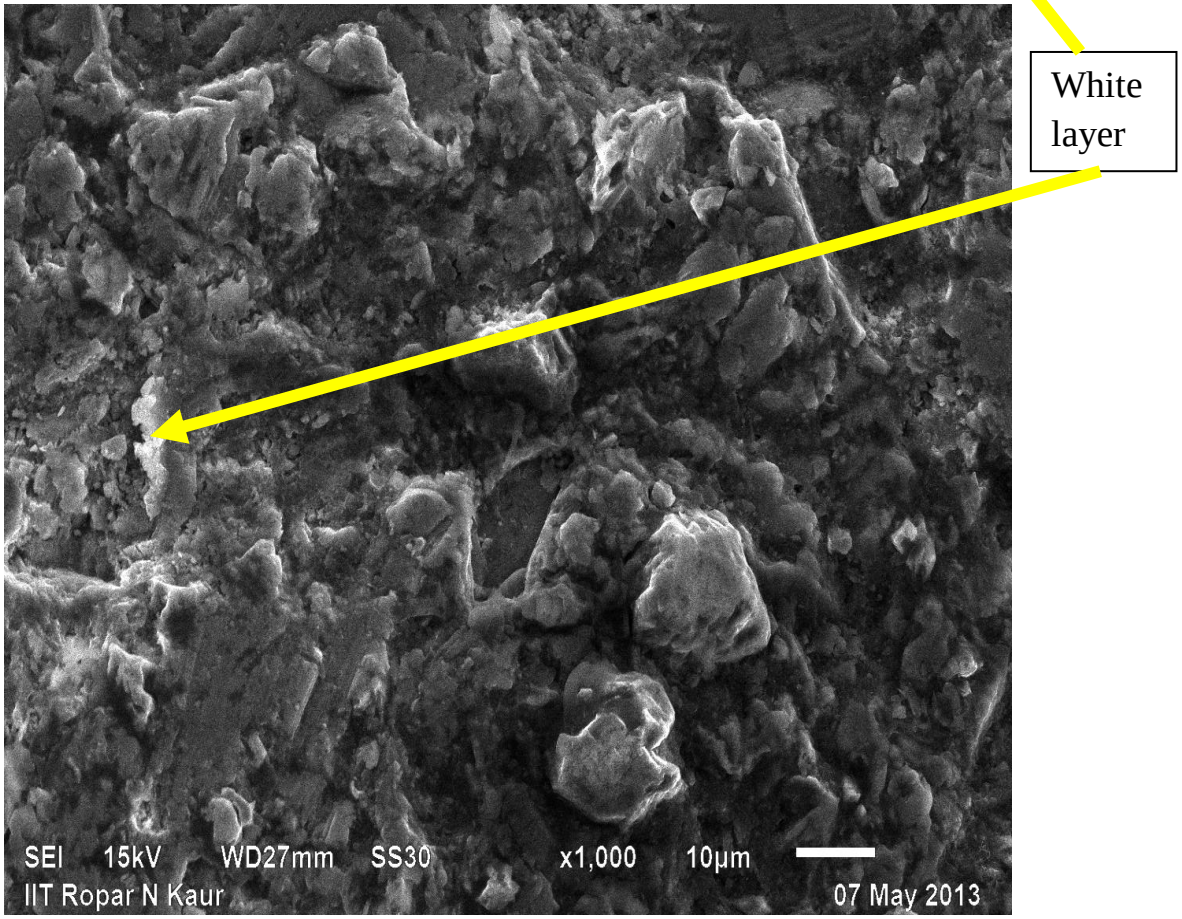

(c) 1000

Figure 9.12: Micrograph of Al/Si Composite machined using HSS tool with Al_2O_3 as abrasive slurry (Grit size Mix, Slurry concentration 25% and Power rating 200W).

Microstructure is shown in above figures; it was observed that as value power rating increases, there are more micro cracks found on the surface. The white layer is formed on the machined surface due to the presence of aluminium oxide. The surface was found rough, because of debris which are not flashed away completely from the machining zone due to the use of larger grit size. The tool also affects the microstructure of machined surface as HSS tool formed more surface roughness and micro crack. Figure 9.25, 9.28, 9.31 and 9.32 shows the white layer deposition of Al_2O_3 on the machined surface.

CHAPTER 10

COMPOSITION OF MACHINED SURFACE (XRD ANALYSIS)

10.1 Introduction

X-ray diffraction (XRD) is a rapid analytical technique primarily used for phase identification of a crystalline material and can provide information on unit cell dimensions. The analyzed material is finely ground, homogenized, and average bulk composition is determined. X-ray diffraction is based on constructive interference of monochromatic X-rays and a crystalline sample. These X-rays are generated by a cathode ray tube, filtered to produce monochromatic radiation, collimated to concentrate, and directed toward the sample.

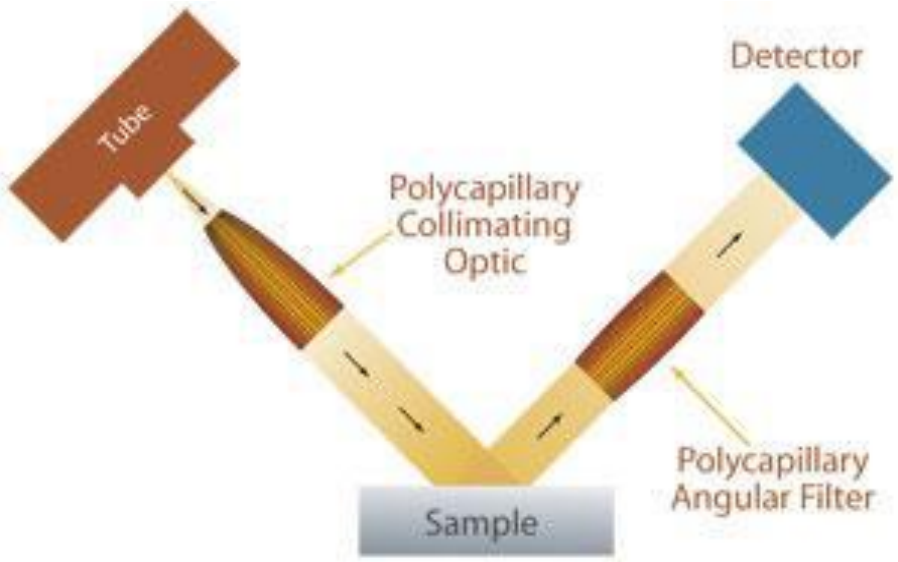

Figure 10.1: X-ray diffraction mechanisms [51]

The interaction of the incident rays with the sample produces constructive interference (and a diffracted ray) when conditions satisfy Bragg's Law ($n\lambda=2d \sin \theta$). This law relates the wavelength of electromagnetic radiation to the diffraction angle and the lattice spacing in a crystalline sample. These diffracted X-rays are then detected, processed and counted. By scanning the sample through a range of 2θangles, all possible diffraction directions of the lattice should be attained due to the random

orientation of the powdered material. Conversion of the diffraction peaks to d-spacings allows identification of the mineral because each mineral has a set of unique d-spacings. Typically, this is achieved by comparison of d-spacings with standard reference patterns. All diffraction methods are based on generation of X-rays in an X-ray tube. These X-rays are directed at the sample, and the diffracted rays are collected. A key component of all diffraction is the angle between the incident and diffracted rays. X-ray diffractometers consist of three basic elements: an X-ray tube, a sample holder, and an X-ray detector. X-rays are generated in a cathode ray tube by heating a filament to produce electrons, accelerating the electrons toward a target by applying a voltage, and bombarding the target material with electrons. When electrons have sufficient energy to dislodge inner shell electrons of the target material, characteristic X-ray spectra are produced. These X-rays are collimated and directed onto the sample. As the sample and detector are rotated, the intensity of the reflected X-rays is recorded. When the geometry of the incident X-rays impinging the sample satisfies the Bragg Equation, constructive interference occurs and a peak in intensity occurs. A detector records and processes this X-ray signal and converts the signal to a count rate which is then output to a device such as a printer or computer monitor. The geometry of an X-ray diffractometer is such that the sample rotates in the path of the collimated X-ray beam at an angle θ while the X-ray detector is mounted on an arm to collect the diffracted X-rays and rotates at an angle of 2θ.

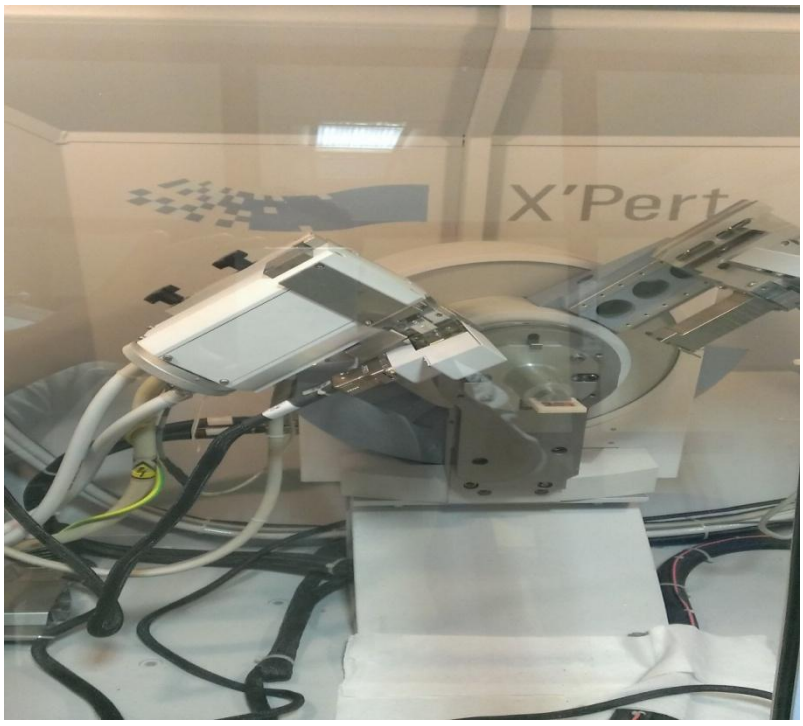

Figure 10.2 X-Ray Diffraction Machine (XRD) (IIT Ropar)

10.2 X-RAY DIFFRACTION Analysis

In XRD, the physical content of constituents present in the samples are indicated in the form of a graphs and tables shows the name and percentage of elements/ compounds present in respective samples. Following figure shows the XRD analysis of Al/Si composites and Al/Cu alloy of different composition.

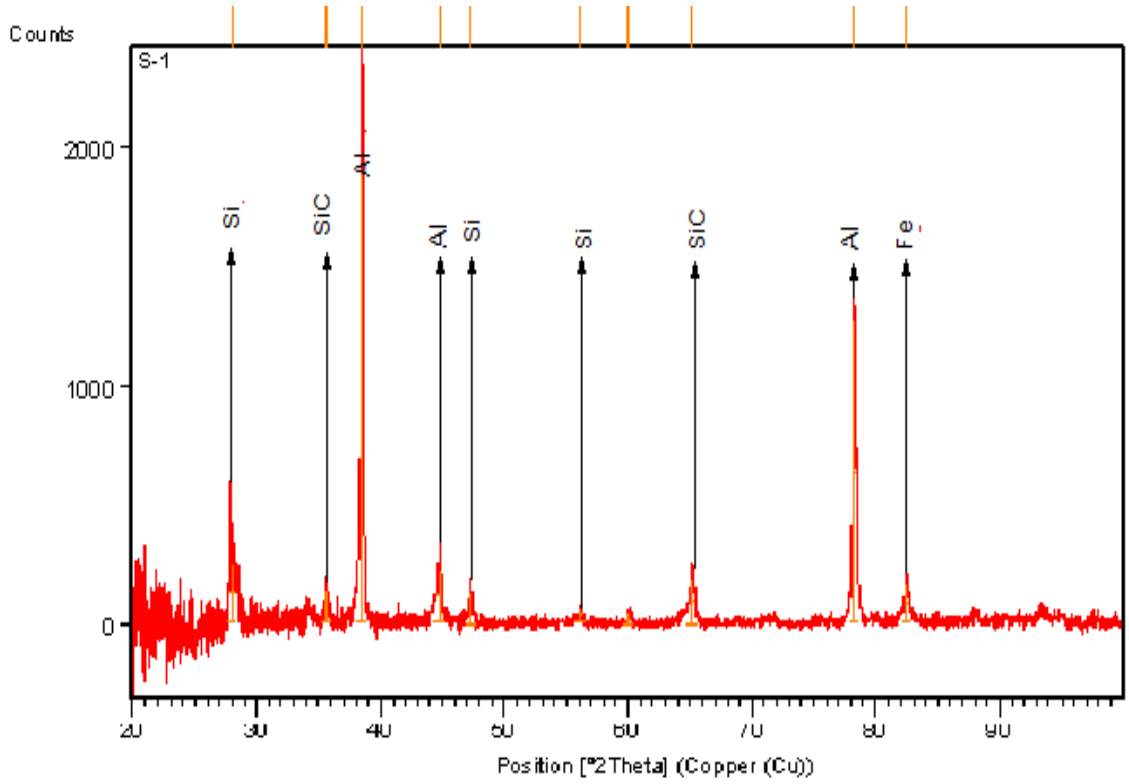

Figure 10.3 X-ray diffraction for Al/Si Composite with SiC of 280 grit size with power rating 100W.

Table 10.1 X-ray diffraction for Al/Si Composite with SiC of 280 grit size

Reference Code	Score	Compound Name	Scale Factor
00-049-1428	20	Silicon Carbide	0.077
03-063-0932	17	Aluminium	0.067
00-003-1050	42	Iron	0.081
01-089-2749	23	Silicon	0.102

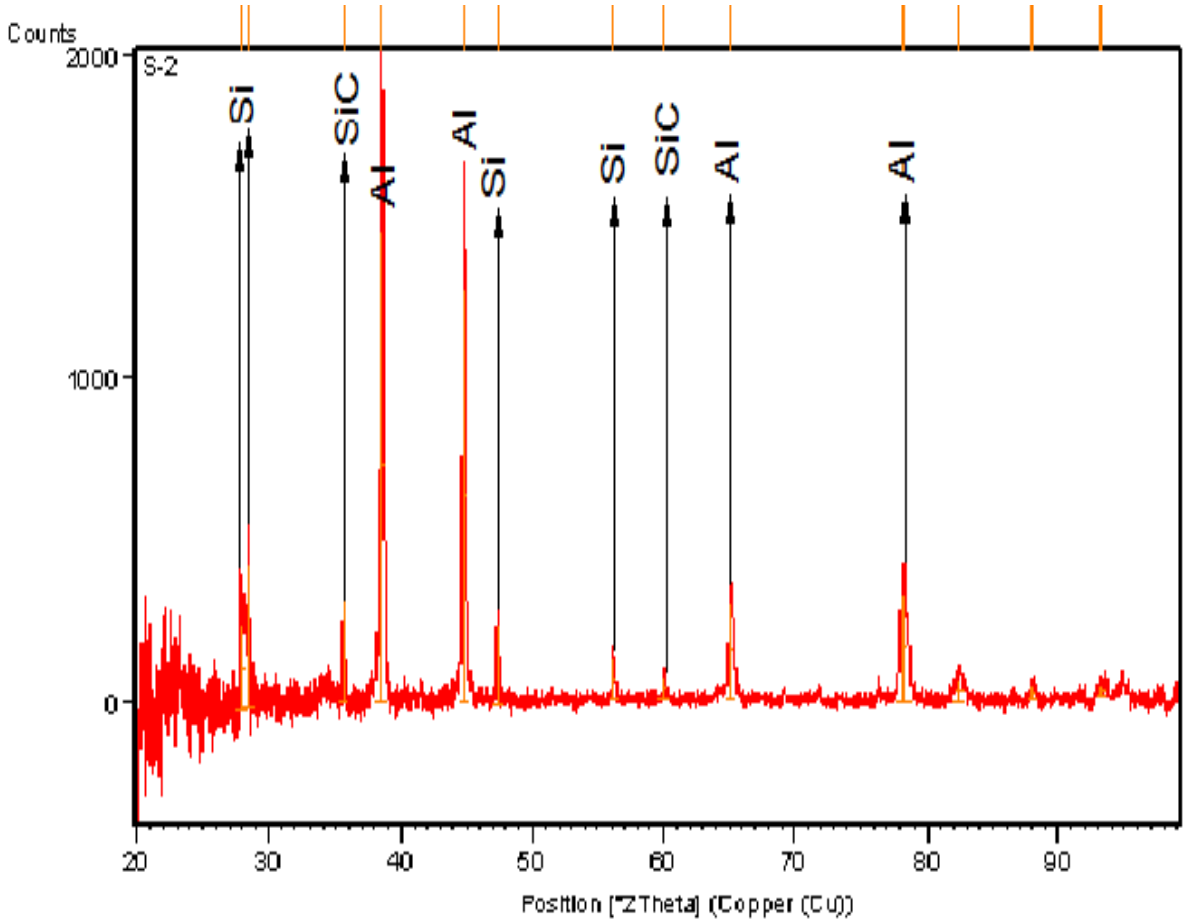

Figure 10.4 X-ray diffraction for Al/Si Composite with SiC of 400 grit size with power rating 200W.

Table 10.2 X-ray diffraction for Al/Si Composite with SiC of 400 grit size.

Reference Code	Score	Compound Name	Scale Factor
03-065-0360	41	Silicon Carbide	0.115
03-065-6323	35	Iron Silicon	0.920
00-003-0932	13	Aluminium	0.127
01-078-2500	7	Silicon	0.059

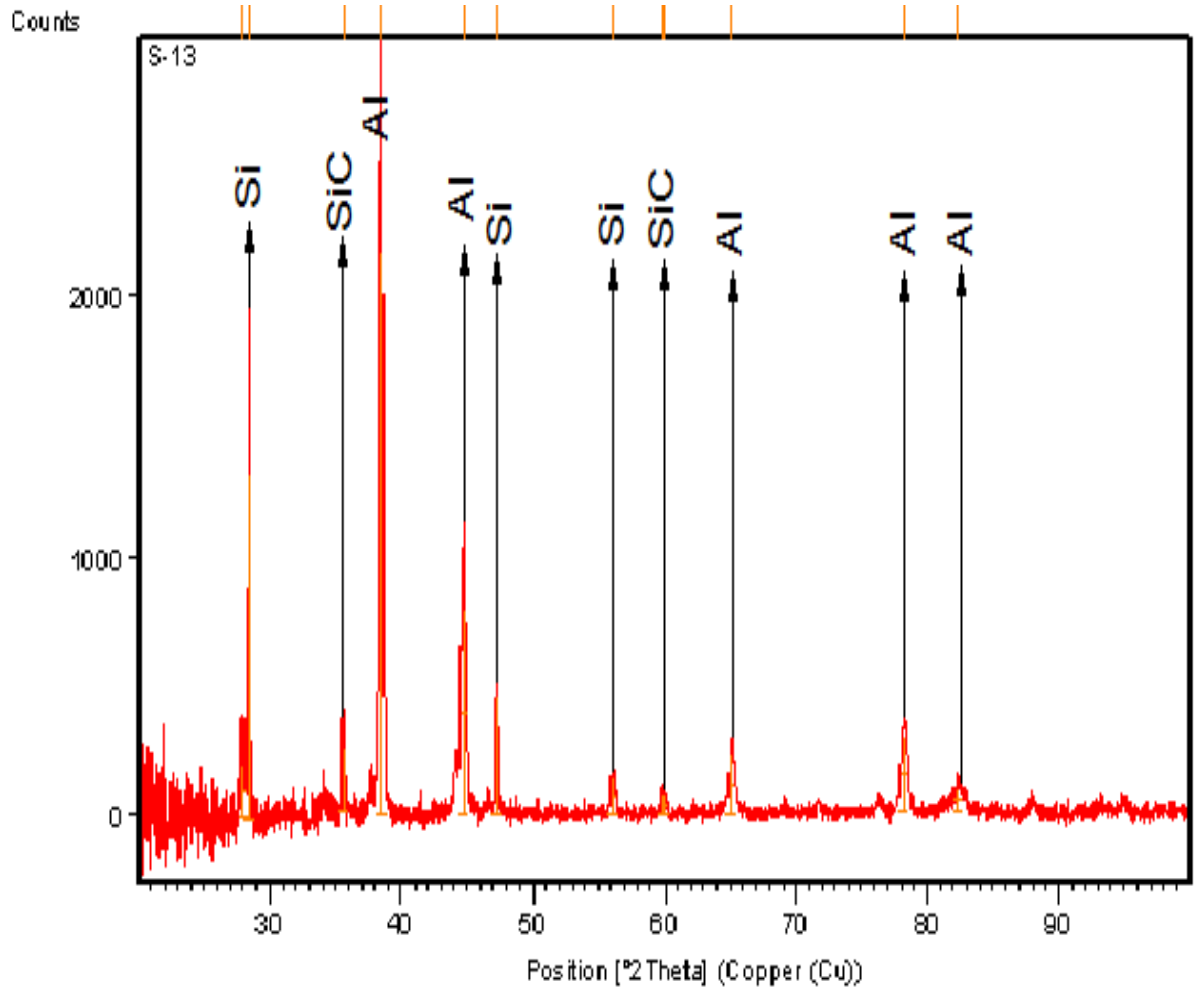

Figure 10.5 X-ray diffraction for Al/Cu Alloy with SiC of 280 grit size with power rating 150W.

Table 10.3 X-ray diffraction for Al/Cu Alloy with SiC of 280 grit size.

Reference Code	Score	Compound Name	Scale Factor
00-049-1428	30	Silicon Carbide	0.096
00-051-0916	13	Copper Silicon	0.139
00-003-0932	16	Aluminium	0.025
00-001-0787	10	Silicon	0.107

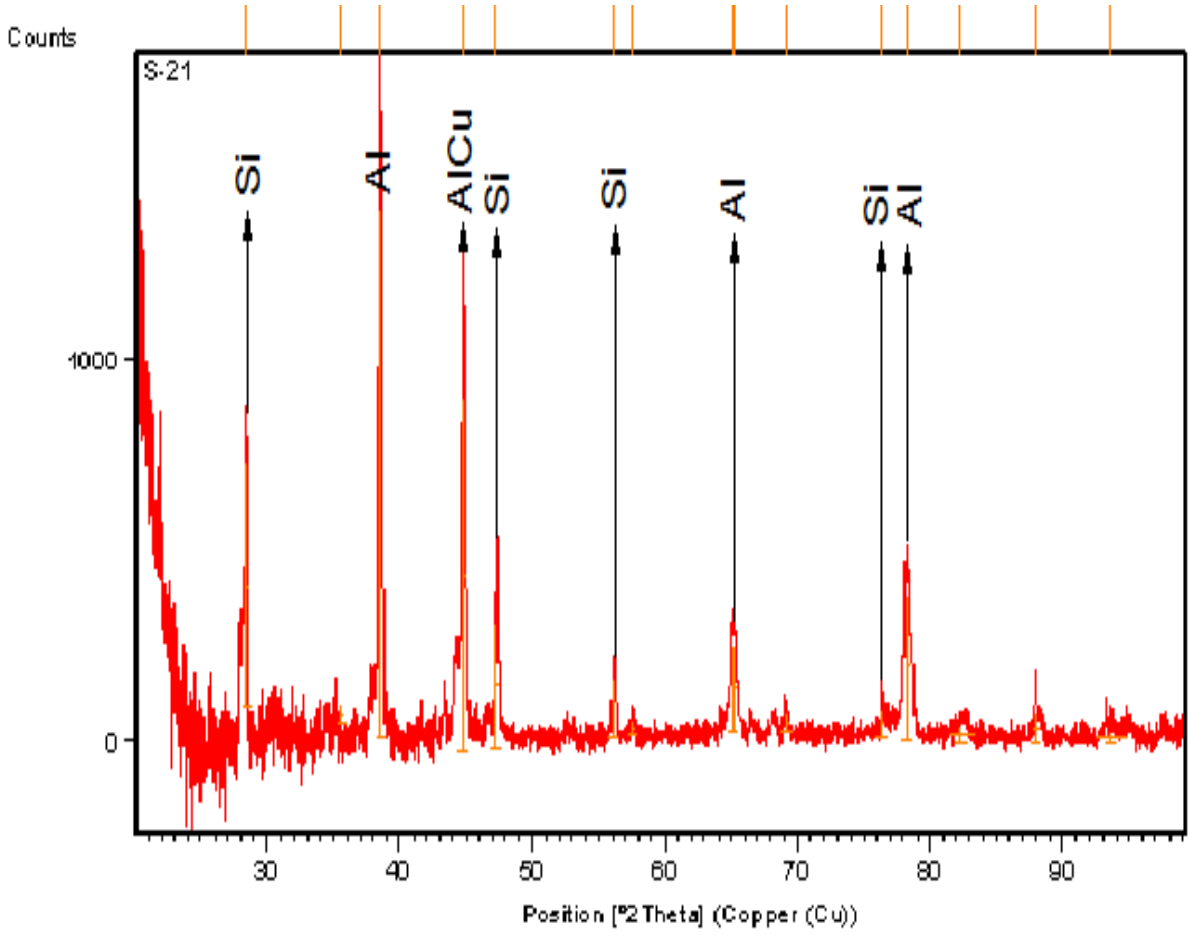

Figure 10.6 X-ray diffraction for Al/Cu Alloy with $Al_2\ O_3$of Mix grit size with power rating 150W.

Table 10.4 X-ray diffraction for Al/Cu Alloy with $Al_2\ O_3$ of Mix grit size.

Reference Code	Score	Compound Name	Scale Factor
03-065-1228	7	Aluminium Copper	0.156
03-065-1060	9	Silicon	0.732
03-065-1428	15	Aluminium	0.054

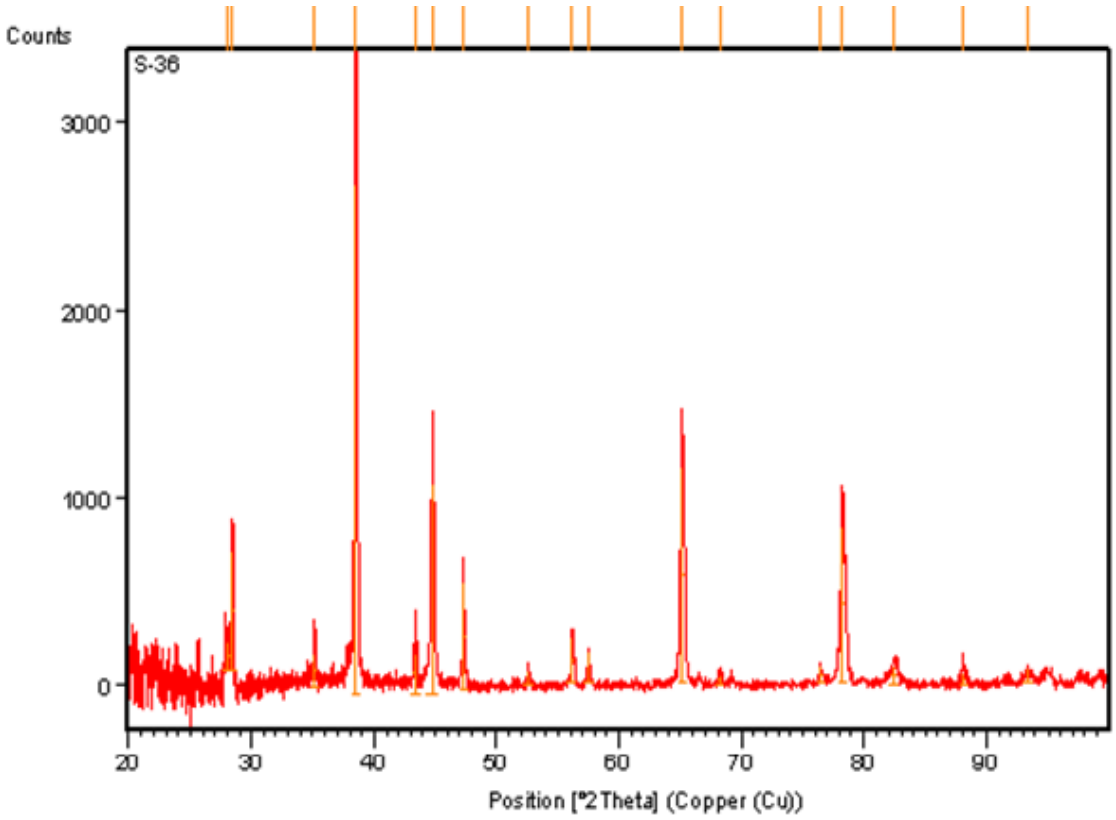

Figure 10.7 X-ray diffraction for Al/Si Composite with $Al_2\ O_3$ of Mix grit size with power rating 200W.

Table 10.5 X-ray diffraction for Al/Si Composite with $Al_2\ O_3$ of Mix grit size.

Reference Code	Score	Compound Name	Scale Factor
01-088-0826	46	Aluminium Oxide	0.078
00-003-0932	45	Aluminium	0.111
00-002-0561	8	Silicon	0.032

CHAPTER 11

RESULTS, CONCLUSIONS AND RECOMMENDATIONS

11.1 RESULTS

ANOVA is used to study the effects of various parameters like tool, work piece, power rating, slurry concentration, type of slurry and grit size. Some of these factor and their interactions found significant in some cases and some of them found insignificant in some cases. The purpose of INOVA was to identify the important parameters in prediction of MRR, TWR, micro hardness, surface roughness. The major results which we can get out from this study are given below:

11.1.1 Material Removal Rate

From the Table 4.2, it was observed that Power Rating was found to be the most significant factor with contribution of 28.71 % followed by Slurry Concentration and Grit Size with a contribution of 25.95% and 12.73% respectively. The Slurry type, type of Tool, Workpiece and interaction between Slurry type and Tool, Slurry type and Workpiece, and Tool and Workpiece was found insignificant.

For S/N ratio Power Rating, Slurry Concentration and Grit Size were found to be significant to MRR for reducing the variation.

Table 4.3 and 4.5 shows the ranks of different factor. 1^{st} rank is given to Power Rating that has highest contribution to MRR. 2^{nd} rank is given to Slurry Concentration , 3^{rd} rank is given to Grit Size, 4^{th} rank is given to type of Slurry, 5^{th} rank is given to Workpiece and the 6^{th} is given to the Tool that has minimum contribution to MRR.

Highest MRR is observed when Workpiece is machined on Power Rating of 150, Slurry Concentration of 35% and 280 as its Grit Size. With 95% Confidence Interval mean value of MRR was found to be 4.42 ± 0.48 mm^3/min.

11.1.2 Tool Wear Rate

From the Table 5.2, it was observed that Power Rating was found to be the most significant factor with contribution of 28.59% followed by Slurry Concentration and Grit Size with a contribution of 25.83% and 13.83% respectively. The Slurry type, type of Tool, Workpiece and interaction between Slurry type and Tool, Slurry type and Workpiece, and Tool and Workpiece was found insignificant.

For S/N ratio Power Rating, Slurry Concentration and Grit Size were found to be significant to TWR for reducing the variation.

Table 5.3 and 5.5 shows the ranks of different factor. 1^{st} rank is given to Power Rating that has highest contribution to MRR. 2^{nd} rank is given to Slurry Concentration , 3^{rd} rank is given to Grit Size, 4^{th} rank is given to type of Slurry, 5^{th} rank is given to Workpiece and the 6^{th} is given to the Tool that has minimum contribution to TWR.

Lowest TWR is observed when Workpiece is machined on Power Rating of 100, Slurry Concentration of 30% and Mix as its Grit Size. With 95% Confidence Interval mean value of TWR was found to be $0.3697 \pm 0.051\ mm^3$/min

11.1.3 Surface Roughness

From the Table 6.2, it was observed that Power Rating was found to be the most significant factor with contribution of 34.32% followed by Grit Size with a contribution of 18.39% and interaction between Slurry type and type of Tool was found significant with contribution of 8.40%. The Slurry type, Slurry concentration, type of Tool, Workpiece and interaction between Grit size and Slurry Concentration, Grit size and Power Rating was found insignificant.

For S/N ratio Power Rating, Grit Size and interaction between Slurry type and type of Tool were found to be significant to MRR for reducing the variation.

Table 6.3 and 6.5 shows the ranks of different factor. 1^{st} rank is given to Power Rating that has highest contribution to Surface Roughness. 2^{nd} rank is given to Grit Size, 3^{rd} rank is given to Slurry Concentration, 4^{th} rank is given to the Tool, 5^{th} rank is given to the type of Slurry and 6^{th} rank is given to the Workpiece that has minimum contribution to Surface Roughness.

Lowest Surface Roughness is observed when Workpiece is machined on Power Rating of 150 and Mix as its Grit Size. With 95% Confidence Interval mean value of Surface Roughness was found to be $1.87 \pm 0.09 \ \mu m$.

11.1.4 Hardness

From the Table 7.2, it was observed that Workpiece was found to be the most significant factor with contribution of 81.86 % followed by the type of Tool and Power Rating with a contribution of 5.21% and 2.44% respectively. The Slurry type, Grit size, Slurry Concentration and interaction between type of Tool and Grit size, type of Tool and Power Rating, and Grit size and Power Rating was found insignificant.

For S/N ratio Workpiece, type of Tool and Power Rating, Slurry Concentration and Grit Size were found to be significant to Hardness for reducing the variation.

Table 7.3 and 7.5 shows the ranks of different factor. 1^{st} rank is given to Workpiece that has highest contribution to Hardness. 2^{nd} rank is given to the type of Tool, 3^{rd} rank is given to Power Rating, 4^{th} rank is given to Grit Size, 5^{th} rank is given to the type of Slurry and the 6^{th} is given to the Slurry Concentration that has minimum contribution to Hardness.

Highest Hardness is observed when the Al/Si Workpiece is machined with High Speed Steel as Tool Material on Power Rating of 150. With 95% Confidence Interval mean value of Hardness was found to be 36.59 ± 0.407 HRB.

11.1.5 Microstructure Analysis

Optical microstructure and SEM were analyzed to observe the presence and distribution of particles in aluminium silicon composite and aluminium copper alloy. Various SEM images were taken at different magnifications like 250X, 800X and 1000X. It was observed that micro crack was found as the power rating increases. Al/Si composite when machined by HSS shows more surface roughness.

11.2 Conclusions

The following conclusions were drawn from present study:-

1. The MRR is mainly affected by Power Rating and Slurry Concentration.

2. The TWR is mainly affected by Power Rating and Slurry Concentration.

3. Maximum effect on machined surface finish is due to Grit Size and Power Rating.

4. Rockwell Hardness depends on Workpiece, Tool and Power Rating.

11.3 Recommendation for Future Work

a) Different type of slurry, such as (Boron carbide) and Grit size (220-600) can be used to know the variation in the results.

b) Different type of tool material lighter in weight, also harder than HSS and SS can be used and the variation in results can be found.

c) Comparison of SEM analysis can be done of various composites and alloy, machining with USM and the variations can be found.

REFERENCES

[1] Adithan M. (1981), "Tool Wear characteristics in ultrasonic drilling", Tribology International, Vol. 14, No. 6, pp. 351-356.

[2] Anantha Ramu B.L. and Krishnamurthy R. (1989), "Machining performance of toughened zirconia ceramic and cold compact alumina ceramic in ultrasonic drilling", Journal of Mechanical Working Technology, Vol.20, pp.365-375.

[3] Azarhoushang B. and Akbari J. (2007) "Ultrasonic-assisted drilling of Inconel 738-LC" International Journal of Machine Tools & Manufacture, Vol. No.-47, pp.1027-1033.

[4] Babitskya V.I., Astashevb V.K., Meadows A. (2007) "Vibration excitation and energy transfer during ultrasonically assisted drilling" Journal of Sound and Vibration. Vol. No. 308. pp. 805-814.

[5] Brehl D., Dow T. (2008), "Review of vibration-assisted machining" Precision Engineering, Vol. No. 32, pp. 153-172.

[6] Chang S. and Bone G.M. (2005), "Burr size reduction in drilling by ultrasonic assistance", Robotic and Computer-Integrated manufacturing, Vol. 21, pp. 442-450.

[7] Chang Simon, Bone Gary (2010), "Burr height model for vibration assisted drilling of aluminium 6061-T6" Precision Engineering, Vol. No. 34, pp. 369-375.

[8] Choi J.P., Jeon B.H., Kim B.H., (2007), "Chemical assisted ultrasonic machining of glass," Journal of Materials Processing Technology, pp.153-156.

[9] Dam H.; Quist P, and Schreiber M. (1995), "Productivity, surface quality and tolerances in ultrasonic machining of ceramics", Journal of Materials Processing Technology, Vol.51, No. 1-4, pp.358-368.

[10] Deng Jianxin and Lee Taichiu (2002), "Ultrasonic machining of ceramic composites",Journal of the Euoropean Ceramic Society, vol.22, No.8, pp. 1235-1241.

[11] Dvivedi A and Kumar P. (2007), "Surface quality evaluation in ultrasonic drilling through the Taguchi technique" Int J Adv Manuf Technol, Vol. 34, pp 131-140.

[12] El-Hofy Hassan (2005), "Advanced Machining Processes", McGraw-Hill, Production Engineering Department, Alexandria University, Egypt, ISBN 0-07-145334-2.

[13] Gao G., Zhao B., Xiang D., Kong Q. (2009), "Research on the surface characteristics in ultrasonic grinding nano-zirconia ceramics" Journal of materials processing technology, Vol. No. 209, pp. 32-37.

[14] Guzzo P.L., Raslan A.A., Mello De J.D.B. (2003), " Ultrasonic abrasion of Quartz Crystals", Wear, Vol.255, pp. 67-77.

[15] Guzzo P.L., Raslan A.A., Shinohara A.H., Suzuki C.K., Mikawa Y.(2001) "Characterization of synthetic quartz crystals grown from cylindrical seeds produced by ultrasonic machining", Journal of Crystal Growth, Vol. No. 229, pp.275-282.

[16] Hsu C.Y., Lin Y., Lee W.S., Lo S.P. (2008) "Machining characteristics of Inconel 718 using ultrasonic and high temperature-aided cutting journal of materials processing technology, Vol. No. 9 8,pp. 359-365.

[17] Ichida Y., Sato R., Morimoto Y., Kobayashi K. (2005) "Material removal mechanisms in non-contact ultrasonic abrasive machining", Wear Vol. No.258, pp. 107-114.

[18] Jadoun R.S., Kumar Pradeep, Mishra B.K. (2009), "Taguchi's optimization of process parameters for production accuracy in ultrasonic drilling of engineering ceramics", Prod. Eng. Res. Devel.,Vol. 3, pp. 243-253.

[19] Jatinder Kumar and Vinod Kumar (2012), "Evaluating the Tool Wear Rate in Ultrasonic Machining of Titanium using Design of Experiment Approach", World Academy of Science, Engineering and Technology, Vol. No. 81, pp 803-808.

[20] Khoo C.Y., Hamzah Esah, Sudin Izman (2008), "A review on the rotary ultrasonic machining of advanced ceramics", Journal Mekanikal, Vol. No. 25, pp. 9-23.

[21] Komariah M. and Reddy P.N. (1993), "Relative Performance of tool materials in ultrasonic machining", Wear, Vol.161, No.1-2, pp. 1-10.

[22] Kumar Jatinder and Khamba J.S. (2010), " Modeling the material removal rate in ultrasonic machining of titanium using dimensional analysis", Int J Adv Manuf Technology Vol. No. 48, pp. 103-119.

[23] Kumar Vinod and Khamba J.S. (2009) "Parametric optimization of ultrasonic machining of Co-based super alloy using the Taguchi multi-objective approach" Journal of Prod. Eng. Res. Devel., Vol. No.3,pp. 417 – 425.

[24] Kumar Jatinder, Khamba J.S., Mohapatra S. (2008) "An investigation in the machining characteristics of titanium using ultrasonic machining:, Int. J. Machining and Machinability of Materials, Vol. 3, Nos. ½.

[25] Kumar Vinod (2009), "Ultrasonic Machining of Tungsten Carbide, Stellite and Diamond", ME THESIS. THAPAR UNIVERSITY, PATIALA.

[26] Lee T.C., Chan C.W. (1997), "Mechanism of the ultrasonic machining of ceramic composites", Journal in materials Processing Technology", Vol. 17, pp.195-201.

[27] Lia Z.C., Caib Liang-Wu, Peia Z.J., Treadwell C. (2006), "Edge-chipping reduction in rotary ultrasonic machining of ceramics: Finite element analysis and experimental verification" International Journal of Machine Tools & Manufacture, Vol. No. 46, pp. 1469-1477.

[28] Liao Y.S., Chen Y.C., Lin H.M (2007) "Feasibility study of the ultrasonic vibration assisted drilling of Inconel super alloy", International Journal of Machine Tools & Manufacture, Vol. No. 47, pp.1988-1966.

[29] Liu DeFu, Cong W.L., Pei Z.J, Tang YongJun (2012), "A cutting force model for rotary ultrasonic machining of brittle materials" International Journal of Machine Tools & Manufacture, Vol. No. 52, pp-77-84.

[30] Li Z.C., Jiao Y., Deine T.W., Pei Z.J., Treadwell C. (2005), "Rotary ultrasonic machining of ceramic matrix composites: feasibility study and designed experiments", International Journal of Machine Tools & Manufacture, Vol. 33, pp. 1402-1411.

[31] Li Z.C., Jiao Y., Deine T.W., Pei Z.J., Treadwell C. (2006), "Investigation of surface roughness and accuracy in ultrasonic machining", International Journal of Machine Tools & Manufacture, Vol. 46, pp. 1469-1478.

[32] Majeed M.A., Vijayaraghvan L., Malhotra S.K., KrishnaMurthy R. (2008), "Ultrasonic Machining of Al2O3/LaPO4 Composites", International Journal of Machine Tools & Manufacture, Vol. 48, pp. 40-46.

[33] Module 9 Non conventional machining – Lesson 36 Ultrasonic Machining (USM) – Version 2 ME, IIT Kharagpur.

[34] Pandey P.C and Shan H.S (1980), "Modern Machining Processes", Tata McGraw-Hill, N.D., pp. 7-38.

[35] Pujana J., Rivero A., Celaya A.,Lacalle L.N. (2009) "Analysis of ultrasonic-assisted drilling of Ti6Al4V", international Journal of Machine Tools & Manufacture, Vol. No. 49, pp.500-508.

[36] Ramulu M. (2005), "Ultrasonic machining effects on the surface finish and strength of silicon carbide ceramics", International Journal of Manufacturing Technology Management Vol. 7, No.2/3/4, pp. 107-125.

[37] Shen Xue-Hui, Zhang Jianhua, Xing Dongliang Xing, Zhao Yunfeng, (2012), "A study of surface roughness variation in ultrasonic vibration-assisted milling", Int J Adv Manuf Technol, Vol. No. 58, pp. 553-561.

[38] Singh M.K. (2008), "Unconventional Manufacturing Processes", New Age International Publishers, ISBN (13): 978-81-224-2244-3.

[39] Singh R. and Khamba J.S. (2007), "Taguchi technique for modeling material removal rate in ultrasonic machining of titanium, "Journal of Materials Science and Engineering, Vol. A 460-461, pp. 365-369.

[40] Singh R. and Khamba J.S., (2008) "Comparison of slurry effect on machining characteristics of titanium in ultrasonic drilling", journal of materials processing technology, Vol. 1 97,pp. 200-205.

[41] Singh Rupinder and Khamba J.S. (2006), " Ultrasonic machining of titanium and its alloys" Journal of Materials Processing Technology, Vol. No. 173, pp-125-135

[42] Tawakoli Taghi, Azarhoushang Bahman (2008), "Influence of ultrasonic vibrations on dry grinding of soft steel," International Journal of Machine Tools & Manufacture, Vol. No. 48, pp. 1585-1591.

[43] Thomas P., Babitskya V.I. (2007) "Experiments and simulations on ultrasonically assisted drilling" Journal of Sound and Vibration. Vol. No. 308. pp. 815-830.

[44] Wang Qiangguo, Cong Weilong, Pei Z.J., Gao Hang, Kan Renke (2009) " Rotary ultrasonic machining of potassium dihydrogen phosphate (KDP) crystal: An experimental investigation on surface roughness" Journal of Manufacturing Processes, Vol. No. 11, pp. 66-73.

[45] Wei B., Denga X., Fang Z. (2007) "Study on ultrasonic-assisted lapping of gears" International Journal of Machine Tools & Manufacture, Vol. No. 47, pp. 2051-2056.

[46] Wiercigroch M., Neilson R.D., Player M.A. (1999) "Material removal rate prediction for ultrasonic drilling of hard materials using an impact oscillator approach", Physics Letters A Vol. No. 259, pp. 91-96.

[47] Wiercigrocha M., Wojewadab J., Krivtsovc A. (2005), "Dynamics of ultrasonic percussive drilling of hard rocks" Journal of Sound & Vibration, Vol. No. 280, pp. 739-757.

[48] Yeo S.H, Tan P.C (2011),"A new approach for force measurement and workpiece clamping in micro-ultrasonic machining" Int J Adv Manuf Technology, Vol. 53, pp 517-522.

[49] Zhang C., Rentsch R., Brinksmeier E. (2005) "Advances in micro ultrasonic assisted lapping of microstructures in hard-brittle materials: a brief review and outlook" International Journal of Machine Tools & Manufacture, Vol. No. 45, pp. 881-890.

[50] www.google.com